UNIVERSITÉ DE SHERBROOKE

Studying the beginning of the end: The roles of Tbf1 and Reb1 at subtelomeres

Par Alexandra Krallis
Département de Microbiologie et d'Infectiologie

Mémoire présentée à la Faculté de Médecine et des Sciences de la Santé en vue de l'obtention du grade de maître ès sciences (M. Sc.) en Microbiologie

Sherbrooke, Québec, Canada Avril, 2020

Membres du jury d'évaluation
Pr Raymund J. Wellinger, Département de Microbiologie et d'Infectologie Pr Benoit Chabot, Département de Microbiologie et d'Infectologie
Pr François Bachand, Département de Biochimie

Résumé

Studying the beginning of the end: The roles of Tbf1 and Reb1 at subtelomeres

Par Alexandra Krallis
Programme de Microbiologie

Mémoire présenté à la Faculté de médecine et des sciences de la santé en vue de l'obtention du diplôme de maitre en sciences (M. Sc.) en Microbiologie, Faculté de Médecine et des Sciences de la Santé, Université de Sherbrooke, Sherbrooke, Québec, Canada, J1H 5N4

Les séquences télomèriques chez *S. cerevisiae* recrutent une multitude de protéines afin de remplir ses fonctions essentielles pour le maintien de l'integrité genomique : la réplication complète des chromosomes et la protection des mécanismes de réparation de l'ADN. Cependant, il y a des indices que les régions sous-télomèriques, qui se trouvent directement à l'intérieur des répétitions télomèriques, peuvent aussi affecter les fonctions des extrémités chromosomiques. Deux des principales protéines recrutées aux sous-télomères sont Tbf1 et Reb1. Bien qu'elles se lient aux régions promotrices d'une multitude de gènes, leurs fonctions aux extrémités chromosomiques ne sont pas encore comprises.

Des études précédentes suggèrent que Tbf1 et Reb1 pourraient jouer un rôle dans le maintien de la longueur des télomères et en empêcher la propagation de répression transcriptionnel des gènes près des télomères. Comme beaucoup de ces études ont été réalisées en l'absence de régions sous-télomèriques ou avec des allèles mutants, on ne sait pas si les phénotypes observés proviennent de changements dans les régions sous-télomèriques ou des altérations de la transcription des cibles Tbf1 ou Reb1. Afin d'éviter ces complications, un système a été conçu pour étudier les effets de l'absence de Tbf1 et Reb1 des sous- télomères avec des structures naturelles.

L'utilisation de ce système a permis de découvrir que, Tbf1 et Reb1 ne sont pas très importantes pour le maintien de la longueur des télomères ou pour limiter la propagation de répression transcriptionnel. Cependant, il a été observé que Tbf1 et Reb1 ont un rôle dans la répression de TERRA, un ARN long non codant transcrit à partir des régions sous-télomèriques. Récemment, il a été suggéré que TERRA pourrait jouer un rôle dans le maintien des télomères. Toutefois, il est crucial de limiter la transcription du télomère, car elle pourrait mener à une cassure de l'ADN et l'instabilité génomique. Cette étude souligne l'importance de travailler avec des régions sous-télomèriques non-modifiées ou modifiées en étudiant les télomères et offre un nouvel aperçu de la régulation de TERRA.

Mots-clés : Tbf1, Reb1, télomère, transcription, TERRA

Summary

Telomeres protect the ends of linear chromosomes from being recognized as DNA breaks, helping to avoid events that could lead to genomic instability. The telomeric sequences in budding yeast recruit a multitude of proteins in order to carry out essential functions in end replication and protection from DNA repair machinery. However, there is evidence that subtelomeres, which lie directly interior to the telomeric repeats, may also affect the properties of the chromosomal ends. Two of the main proteins recruited to the subtelomeres are Tbf1 and Reb1. While they bind at promoter regions of a multitude of genes, their function at the chromosomal ends is still unclear.

TBF1 and *REB1* are both essential genes, with some overlapping targets and functions in fine tuning transcription and creating nucleosome free regions. Past work suggests both Tbf1 and Reb1 could have roles in telomere length maintenance and limiting the spread of telomere silencing. As many of these studies were done in the absence of subtelomeric regions, or with mutant alleles, it is unclear if the telomere phenotypes observed stem from changes in the subtelomere regions or from alterations in transcription of Tbf1 or Reb1 targets. This is evidenced by different studies producing conflicting evidence pertaining to the functions of these proteins. In order to avoid such complications, a system was designed to study the effects of the absence of Tbf1 and Reb1 at subtelomeres with otherwise native structures.

Through the use of this system, it was found that Tbf1 and Reb1 may not be very important for telomere length maintenance or limiting the spread of telomere silencing. However, it was discovered that Tbf1 and Reb1 have a role in repressing TERRA, a long non-coding RNA transcribed from the subtelomere and telomeric repeats. Recent work suggests TERRA may have a role in telomere maintenance in the absence of telomerase. However, limiting transcription of the telomere is crucial, as it could lead to replication fork stalling, DNA breaks and genomic instability. This study underlines the importance of working with natural subtelomere regions when studying telomeres and offers a new insight into TERRA regulation.

Keywords: Tbf1, Reb1, telomere, transcription, TERRA

Table of Contents

List of Figures

List of Tables

Acknowledgements

I would like to first thank my research director, Professor Raymund Wellinger, for welcoming me into his laboratory first as an intern and again as a masters student. I truly appreciate the enjoyable and friendly environment in the Wellinger Lab and would like to thank all Lab members, as well as Pr. Wellinger for their support, encouragement and positivity. I would like to especially thank Emeline Pasquier for mentoring me during my internship and continuing to offer so much invaluable advice and help and throughout my experience in the lab. I would also like to thank Erin Bonnell for the strains provided, as well as her support and advice on all things Tbf1. Finally, I would like to thank Pr. François Bachand and Pr. Benoit Chabot for agreeing to be part of my jury committee.

List of Abbreviations

Δ: delta, identifies a deletion
°C: degrees Celsius µg: microgram
µl: microliter µM: micromolar
3’: 3’ extremity of a nucleotide, free OH group on the 3’ carbon of ribose ring
5’: 5’ extremity of a nucleotide, free OH group or phosphate ester on 5’ carbon of ribose ring
5-FOA: 5-Fluoroorotic acid
A: adenosine
ALT: alternative lengthening of telomeres
ARS: Autonomously replicating sequence
b: base(s)
bp: base pair(s)
BIR: Break-induced replication
BSA: bovine serum albumin
C: cytosine
ChIP: Chromatin Immunoprecipitation
ChIP-seq: Chromatin Immunoprecipitation-sequencing
CRAC: Cross-linking and analysis of cDNA sequencing
C-terminal: carboxy-terminal
dCTP: deoxycytidine triphosphate
dGTP: deoxyguanosine triphosphate
DNA: Deoxyribonucleic acid
DSB: Double-strand break
dsDNA: double-stranded DNA
dNTP: deoxynucleoside triphosphate
DTT: Dithiothreitol
ECL: Electrochemiluminescence or electro generated chemiluminescence
EDTA: Ethylenediaminetetraacetic acid
G: guanosine
GBD: Gal4 binding domain
GRF: General regulatory factor
HEPES: 4-(2-hydroxyethyl)-1-piperazineethanesulfonic acid
HO: Homothallic switching endonuclease
HR: Homologous recombination
HDR: Homology directed repair
HTF: 6xHis-TEV-3xFlag
ITS: interstitial telomeric repeat sequence
IGR: Intergenic region
IgG: Immunoglobulin G
IP: Immunoprecipitation
kb: kilobase
kDa: kiloDalton

LB: Luria Broth medium
M: molar
m/v: mass per volume
NEB: New England Biolabs
NDR: Nucleosome depleted region
NHEJ: Non-Homologous End-Joining
nM: nanomolar
NS: non-specific
nt: nucleotide
N-terminal: amino terminal
ORC: Origin Recognition Complex
ORF: Open Reading Frame
PBS: phosphate-buffered saline
PBS-T: phosphate-buffered saline with 0.1% Tween-20
PCR: Polymerase Chain Reaction
pH: measure of acidity or basicity of a solution
PMSF: phenylmethylsulfonyl fluoride
RNase: Ribonuclease
RS: sequence recognized by Recombinase R
SDS: sodium dodecyl sulfate
SDS-PAGE: SDS-Polyacrylamide Gel Electrophoresis
snoRNA: small nucleolar RNA
SPP: Service de Purification de Protéines at Université de Sherbrooke
SSC: Saline sodium citrate
ssDNA: single-stranded DNA
STARs: SubTelomeric Anti-silencing Regions
STEX: Single Telomere Extension assay
STR: Subtelomeric repeated elements
T: Thymidine
T_x: Time point X (T_1 = Time point 1)
TAE: 40 mM Tris, 20 mM glacial acetic acid, 1 mM EDTA pH 8.0
TAP: Tandem Affinity Purification
Taq: DNA polymerase from *Thermophilus aquaticus*
TBE: 40 mM Tris, 20 mM borate, 1 mM EDTA pH 8.0
TCA: Trichloroacetic acid
TEL01Lmod: modified TEL01L telomere
TEL03Lmod: modified TEL03L telomere
$TEL07L^{tr}$: truncated TEL07L telomere, lacking subtelomere
Teloblots: Southern blots measuring telomere length
TERRA: Telomeric repeat containing RNA
TEV: Tobacco etch virus protease
TdT: Terminal deoxynucleotidyl Transferase
TN150: 50 mM Tris-HCl pH 7.8, 150 mM NaCl, 0.1% NP-40
TN1000: 50 mM Tris-HCl pH 7.8, 1 M NaCl, 0.1 % NP-40

TPE: Telomere Position Effect
TRF: Terminal Restriction Fragment
ts: temperature sensitive
UAS: Upstream activation sequence
UTR: Untranslated region
WCE: whole cell extract
XCR: X-element combinatorial repeats
XCRmut: XCR containing point mutations in Tbf1 and Reb1 binding sites
v/v: volume per volume
V: Volt
YC: Yeast Complete synthetic media
YEPD: Yeast Extract Peptone Dextrose complete medium

Introduction

Telomeres

Eukaryotic genomes are arranged into multiple linear chromosomes beginning and ending with structures protecting them, named telomeres. These structures were first characterized by Herman Muller and Barbara McClintock (1939, 1941), who each noted that broken chromosomal ends were highly unstable and prone to fusion, while native chromosomal ends were resistant to chromosome fusion (McClintock, 1941; McClintock, 1939; Muller, 1938). The structures at the chromosomal ends were named by Herman Muller (1938) after the Greek “telos” (end) “meros” (part) and are known to be essential for the maintenance of genome stability due to their ability to inhibit chromosome-chromosome fusions.

The structure of telomeres is conserved throughout eukaryotes, while the exact sequence varies across species. Telomeric DNA is comprised of non-coding G-rich repeat sequences, with a double stranded portion and 3’ single stranded overhang (Larrivée et al., 2004; McElligott and Wellinger, 1997; Wellinger et al., 1993). The lengths of double and single stranded sections vary across different species. The telomeres carry out their main function, maintenance of genome stability, by recruiting various protein complexes. For example, in human cells, the TTAGGG (T_2AG_3) telomeric repeats (de Lange et al., 1990) form 5-15 kilobases (kb) of double stranded DNA and a 50-300 nucleotide (nt) 3’ single stranded overhang (McElligott and Wellinger, 1997). The T_2AG_3 sequence is conserved in all mammalian species, while the length of double strand and single strand sections of the telomeres can vary. This telomeric DNA associates with the shelterin complex, consisting of 6 protein subunits (Chen, 2019; De Lange, 2005). The shelterin complex specifically binds telomeres by proteins TRF1, TRF2 and POT1, which directly bind DNA in a sequence specific manner. TRF1 and TRF2 bind double stranded T_2AG_3 repeats through their two SANT/Myb type DNA binding domains, while POT1 binds the single stranded portion (Chen, 2019). Proteins Rap1, TIN2 and TPP1 bind and interconnect the DNA binding

proteins. Association with the shelterin complex remodels the telomeric DNA and recruits additional proteins to facilitate telomeric functions, such as inhibiting DNA repair mechanisms and maintaining telomere length homeostasis (Chen, 2019).

Telomeres of S. *cerevisiae* (budding yeast), are structured similarly, although they do not interact with an analogous set of proteins. Telomeric DNA consists of 300 $\pm$ 75 bp of double standed DNA with a $TG_{1\text{-}3}$ degenerate repeat sequence (Wellinger and Zakian, 2012). The 3'-single stranded overhang is also G-rich, with the same $TG_{1\text{-}3}$ repeats and is 12-15 nt long (Larrivée et al., 2004). Like the human telomere, budding yeast telomeres are bound by several protein factors. Although the proteins themselves vary, they too associate with telomeric DNA to allow the telomeres to carry out essential telomeric functions (Wellinger and Zakian, 2012). The yeast telomere and its binding factors are represented in Figure 1. Double stranded yeast telomeric DNA is covered with Rap1, an ortholog to human Rap1 (Li et al., 2000; Wellinger and Zakian, 2012). While the hRap1 does not directly bind DNA, scRap1 binds telomeric DNA via its double myb domain and recruits Sir3/Sir4 and Rif1/Rif2 (Buck and Shore, 1995; Graham et al., 1999; Hardy et al., 1992; Moretti and Shore, 2001; Moretti et al., 1994; Wotton and Shore, 1997). The Sir proteins form a complex involved in repressing transcription at the chromosomal ends and also interact with other proteins important for telomeric functions. In addition to this, Sir4 is involved in tethering the telomeres to the nuclear envelope, where they form foci in the G1-S-phase (Andrulis et al., 2002; Bupp et al., 2007; Taddei et al., 2004). Proteins Rif1 and Rif2 are important for telomere length homeostasis (Wellinger and Zakian, 2012).

As in human telomeres, the 3' single strand overhang is bound by a protein that recognizes single stranded DNA. Cdc13 binds single stranded $TG_{1\text{-}3}$ repeats and interacts with different proteins, depending on the cell cycle phase (Mersaoui and Wellinger, 2018). Cdc13 is involved in a variety of functions such as telomere elongation, telomere replication and chromosomal capping, by interacting with various proteins at different stages of the cell cycle (Mersaoui and Wellinger, 2018; Wellinger and Zakian, 2012). Telomeres are also bound by yKu70 and yKu80 proteins, which form a ring shaped yKu complex. The complex can either directly bind DNA or be recruited through interactions

between yKu80 and Sir4 (Gravel et al., 1998; Larcher et al., 2016; Roy et al., 2004). The yKu complex plays a role in chromosomal end capping, repression of transcription near telomeres, clustering telomeres near the nuclear envelope and telomere length maintenance (Boulton and Jackson, 1998; Fisher et al., 2004; Gallardo et al., 2011; Laroche et al., 1998; Polotnianka et al., 1998). However, it also has roles in DNA repair at double stranded breaks within the genome (Fell and Schild-Poulter, 2015). Many of the proteins involved in telomere functions also have roles in transcription or DNA repair pathways when bound at other genomic loci, some of which will be discussed below (Wellinger and Zakian, 2012).

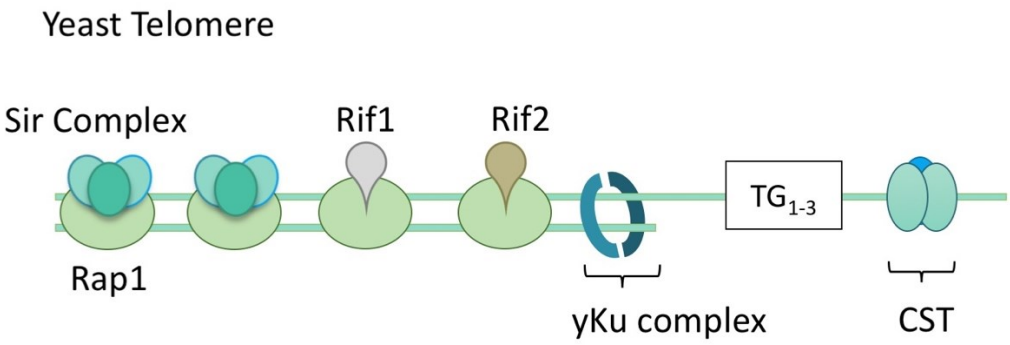

Figure 1: Schema of the telomere nucleoprotein structure in S. cerevisiae
Double stranded DNA is bound by Rap1, which recruits proteins Sir2/3/4 to form the Sir complex. Rap1 also recruits Rif1 and Rif2 to negatively regulate telomere elongation. The yKu complex is formed by proteins yKu70 and yKu80 and binds at the double strand/single strand junction to function in end capping. The CST complex, a complex containing Cdc13, Stn1 and Ten1, binds to single stranded TG_{1-3} repeats.

Essential functions of telomeres: chromosome capping

As Muller (1938) and McClintock (1939) described in their experiments observing stable chromosome ends, the telomeres prevent fusion between chromosomes, which is essential for genome stability in a healthy cell. When DNA breaks occur within a chromosome, the cell must repair it through DNA repair mechanisms such as non-homologous end joining (NHEJ) or homologous recombination (HR). Recognition of

the telomeres as double stranded breaks would lead to the fusion of chromosomes by DNA repair mechanisms and create dicentric chromosomes. This process is propagated in daughter cells in a cycle called the breakage-fusion-bridge cycle and results in gross genomic instability (McClintock, 1939). NHEJ is particularly hazardous for unprotected chromosomal ends, as this DNA repair mechanism recognizes double stranded breaks and joins the DNA together, regardless of sequence. To prevent these events, the telomere nucleoprotein structures protect the chromosomal ends from recognition by DNA repair machinery as a double stranded break. This function is called chromosome capping (Garvik et al., 1995; Wellinger and Zakian, 2012).

There are multiple proteins contributing to the capping functions of telomeres, however, many of these proteins have additional telomeric and non-telomeric functions. As is represented in Figure 1, Rap1 binds double stranded $TG_{1\text{-}3}$ repeats (Conrad et al., 1990; Gilson et al., 1993). In addition to Rap1 contributing to telomere capping by limiting resection of the C-rich strand, it recruits Rif2 and Sir4 proteins, which decrease chromosomal fusion by 2 different pathways (Marcand et al., 2008; Vodenicharov et al., 2010). Rif2 is thought to inhibit telomere-telomere fusion by inhibiting the MRX complex required for NHEJ from functioning. Sir4 contributes to decreasing telomere-telomere fusion, possibly through interactions with yKu80. The yKu complex is a protein with functions at non-telomeric loci (Downs and Jackson, 2004). yKu facilitates NHEJ repair of double stranded breaks by binding to DNA at the breaks in a sequence independent manner and preventing MRX dependent 5' end resection (Bonetti et al., 2010). When binding telomeres, for example after replication fork collapses, the yKu complex is implicated in telomere capping by inhibiting 5'-end resection (Gravel et al., 1998; Larcher et al., 2016; Vodenicharov et al., 2010). The single stranded telomeric repeats are bound by Cdc13, which carries out its protective functions by recruiting essential proteins Stn1 and Ten1 to form the CST complex (Wellinger and Zakian, 2012). This complex protects the telomere from C-strand degradation and subsequent activation of DNA damage checkpoints (Garvik et al., 1995). The additional functions of Cdc13 in end-replication and telomere elongation events will be discussed below.

Essential functions of telomeres: chromosome end replication

In addition to linear chromosomes being vulnerable to degradation and chromosomal fusion, they also present a problem for conventional DNA replication machinery. Each round of DNA replication causes a slight loss of terminal sequences at one end of each chromosome, represented in Fig. 2 (Olovnikov, 1973; Soudet et al., 2014). Replication of the leading and lagging strands at the ends of the chromosomes produces two different types of DNA ends (Lingner et al., 1995). The lagging strand is replicated *via* short Okazaki fragments, using the G-rich strand as a template. The degradation of the last short RNA primer after DNA replication results in the 3' single stranded overhang required for the functional telomere structure and does not result in a loss of terminal sequences (Soudet et al., 2014). Replication of the leading strand in the 5' to 3' direction uses the C-rich strand as a template and continues until the end of the template (Olovnikov, 1973). The loss of terminal sequence occurs upon generation of the 3' single stranded overhang. The newly replicated 5' strand is resected in the 5' to 3' direction by an exonuclease and then filled in, leaving a 3' overhang of 12-15 bp (Soudet et al., 2014). Thus, the newly synthesized G-rich leading strand is now 12-15 bp shorter than the original G-rich lagging strand.

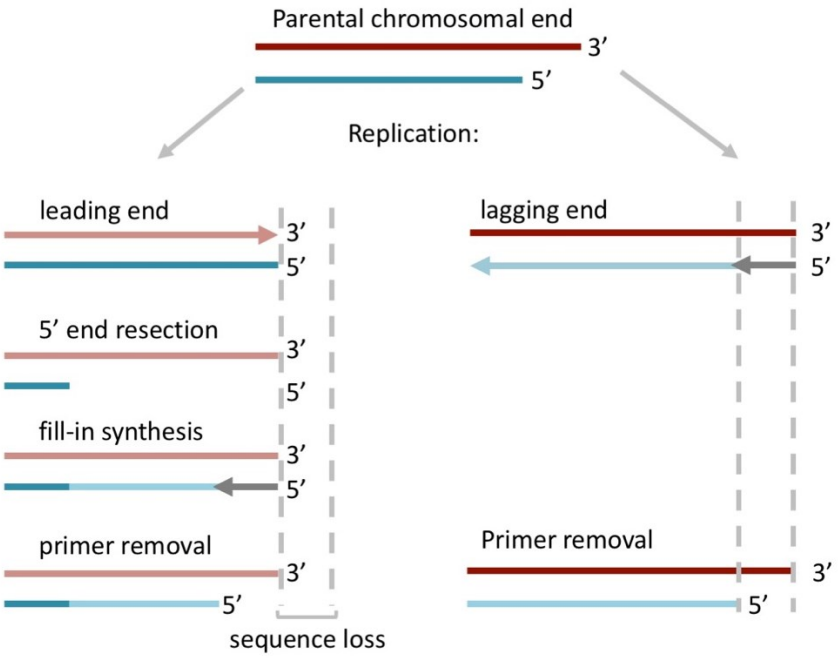

Figure 2: End-replication problem.
Parental 5′ and 3′ strands are indicated in dark blue and dark red respectively. Daughter 5′ and 3′ strands are indicated in light blue and dark blue strands. After replication of the leading 5′ end, the 5′ strand is resected and subsequently filled in (light blue). RNA primers are shown by grey arrow. Sequence loss after replication of 5′ strand is indicated by dashed grey lines.

As the telomeres are made of non-coding sequences, the gradual loss of DNA does not lead to a loss of coding genetic material. However, telomeric proteins involved in capping require certain lengths of telomeric sequences in order to bind effectively and carry out capping functions. Thus, human cells have a limit of cell divisions (Hayflick Limit) due to the progressive shortening of telomeric sequences that comes with DNA replication and cell division (Hayflick and Moorhead, 1961; Lundblad and Szostak, 1989). After somatic cells have reached this limit, they enter a G_0 state and do not replicate further. This also serves to limit the accumulation of mutations, which could eventually lead to genetic instability and cancer. However, mammalian germ and stem cells, as well as yeast cells, have unlimited dividing potential. This is due to the presence of a reverse transcriptase called telomerase, which is able to counteract the progressive shortening of chromosomal ends by elongating telomeric sequences (Greider and Blackburn, 1985, 1987; Morin, 1989).

Telomerase consists of an RNA scaffold that also encompasses a template for telomeric sequences, a catalytic protein subunit and several other proteins essential for *in vivo* function. In S. *cerevisiae*, the RNA moiety of the ribonucleoprotein, called TLC1, is a long non-coding RNA that possesses multiple distinct elements represented in Figure 3 (Singer and Gottschling, 1994). Near the 17 nt template region at the center of the RNA is a template boundary element and a pseudo-knot structure (Dandjinou et al., 2004). The RNA is folded into 3 stem loops such that the 3' end is in proximity with the 5' end. The catalytic subunit, Est2 (ever shorter telomere), binds to the central area containing the template for elongation of the G-rich 3' overhang (Chappell and Lundblad, 2004; Livengood et al., 2002). The Est1 accessory protein binds to a bulge on the third stem loop, with the Est3 protein bridging Est1 and Est2 (Seto et al., 2002; Tucey and Lundblad, 2014). These proteins are all named for their "ever shorter telomere" phenotype, as their deletion causes progressive telomere shortening, eventually leading to genomic instability and cell death (Lendvay et al., 1996; Lundblad and Szostak, 1989). Proteins Pop1, Pop6 and Pop7 are thought to stabilize the complex by binding the same bulge as Est1, potentially interacting with Est1 and Est2 (Lemieux et al., 2016; Laterreur et al., 2018). The 3' end of the RNA is bound by the Sm_7 complex, which also contributes to the stability of the molecule (Seto et al., 1999). In order to import and retain the telomerase molecule in the nucleus, the yKU complex binds a 48 nt stem loop called the yKu binding stem (Gallardo et al., 2008; Seto et al., 1999; Stellwagen et al., 2003).

Telomerase is only recruited to specifically short telomeres in the late S phase of the cell cycle (Teixeira et al., 2004). At long telomeres, more Rap1 is associated to the double stranded $TG_{1\text{-}3}$ repeats, recruiting Rif1 and Rif2. Rif2 inhibits 5' to 3' end resection by the MRX complex (Marcand et al., 2008). This limits the amount of 3' single stranded overhang available for telomerase to associate with, thus limiting telomere elongation by telomerase. At short telomeres, less Rap1 is present, as there are less double stranded $TG_{1\text{-}3}$ repeats, leading to a decreased presence of Rif2 (Levy and Blackburn, 2004; Marcand et al., 1997). This allows MRX to be activated by the Tel1 kinase, leading to resection of the C-rich strand (Goudsouzian et al., 2006; Martina et al., 2012). The

3’ single strand overhang produced then binds Cdc13, which, at this stage in the cell cycle, is not associated with Stn1 and Ten1, but recruits telomerase to the telomere *via* interactions with Est1 (Chen, 2019; Evans and Lundblad, 1999; Wu and Zakian, 2011). The 3’ single stranded overhang is elongated. In the G2 phase, Cdc13 begins to associate with Stn1 and Ten1 to form the CST complex and recruit DNA polymerase α to fill in the telomeric C- strand, completing telomere elongation (Chandra et al., 2001; Grossi et al., 2004; Mersaoui and Wellinger, 2018).

In the absence of telomere elongation by telomerase, telomeres will gradually shorten, and cells will enter a permanent cell cycle arrest and senesce (Lundblad and Szostak, 1989; Singer and Gottschling, 1994). The same can happen due to the presence of a single, critically short telomere when it is unable to be repaired by telomerase (Abdallah et al., 2009; Hackett et al., 2001; Khadaroo et al., 2009). However, a certain subset of these cells can evade replicative senescence and regain replicative capacities (Lundblad and Blackburn, 1993; Teng and Zakian, 1999). These so-called “survivors” maintain their telomere length by break induced replication (BIR), a form of homologous recombination (Kass- Eisler and Greider, 2000; Lundblad and Szostak, 1989). BIR occurs at collapsed replication forks, eroded, uncapped telomeres and is also recruited at RNA-DNA hybrids called R- loops (Balk et al., 2013; Lydeard et al., 2007). This alternative form of telomere maintenance can cause two different DNA arrangements at the chromosomal ends, causing cells to be classified as type I and type II survivors (Lundblad and Blackburn, 1993; Teng and Zakian, 1999). Type I survivors are characterized by an amplification of Y’ elements and only short tracts of double stranded $TG_{1\text{-}3}$ repeats. The formation of a type I survivor requires *RAD52, RAD51, RAD54, RAD55* and *RAD57* (Larrivée and Wellinger, 2006; Lundblad and Blackburn, 1993). Type II survivors have only a slight amplification of the Y’ elements, but have an extremely variable extension of $TG_{1\text{-}3}$ repeats, some arriving to be over 12 kb in length (Teng and Zakian, 1999; Teng et al., 2000). The process to form type II survivors requires the MRX complex, *TEL1*, *SGS1* and *RAD59*. While type I survivors often form first in a population, they grow slowly and are frequently outcompeted by type II survivors in liquid cultures (Lundblad and Blackburn, 1993; Teng et al., 2000).

Subtelomeres

The length of telomeres in S. *cerevisiae* can sometimes vary by approximately 150 bp from telomere to telomere. Even in humans, some chromosomes have been noted to have consistently longer or shorter tracts of telomeric repeats (Martens et al., 1998). This could be influenced by the subtelomeric regions, which vary across chromosomal ends (Gilson and Londoño-Vallejo, 2007). In S. *cerevisiae*, telomeres can be divided into two classes, depending on their subtelomeric areas (Figure 3). XY' telomeres posess both X and Y' subtelomeric elements, while X-only telomeres only have X-elements. Y'elements are present at approximately half of the chromosomal ends in 1-4 copies and exist in two forms; Y' short (5.2 kb) and Y' long (6.7 kb) (Chan et al., 1983; Chan and Tye, 1983). These elements are homogenous in sequence, only differing from each other in some insertions and deletions and undergo frequent mitotic recombination (Horowitz et al., 1984; Louis and Haber, 1992). Furthermore, Y'elements contain nucleosomes and are transcriptionally active, although many contain dubious or uncharacterized ORFs (Mak et al., 2009; Zhu and Gustafsson, 2009). At XY' telomeres, the Y' element is bordering the telomeric repeats, with the X-element on the centromere proximal side of the Y' element (Figure 3).

X-elements are distinct from the Y' elements in that they are present at every chromosomal end and are more heterogenous in size and sequence. In contrast to the Y' elements, they have been reported to lack nucleosomes, but appear in a heterochromatic structure similar to telomeric repeats (Takahashi et al., 2011; Zhu and Gustafsson, 2009). The X-Core is a relatively homogenous sequence of approximately 475 bp, comprises an autonomously replicating sequence (ARS) and is present in all X-elements. Most X-elements also have XCR (X-element combinatorial repeats) sequences, made of different combinations of four subtelomeric repeated elements (STR- A, STR-B, STR-C, STR-D). The sequences of the individual STRs are quite conserved in telomeres of the same strains (Louis et al., 1994). STR-A contains at least one TTAGGG sequence, along with several degenerate copies. STR-B, STR-C and STR-D are conserved in length, with STR-C containing a TG_{1-3}-like sequence TGGTGGT (Louis et al., 1994). STRs A-C all contain a

G-rich strand. Although each of these elements are individually more conserved than the X-Core sequence, they are combined differently amongst the individual X-elements, such that the XCR regions are variable in sequence and in length. Thus, X-elements range from 0.5-4 kb in length. X-only telomeres have the XCR sequence directly bordering telomeric repeats, with the X-Core sequence on the centromere proximal side of the XCR (Figure 3). In XY' telomeres, the X-element is separated from the telomeric repeats by the Y' element. Some subtelomeres contain telomeric sequences between X and Y' or Y' and Y' junctions (Walmsley et al., 1984). These are called interstitial telomeric repeat sequences (ITS).

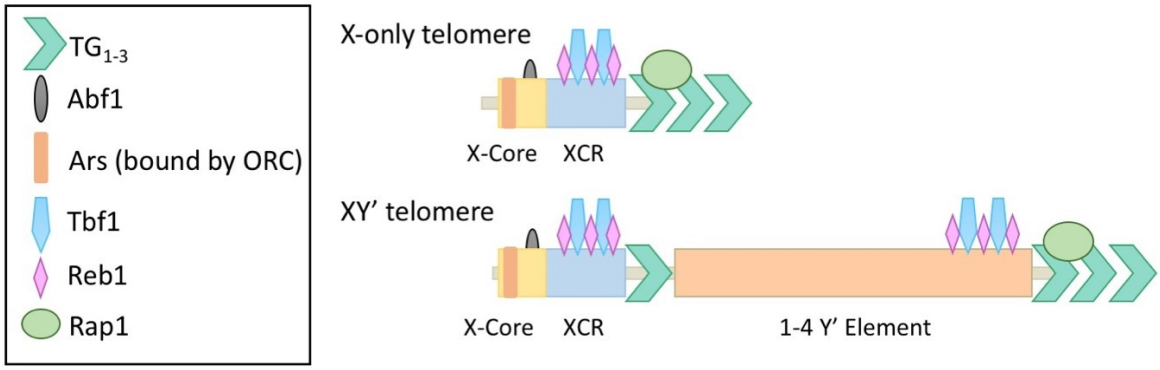

Figure 3: Subtelomeric sequences and binding proteins.
The X-Core is approximately 475 bp long, is present at all chromosomal ends and has an ARS, bound by the Orc complex and Abf1 binding site. 15 of the 16 chromosomal ends contain the XCR, which contains binding motifs for Tbf1 and Reb1. 1-4 Y' elements are present at approximately 50% of telomeres and exist in sizes of either 5.2 kb 6.7 kb. Y' elements also contain binding sites for Tbf1 and Reb1 at the telomere proximal end. X-Y' element junctions sometimes contain telomeric repeats, called interstitial telomeric repeat sequences (ITS).

One manner in which the subtelomeric sequences could influence the properties of the downstream telomeres is by recruiting different proteins in a sequence specific manner. The X-Core sequence, containing an ACS, can recruit ORC (origin recognition complex) and the Abf1 transcription factor, both of which influence chromatin silencing when bound at *HM* loci (Diffley and Stillman, 1989; Kurtz and Shore, 1991). Most telomeres also recruit essential proteins Tbf1 and Reb1 (Koering et al., 2000). Both proteins have roles in transcriptional regulation when bound at other genomic loci and

have similar binding motifs at subtelomeres (Bosio et al., 2017; Koering et al., 2000; Liu and Tye, 1991). The subtelomeric proteins Abf1, Tbf1, Reb1, as well as the telomere repeat binding protein Rap1, are a group of general regulatory factors (GRFs), as they bind at a multitude of promoters throughout the genome and have various functions in transcriptional regulation at their targets (Bosio et al., 2017; Fourel et al., 2002; Koering et al., 2000). X-only telomeres contain Tbf1 and Reb1 consensus sequences in the XCR and one Reb1 binding site in the X-Core (Koering et al., 2000). The telomere of the right arm of chromosome VI (TEL06R), is the only exception, as the X-element of this telomere comprises only the X-Core sequence. XY' telomeres can recruit Tbf1 and Reb1 *via* the X-element and Y' element. Binding sequences for Tbf1 and Reb1 are located in the telomere proximal portion of Y' elements, such that both XY' and X-only telomeres have a cluster of Tbf1 and Reb1 at the telomere-subtelomere junction (Koering et al., 2000). The number of binding sites for these proteins can differ from subtelomere to subtelomere and may introduce differences in their individual properties. In addition to this, multiple transcription factors can bind to different subtelomeric areas in a variety of stress conditions, which could also influence telomeric behaviour (Mak et al., 2009).

Telomeric properties: Telomere Position Effect

The proteins recruited to the telomere repeats give the DNA in these areas' unique properties. One of these properties is the telomere position effect (TPE), which describes the transcriptional silencing of DNA interior to the telomeric repeats (Gottschling et al., 1990). This was initially thought to be directly dependent only on the Sir proteins and on the yKu complex (Boulton and Jackson, 1998). Rap1 recruits Sir3 and Sir4 to the telomere, followed by the recruitment of Sir2, a histone deacetylase, by Sir4 (Moretti and Shore, 2001; Moretti et al., 1994). yKu is also able to recruit Sir2 via its interactions with Sir4 (Tsukamoto et al., 1997). The deacetylation of histone tails by Sir2 is propagated far from the telomeric repeats due to Sir3 and Sir4 interactions with histones H3 and H4 (Hecht et

al., 1995; Strahl-Bolsinger et al., 1997). TPE was discovered by inserting a *URA3* gene adjacent to a truncated telomere TEL07L^{tr} (URA-tel), lacking its subtelomeric sequence (Gottschling et al., 1990). Although cells expressing the *URA3* gene are normally dead in the presence of 5-fluorotic acid (FOA), some cells with the URA-tel construct were resistant to FOA. This phenomenon was observed with various additional genes when localized near telomeric repeats (Gottschling et al., 1990).

It was initially proposed that TPE gradually diminished with increasing distance from the telomeric repeats (Renauld et al., 1993). However, at natural telomeres possessing wild type X and Y' elements there are large telomere dependent variations in TPE and its continuity, with some telomeres not exhibiting TPE at all (Pryde and Louis, 1999). This is thought to be due to different transcription factors binding to different subtelomeric areas and acting as boundary elements, inhibiting TPE spread, or contributing to increased silencing (Fourel et al., 1999; Mak et al., 2009). The X-elements were found to have TPE increasing properties in the ACS of the X-Core, while sequences of the XCR were coined subtelomeric anti-silencing regions (STARs) (Fourel et al., 2001; Power et al., 2011). The discontinuity of TPE spreading was also observed in levels of the Sir proteins near telomeres (Ellahi et al., 2015; Zill et al., 2010). Sir proteins are found at telomeric repeats and spanning the X-elements, with the highest enrichments at the X-Core, potentially recruited by the ORC complex and Abf1 that bind there (Ellahi et al., 2015). However spreading and gradual dissipation was not observed. Although transcription levels of genes within a distance of 20 kb were low, these areas are not transcriptionally silent (Ellahi et al., 2015; Wyrick et al., 1999). Furthermore, Sir proteins contribute to silencing of only 20 genes, most of which are located close to the telomere. (Wyrick et al., 1999). Thus, TPE may not be exclusively mediated by Sir proteins, as initially proposed. However, there seem to be other mechanisms in place to decrease transcription near chromosome ends, as evidenced by low transcription levels in these areas. For example, histone deacetylase I (HdaI), is responsible for repressing approximately 40 % of genes 10-25 kb from telomeres (Mak et al., 2009; Robyr et al., 2002). Silencing at chromosomal ends could be important for the repression of these

genes, as many of them are related to stress responses. In support of this idea, subtelomeres have been found to recruit various transcription factors in different stress conditions (Mak et al., 2009).

Telomeric Properties: Telomeric repeat containing RNA

The telomeres of many eukaryotes are transcribed into long non-coding RNAs called telomeric repeat containing RNA (TERRA) (Azzalin et al., 2007; Feuerhahn et al., 2010). In mammalian cells, TERRA was found to be involved in the regulation of telomerase, cellular differentiation and heterochromatinization of telomeres (Wang et al., 2015). In budding yeast, TERRA may also have a role in regulating telomere length (Cusanelli and Chartrand, 2014). The transcription start site of TERRA has been mapped to the X-Core of telomere 1L and telomere proximal ends of some Y' elements (Pfeiffer and Lingner, 2012). Thus, each TERRA RNA comprises sequences specific to the telomere it is transcribed from, as well as a G-rich sequence transcribed from telomeric repeats. TERRA is transcribed by RNA polymerase II to produce transcripts ranging in 100-1200 nt in length, some of which are poly-adenylated by poly(A) polymerase Pap1 (Luke et al., 2008). TERRA levels in yeast are extremely low, which is partially due to the degradation of these molecules by the Rat1 5' to 3' exonuclease (Luke et al., 2008). TERRA is also regulated on a transcriptional level *via* different pathways, depending on what telomere is being transcribed (Iglesias et al., 2011). Rap1 binds telomeric repeats and recruits Rif1/2 and Sir2/3/4 proteins, which have been found to regulate TERRA transcription. The deletion of any Sir proteins strongly derepresses TERRA transcription at X-only telomeres, but does not affect the transcription of XY' telomeres. This is in accordance with findings indicating that Sir proteins are largely not localized in Y' elements and would thus not be regulating transcription of these areas (Zhu and Gustafsson, 2009). Rif1 and, to a lesser extent, Rif2 contribute to transcriptional repression at all telomeres (Iglesias et al., 2011).

Multiple experiments have indicated that TERRA could be somehow involved in

regulating telomere length. Using a short inducible telomere, it was shown that TERRA transcription is increased upon telomere shortening and that the levels of TERRA from this telomere decrease gradually as the telomere is elongated by telomerase (Cusanelli et al., 2013). By observing TERRA through live-cell imaging, it was found that TERRA forms foci along the nuclear periphery. Some of these foci colocalized with previously observed telomerase clusters (T-Recs). In addition, TERRA was found to associate with its telomere of origin in a manner dependent on Mre11, Tel1 and yKu70, which are factors also involved in telomerase recruitment. These observations suggest that TERRA transcribed from a short telomere recruits clusters of telomerase specifically for the elongation of the short telomere of origin. However, it was also observed that TERRA transcription may cause telomere shortening *in cis,* by impeding with the yKu complex's function in blocking Exo1 resection activity at telomeres (Pfeiffer and Lingner, 2012).

As TERRA transcription is generally increased in telomerase negative (*tlc1Δ*) cells (Cusanelli et al., 2013), it has been proposed by multiple groups that TERRA transcription plays a role in maintaining telomeres through recombination pathways. In humans, increased TERRA levels have been identified as one of the hallmarks of ALT (alternative lengthening of telomeres) cells, in which telomeres are maintained by homologous recombination pathways in the absence of telomerase (Cesare and Reddel, 2010; Episkopou et al., 2014; Schoeftner and Blasco, 2008). This has recently been observed in yeast as well (Graf et al., 2017; Misino et al., 2018). It was found that an increase of TERRA can delay senescence by aiding in the formation of type II survivors. In telomerase negative yeast cells, telomeres are most likely maintained by break induced replication (BIR), which is triggered by the increased formation of DNA-RNA hybrids called R-loops (Balk et al., 2013; Lydeard et al., 2007). It was observed that TERRA forms such R-loops at the telomere it is transcribed from, by base pairing with subtelomeric and telomeric sequences (Graf et al., 2017). Degradation of "free" TERRA, not in R-loops, is mediated by Rat1 around the time of replication. An increase in TERRA and R-loops was observed in telomerase negative cells, particularly at critically short telomeres. The accumulation of TERRA originating specifically from short telomeres was attributed to a decrease in Rat1

mediated degradation, but not an increase in transcription, at these telomeres (Graf et al., 2017). Degradation of R-loops is mediated by RnaseH1 and RNaseH2, which are recruited by Rif2 (Graf et al., 2017; Misino et al., 2018). The increase in R-loops correlates with increased HDR events to elongate telomeres and delay senescence (Balk et al., 2013; Graf et al., 2017). HDR is presumably promoted by the DNA damage response due to the accumulation of Rad51 observed at very short telomeres with increased R-loops (Graf et al., 2017). Supporting this, the overexpression of RNase H1 and subsequent increase in R-loop degradation were found to slow the growth rates of type II survivors (Misino et al., 2018; Yu et al., 2014). The increase in TERRA levels and formation of these R-loops occur in the G1/S transition, preceding the passage of the replication fork through the telomere. At short telomeres, it was proposed that a decrease in RNase H2 recruitment by Rif2 allowed for the persistence of R-loops, leading to an increased possibility of a collision event with the replisome. This could lead to Rad51 inducing a DNA damage response, leading to HDR to elongate the telomere. The Rif2 mediated recruitment of RNase H2 was proposed to be the manner in which the cells inhibit R-loop accumulation at long telomeres, as the presence of Rif2 is decreased at short telomers (Graf et al., 2017; McGee et al., 2010).

Tbf1

Although many experiments implicate this essential protein in both telomeric and non-telomeric processes, its exact role remains elusive. It has been implicated in DNA damage response, telomere maintenance, transcription and chromatin remodelling (Arnerić and Lingner, 2007; Berthiau et al., 2006; Bonetti et al., 2013; Preti et al., 2010; Ribaud et al., 2012). Tbf1 was first identified by DNase I footprinting as telomere binding factor α (Tbfα), due to its ability to bind TTAGGG sequences, which are mammalian telomere repeats (Liu and Tye, 1991). While Tbf1 is not able to bind yeast telomeric repeats, it was shown to associate to TAGGG consensus sequences located at the junction

of the telomere and subtelomeric repeats (Brigati et al., 1993; Koering et al., 2000; Liu and Tye, 1991). Tbf1 has similarities to the human proteins TRF1 and TRF2, as they all bind TTAGGG sequences conserved in many organisms (Brigati et al., 1993; Zhong et al., 1992). These proteins are able to specifically bind T_2AG_3 like motifs due to their telomeric DNA binding motifs, named the telobox (Bilaud et al., 1996). The telobox is conserved from plants to yeast to animals and binds to a core TAGGG motif (Bilaud et al., 1996; Koering et al., 2000). The telobox is related to the Myb-binding domain, however it only contains one out of the three tandem repeats typically seen in Myb binding motifs and thus does not bind typical Myb DNA binding sites (Bilaud et al., 1996; Vassetzky, 1999).

Although Tbf1 binds subtelomeric repeats *via* a TAGGG motif found in both the X and Y' elements, it is also found at a multitude of promoters in the genome (Koering et al., 2000; Lavoie et al., 2010; Preti et al., 2010). It is suspected that its essential role is related to transcriptional regulation at non-telomeric loci (Bilaud et al., 1996). Due to the multitude of binding sites throughout the genome and its involvement in modulating chromatin structure and transcription, Tbf1 is considered a general regulatory factor (GRF) (Ko et al., 2008). In addition to binding upstream over 200 protein coding genes, such as ribosome biogenesis genes, Tbf1 also binds promoters of approximately 90 % of snoRNA genes (Bosio et al., 2017; Lavoie et al., 2010; Preti et al., 2010). Interestingly, Tbf1 may be involved in the regulation of its own expression, as it binds its own promoter (Lavoie et al., 2010). At snoRNA promoters, it is suspected that Tbf1 is important for fine tuning snoRNA transcription (Preti et al., 2010). Its role at protein coding genes is quite different. In these areas, it binds with Vid22 and Env11 to form nucleosome depleted regions (NDR), indicating a role in chromatin remodeling (Badis et al., 2008; Preti et al., 2010). The association of Tbf1 and Vid22 was also found to be important in DNA damage responses at double stranded breaks (Bonetti et al., 2013). Strains expressing loss of function Tbf1 and Vid22 alleles were shown to be more sensitive to DNA damage inducing drugs. This sensitivity is hypothesized to be connected to Tbf1's role in generating an NDR, since the deletion of the histone deacetylase Rpd3 eliminated sensitivity to DSB inducing agents in *tbf1* strains. Furthermore, Tbf1 and Vid22 were shown to be important

for the generation of 3' single stranded DNA at HO-induced DSBs, which is necessary for DNA repair by homologous repair (HR). However, it is unknown how Tbf1 could be recruited to these DSBs, as its DNA binding is sequence specific (Bonetti et al., 2013; Preti et al., 2010). In general, the Longhese Lab suggests that the role of Tbf1 in chromatin compaction could impact 3' end processing, thus affecting DDR pathways (Bonetti et al., 2013).

Given that Tbf1 is associated with 15 of the 16 chromosomal ends in S. *cerevisiae*, it is expected to have an important telomeric function (Preti et al., 2010). Studies done thus far have implicated that Tbf1 could participate in a variety of telomeric functions (Berthiau et al., 2006; Fourel et al., 1999; Hediger et al., 2006; Ribaud et al., 2012). More than one study suggests Tbf1 could have a role as a back-up length regulator, when telomerase is not functioning properly (Arnerić and Lingner, 2007; Berthiau et al., 2006; Ribaud et al., 2012). Monitoring the extension of single telomeres by STEX (Single Telomere Extension) assay revealed that in *tel1Δ* strains with short telomeres, the presence of the subtelomere or of Tbf1 near $TG_{1\text{-}3}$ telomeric repeats restores the preferential elongation of short telomeres (Arnerić and Lingner, 2007). In *tel1Δ* strains, this property is lost in telomeres lacking a subtelomere. In these experiments, Tbf1 was expressed in fusion with a Gal4 binding domain (GBD) and tethered to truncated TEL07L ($TEL07L^{tr}$), lacking a subtelomeric area, by introducing UAS_G sites in the subtelomeric area to recruit the GBD-Tbf1N. A different study suggests that tethering GBD-Tbf1N to $TEL07L^{tr}$ in *tel1Δ* backgrounds has a function in protecting this telomere from access to telomerase, as telomeres became increasingly shorter as more GBD-Tbf1N was tethered to the chromosomal ends (Berthiau et al., 2006). The conflicting results of these two studies can be explained by an experiment investigating the potential capping functions of Tbf1 when bound to *de novo* formed T_2AG_3 telomere repeats (Ribaud et al., 2012). The assay used to examine the formation of *de novo* telomere repeats involved integrating T_2AG_3 sequences of either 60 or 230 bp flanking an HO endonuclease recognition site in opposing orientations (Diede and Gottschling, 1999; Ribaud et al., 2012). After a cleavage by the HO endonuclease at the HO recognition site between the vertebrate repeats, these

would mimic the behaviour of short (60 bp) or long (230 bp) telomeres. A functional Tbf1 was an important factor in regulating the length of the T_2AG_3 sequences. Telomerase was preferentially recruited to rapidly lengthen short 60 bp tracts, while long tracts were not lengthened (Ribaud et al., 2012). The localization of telomerase and subsequent lengthening of short telomeres, as well as the protection of "normal length", 230 bp tracts, were dependent on a fully functional Tbf1 protein. Furthermore, in cells expressing a deficient *tbf1Δi* allele, long telomeres were recognized as double stranded breaks and caused a delay in the cell cycle. This was not the case in *TBF1* strains. Thus, Tbf1 could be involved in recruiting telomerase to telomeres when present in small amounts, but increasing amounts lead to protection from over-elongation and the DDR (Arnerić and Lingner, 2007; Berthiau et al., 2006; Ribaud et al., 2012).

One of the initial roles proposed for Tbf1 at telomeres is that of an insulator to prevent the spread of TPE (Fourel et al., 1999). Regions called STARs (Subtelomeric Anti-silencing Regions) were identified in X and Y' elements and characterized as sequences with anti-silencing properties. These sequences contain binding sites for both of the main telomeric binding proteins, Tbf1 and Reb1 (Koering et al., 2000). The experiments were done as explained above (see section on TPE), by evaluating the expression of a *URA3* gene placed near telomeric repeats by monitoring resistance to growth on 5-FoA medium. These experiments also showed that when 1-3 Tbf1 binding sites were introduced into the subtelomere, there was a very slight decrease in TPE (Fourel et al., 1999). However, the insertion of 10 TTAGGG sequences in this area produced a stronger effect. The necessity to heavily alter the subtelomere to observe these functions, as well as the fact that the X-Core functions as a proto silencer overshadows the STARs anti-silencing effects and could reduce the importance of Tbf1 as an anti-silencer at the subtelomere (Fourel et al., 1999; Power et al., 2011).

Reb1

In addition to binding motifs for Tbf1, subtelomeres contain sequences that bind the essential general regulatory factor Reb1 (Chasman et al., 1990; Ju et al., 1990; Koering et al., 2000; Morrow et al., 1989). The *REB1* gene was independently discovered several times and carried different names due to the multitude of targets it is associated with throughout the genome. It was first identified as Factor Y, binding to UAS_G, a stretch of upstream activation sequences between *GAL1* and *GAL10* genes to create nucleosome free regions in flanking sequences (Fedor et al., 1988). The same group later renamed the protein GRF2, as they discovered that it binds a multitude of UASs and, through its effects on chromatin structure, has a synergistic effect on transcriptional activation when in proximity to thymidine rich regions (Chasman et al., 1990). Another study identified it as the Q-binding protein (QBP), necessary for the TATA-independent activation of GCN4 transcription (Brandl and Struhl, 1990). Around the same time, a different group found Reb1 as an rRNA enhancer binding protein, as it was found to bind enhancers and protect the bound sequences from access to other proteins and chemicals (Morrow et al., 1989). In addition to binding these enhancer regions, Reb1 binds a second site upstream the origin of transcription for rRNA and affects chromatin conformation. Additional studies found that Reb1 also binds sites in a number of promoters of genes transcribed by RNA polymerase II (Chasman et al., 1990; H. Wang et al., 1990).

We now know that Reb1 is an essential protein with a myb-related binding domain, recognizing a CCGGGTAA consensus sequence (Ju et al., 1990; Morrow et al., 1989). Indeed, it is found in the UASs of many genes involved in ribosome biogenesis (Ribi), along with Abf1, Rap1 and Tbf1, where it is important for the full expression of target promoters (Bosio et al., 2017). In terms of its role in establishing nucleosome free regions (NFRs), it has been shown that Reb1 is able to do so by recruiting the RSC chromatin remodeling complex when bound at promoter regions (Hartley and Madhani, 2009). The same study showed that establishing NFRs is required for the recruitment of H2AZ variant nucleosomes that are characteristic of promoter regions. Furthermore, Reb1

bound to DNA forms a roadblock in order to induce termination of transcription by RNA polymerase II, yielding unstable transcripts that are degraded and impeding RNA pol II from transcribing into the next gene (Colin et al., 2014; Roy et al., 2016). The termination of transcription by Reb1 was found to be independent of NFRs. Reb1 also has a role in regulating the transcriptional start site (TSS) when bound at promoter regions (Challal et al., 2018). This study found that Reb1, as well as GRFs Abf1 and Rap1, are able to limit ectopic transcription by controlling nucleosome positioning such that transcription is initiated at the correct TSS.

Despite these important roles in transcriptional regulation, the function of Reb1 when bound at subtelomeres is not yet understood. Similar to Tbf1, the binding sites for Reb1 in the subtelomeric regions are variations of its consensus sequence, although they contain the core sequence GGGTAA (Koering et al., 2000). Tbf1 and Reb1 have been implicated in many of the same roles at subtelomeres. They have overlapping roles in anti-silencing, limiting the spread of TPE and both have binding sites in STARs (Fourel et al., 1999). Studies investigating the role of Tbf1 in telomere length maintenance have found Reb1 has similar roles in protecting telomeres from telomerase elongation (Berthiau et al., 2006). This study was also done by localizing Reb1 to truncated telomeres, lacking a subtelomere, in *tel1Δ* backgrounds with a short telomere phenotype. However, contrary to Tbf1, Reb1 does not have the same capping abilities, as it does not protect arrays of its consensus sequence from degradation and does not recruit telomerase to elongate these sequences (Ribaud et al., 2012). Thus, in the context of telomeric and non-telomeric functions, Tbf1 and Reb1 overlap in many ways, but also carry out distinct functions.

Objectives

There is clear evidence that both Tbf1 and Reb1 are important for cell function, as they are essential proteins, involved in transcriptional regulation and chromatin structure,

although it is still partially unclear how exactly they participate in these pathways. Despite these proteins being the main binding factors of the subtelomeric areas, their roles there are not yet well understood. Previous studies have shown that Tbf1 and Reb1 localized at chromosomal ends could be involved in telomere length maintenance and the telomere position effect. However, many experiments investigating the roles of Tbf1 and Reb1 at telomeres were done using heavily altered subtelomeres or expressing mutant protein alleles. A global reduction in DNA binding due to the expression of mutant Tbf1 and Reb1 alleles could lead to alterations in transcription at their targets, which could eventually lead to effects at the telomere. Thus, the use of mutant alleles may give an inaccurate picture of the roles of subtelomeric Tbf1 and Reb1. Although inferences can be made, working with heavily altered subtelomeres, or truncated telomeres lacking subtelomeres, also does not give a complete picture of the roles of Tbf1 and Reb1 at native telomeres. Thus, there is a lack of information concerning the function of Tbf1 and Reb1 at native subtelomeres.

The main objective of this project is to construct a system in which the roles of Tbf1 and Reb1 binding at a native subtelomere can be studied. This is achieved by introducing point mutations into Tbf1 and Reb1 binding sites of X-only telomeres TEL01L and TEL03L in order to decrease the binding efficiency at these sites. A further objective is to use this construct to evaluate the roles of Tbf1 and Reb1 in telomere length maintenance and telomere position effect, as these roles have not yet been examined using native subtelomere structures. In addition, the roles of Tbf1 and Reb1 in transcriptional regulation at telomeres is evaluated by monitoring TERRA transcription from wild type and mutated subtelomeres.

As a secondary project, the role of the yKu complex as an RNA binding protein is investigated. yKu also has dual functions, being involved in NHEJ when bound at double stranded breaks and binding at chromosomal ends to carry out functions in silencing, chromosomal end capping and potential telomerase recruitment. The yKu complex also binds the TLC1 RNA, with roles in shuttling and nuclear retention. Recent data from the Wellinger Laboratory suggests that the yKu complex binds two other non-coding RNAs

transcribed from intergenic regions. In order to investigate the RNA binding capacities of the yKu complex, we aim to perform a cross-linking and analysis of cDNA sequencing (CRAC-seq) in collaboration with the Granneman Laboratory. For this project, the objective is to tag the yKu70 and yKu80 proteins with a 6xHis-TEV-3xFlag tag, used in the Granneman Laboratory for CRAC-seq and validate the compatibility of each aspect this tag with the proteins of interest.

Materials and Methods

Plasmid Cloning Methods

All plasmids used in this study are listed in table 1. The plasmids were constructed in multiple steps using various cloning strategies, which will be described in detail below. All oligonucleotides used for plasmid construction are described in table 6. All sequencing for this project was done by the Plateforme de séquençage et génotypage des génomes at the CHU de Québec, Université de Laval (http://www.sequences.crchul.ulaval.ca/).

Table 1: Plasmids referred to throughout this work.

Plasmids used in this study:		
Name	**Description (Use)**	**Reference**
pRS303	*HIS3* (Cloning)	Umen et al., 1996
pRS304	*TRP1* (Cloning)	Sikorski and Hieter, 1989
pRS305	*LEU2* (Cloning)	Sikorski and Hieter, 1989
pRS306	*URA3* (Cloning)	Sikorski and Hieter, 1989
pRS400	*KanMX4* (Cloning)	Brachman et al., 1998
pADB5	*TRP1, RS-ARS1-RS, 4xLexAOp, 4xUASg* (Cloning: intermediate plasmid)	E. Pasquier, Wellinger Lab
pEP21	*ARS/CEN, TRP1, Yku80-13xMYC, promGAL-RecR* (Expression of Recombinase R)	E.Pasquier, Wellinger Lab
pEP19A	*HIS3, TG_{1-3}* (Cloning)	E. Pasquier, Wellinger Lab
pB3	*ARS/CEN, LEU2, promGAL-RecR* (Cloning: Source of promGAL-Recombinase R)	Griesenbeck et al., 2003
pB1539	*6xHIS-TEV-3xFlag, URA3* (Integrative, protein tagging)	Granneman et al., 2009
pTbf1-myc	*KanMX, tbf1-453-13MYC* (Integrative, protein tagging)	E. Bonnell, Wellinger Lab
pFA6a-13Myc-KMX	*13xMYC, HIS3MX6* (Integrative, protein tagging)	Longtine et al., 1998

pFA6a-3HA-HIS3MX	*3xHA, HIS3MX6* (Integrative, protein tagging)	Longtine et al., 1998
pCT300	*~300 bp C_{1-3} repeats EcoRI fragment* (Southern Blot probe)	Bourns et al., 1998
pAK003	*RS-URA3-RS* (Cloning, intermediate plasmid for integrative plasmide in S. cerevisiae)	This work
pAK002	TEL01Lmod WT XCR (Cloning, intermediate for integrative plasmid)	This work
pAK012	TEL01Lmod XCRmut (Cloning, intermediate for integrative plasmid)	This work
pT3F1	TEL03Lmod WT XCR *RS-LEU2-RS* (Cloning, intermediate for integrative plasmid)	This work
pRIM2D	TEL03Lmod XCRmut *RS-LEU2-RS* (Cloning, intermediate for integrative plasmid)	This work
pAK007	TEL03Lmod XCRmut1 *RS-LEU2-RS* (Cloning, intermediate for integrative plasmid)	This work
pAK016	TEL03Lmod WT XCR *RS-LEU2-RS TG_{1-3} repeats* (Integrative plasmid, linearization with NsiI/Eco53kI)	This work
pAK018	TEL03Lmod XCRmut *RS-LEU2-RS TG_{1-3}* repeats (Integrative plasmid, linearization with NsiI/Eco53kI)	This work
pAK007T	TEL03Lmod $XCRmut_1$ *RS-LEU2-RS TG_{1-3} repeats* (Integrative plasmid, linearization with NsiI/Eco53kI)	This work
pAK013	TEL01Lmod XCRmut *RS-URA-RS TG_{1-3}* (Integrative plasmid, linearization with BamHI/ NotI)	This work
pAK014	TEL01Lmod WT XCR *RS-URA-RS TG_{1-3}* (Integrative plasmid, linearization with BamHI/ NotI)	This work

Traditional Cloning

Traditional cloning was carried out by digesting a vector was with one or more restriction enzymes followed by ligation with a DNA fragment with compatible ends. The ligation was done using a Rapid DNA ligation Kit (Thermo Fisher Scientific), following manufacturer's directions. For each ligation reaction, approximately 50 ng of vector plasmid was linearized with 1 or more restriction enzymes. If only one restriction enzyme was used, plasmid re-circularization was prevented with a dephosphorylation reaction.

DNA ends were dephosphorylated using the Alkaline Phosphatase Kit (Roche), in a 10 µl reaction with 1x phosphatase reaction buffer and 1 U Alkaline Phosphatase and incubated for 1 hour at room temperature, following the manufacturer's protocol. The reaction was stopped by the addition of EDTA to a 20 mM final concentration and incubation at 68 ˚C for 10 minutes. Insert DNA was digested with restriction enzymes leaving DNA ends compatible to the vector. Both vector and plasmid DNA were purified on a 0.45 % agarose gel run in TAE, using Spin-X ® (Sigma) centrifuge tube filters. Vector and insert DNAs were combined at a 5:1 molecular ratio for ligation reactions.

All Around the World PCR

To introduce point mutations into a plasmid, primers were designed to span the area to be mutated, with 1-2 nucleotides difference from the plasmid sequence. The ends of the forward and reverse primers were aligned such that the whole plasmid was amplified. Q5 ® High Fidelity DNA polymerase (NEB) was used according to the manufacturer's instructions, using a temperature gradient spanning $\pm$ 5 ˚C of the melting temperatures (Tm) of the forward and reverse primers (as determined by Snapgene software). Template DNA was degraded using the KLD Enzyme Kit (NEB) containing enzyme DpnI to target the cell-derived methylated DNA, as well as kinase and ligase for plasmid circularization. 1 µl PCR reaction was treated in a 10 µl total volume reaction containing 1 µl of enzyme mix and 5 µl 2x reaction buffer for 20 minutes at room temperature. 5 µl of the product was used for transformation into 50 µl One Shot ® Stbl3® chemically competent E. *coli.*

Gibson Assembly

The Gibson Assembly Kit® (NEB) was used to insert 2 or more DNA fragments into a vector plasmid linearized by restriction enzymes in a single step. The DNA fragments were amplified with primers designed to have overhanging flaps to add short regions with homology to the vector or neighbouring fragments. This homology ensures the fragments are assembled in the correct orientation and order. After PCR amplification of the primers from bacterial plasmids or yeast genomic DNA, the fragments were purified either by on a

0.45 % agarose gel in TAE using Spin-X® columns, or on columns from an EZ-10 Spin Column PCR Product Purification Kit (Biobasic). The Gibson Assembly reaction was carried out according to the manufacturer's directions, in a 10 µl reaction. The products were diluted 1:5 in water before transforming 5 µl into One Shot ® Stbl3 ® chemically competent E. *coli.* (Thermo Fisher) (for plasmids containing telomeric repeats) or One Shot ® Top10 ® chemically competent E.*coli* (Thermo Fisher) bacteria as described below.

Construction of TEL01Lmod and TEL03Lmod plasmids

Mutation of TEL01L and TEL03L subtelomeres was achieved by cloning sequences interior to the telomeric DNA in bacterial plasmids and making desired changes using a combination of the cloning techniques described above. The steps used for the modification of TEL01L and TEL03L subtelomeres will be outlined in the following section. The resulting constructs depicted below (Figures 4, 5), are referred to as TEL01Lmod and TEL03Lmod.

Construction of plasmids with modified TEL01L

A plasmid containing the X-element of the TEL01L telomere (pAK002) was constructed using 2 fragment Gibson Assembly. Both fragments were amplified from genomic yeast DNA from the W3749 strain (W303 background) by PCR and cloned by Gibson Assembly into the pRS303 vector, which was linearized by digestion with the NotI restriction enzyme. Fragment 1 (2011 bp), amplified by primers TEL01L_GB_F/TEL01L_GB_RB, contained regions upstream of the subtelomere, including dubious ORFs PAU8 and YAL067W-A. Fragment 2 (primers: TEL01L_GB_R/TEL01L_GB_FB) contained the XCR and X-Core of the TEL01L X-element, as well as DNA upstream of the X-element (1404 bp). The Gibson Assembly reaction product was transformed into One Shot ® Stbl3 ® chemically competent E. *coli* (Thermo Fisher) as described below. The clones were screened by digestion with NsiI restriction enzyme and sent for sequencing with primers Xel-F and Xel-R.

Tbf1 and Reb1 Binding Site Mutation:

The DNA binding sites in the TEL01L XCR for Tbf1 and Reb1 were mapped using the Yeast Transcription Factor Specificity Compendium (YetFaScO, http://yetfasco.ccbr.utoronto.ca/) (Figure 4). Tbf1 and Reb1 binding motifs both contain CCC or GGG in their core binding sequences (Koering et al., 2000). Thus, point mutations were introduced into these sequences of each predicted binding site by "All Around the World PCR". Primer pairs spanning each binding site were designed with one mismatching nucleotide to introduce a point mutation, changing the cytosine nucleotide (C) to a guanosine nucleotide (G), or *vice versa*. All primer pairs used can be found in table 6 under "TEL01Lmod XCR Site directed PCR mutagenesis".

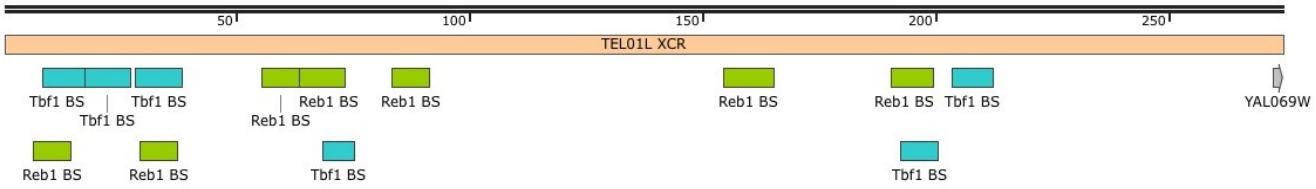

Figure 4: Tbf1 and Reb1 binding sites in TEL01L XCR were mapped by YeTFasCo.
The XCR sequence of TEL01L from the reference genome S288C is depicted, with Tbf1 (blue) and Reb1 (green) binding sites, as identified by the YeTFasCo database.

The PCR product was treated with the KLD Enzyme Mix (NEB) as described above and transformed into One Shot ® Stbl3 ® chemically competent E. *coli* cells. Plasmids were extracted using an EZ-10 Spin Column Plasmid DNA Miniprep Kit (Biobasic), screened by digestion with the XhoI restriction enzyme and sequenced to confirm. The resulting plasmid was subjected to another round of "All Around the World PCR" with primers introducing mutations to a second Tbf1 or Reb1 binding site, followed by the same steps of KLD treatment, transformation and screening. The process was repeated with each of the primer pairs in section "TEL01Lmod XCR Site directed PCR mutagenesis" (Table 6), resulting in the pAK012 plasmid containing point mutations in all Tbf1 and Reb1 binding sites.

Insertion of URA3 flanked by RS sites:

Plasmid pAK003 contains a *URA3* gene flanked by two RS sequences (58 bp) in the same orientation, recognized by the recombinase R (Gartenberg, 2012). It was obtained by classical cloning. The vector pADB5 was linearized with NruI restriction enzyme, which cleaves at a restriction site between two RS sites. *URA3* was amplified from the pRS303 bacterial plasmid with primers URA3_NruI_F and URA3_HpaI_R, PCR purified and digested by NruI and HpaI. Vector and insert were purified on 0.45 % agarose gel gel prior to ligation with Rapid DNA Ligation Kit (Thermo Fisher), as described above. The plasmid was screened by digestion with StuI and PvuII restriction enzymes and confirmed by sequencing. The *RS-URA3-RS* sequence was cloned into the pAK012 (01L-XCRmut) and pAK002 (01L-WT XCR). pAK003 was digested by PvuII to obtain the RS flanked *URA3* insert, which was cloned into the vector plasmids linearized by HpaI. Clones of these intermediate plasmids were screened by digestion with the XhoI restriction enzyme and sequenced.

Addition of telomeric repeats and integration into S. *cerevisiae*:

Telomere repeats were amplified from the pEP19A plasmid with primers QP4-F and SSb-pRS1-F using the GoTaq ® Long PCR MasterMix (Promega) and then purified from a 1 % agarose gel by Spin-X ® column. The fragment was then digested with XbaI and SalI restriction enzymes, for cloning into vectors pAK002+*RS-URA3-RS* and pAK012+*RS-URA3-RS*, digested with the same enzymes (see above protocol), and cloned in One Shot ® Stbl3 chemically competent E. *coli*. Clones were screened by digestion with XhoI restriction enzyme and confirmed by sequenced, constructing final integrative plasmids pAK014 (01L- WT XCR) and pAK013 (01L-XCRmut).

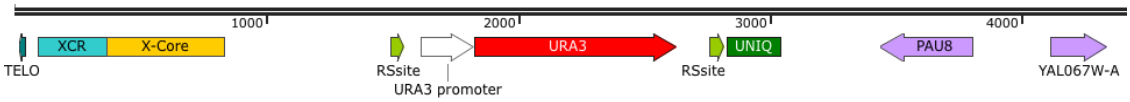

Figure 5: TEL01Lmod integrative plasmid
Schema of TEL01Lmod integrative plasmids (pAK014/pAK013) linearized by BamHI and NotI.Purple arrows indicate ORFs upstream of subtelomere.

Construction of plasmids with modified TEL03L

1 Fragment Gibson Assembly was used to clone the TEL03L X-element and approximately 500 bp of upstream DNA into the pRS303 integrative plasmid. pRS303 was linearized by NotI and NsiI restriction enzymes and the Gibson Fragment was generated by PCR amplification of genomic yeast DNA from a W303 background strain, using primers GB_TY5_F and GB_X_R. The Gibson Assembly reaction products were transformed into One Shot ® Stbl3 chemically competent E. *coli* and plasmid DNA was extracted Miniprep Kit (Biobasic). Clones were screened by digestion with EcoRI restriction enzyme and confirmed by sequencing.

Insertion of LEU2 flanked by RS sites:

Gibson Assembly was used to insert the LEU2 marker flanked by RS sequences between the X-element and upstream genomic DNA cloned on the TEL03L intermediate plasmid. The TEL03L intermediate plasmid was amplified (primers: GB_X_F and GB_TY_R) to serve as a vector and the *RS – LEU2 – RS* DNA fragment was amplified (RS_LEU2_F and RS_LEU2_R) from plasmid pB3 (Griesenbeck et al., 2003). Vector and insert were purified on agarose gel by Spin-X ® column prior to Gibson Assembly reaction and transformation into One Shot ® Stbl3 ® chemically competent E. *coli*. Plasmid DNA was extracted by Miniprep Kit (Biobasic), screened by digestion with EcoRI and sequenced, producing the pT3F1 plasmid.

Mutation of Tbf1 and Reb1 Binding sites:

The binding site mutation process proceeded as with the plasmid containing the TEL01L subtelomere sequence. Tbf1 and Reb1 binding sites were mapped on the XCR of the TEL03L subtelomere using the YetFaSCo database (Figure 6). pT3F1 underwent 6 rounds of All Around the World PCR with the Q5 Mutagenesis Kit using primers found in table 6 under “TEL03L XCR mutation”, as described above. All mutations were verified by sequencing and plasmids were cloned in One Shot ® Stbl3 ® chemically competent E. *coli*. Two mutant versions were produced. Plasmid pRIM2D contained point mutations in all

Tbf1 and Reb1 binding sites, while pAK007 had two Reb1 binding sites without mutations.

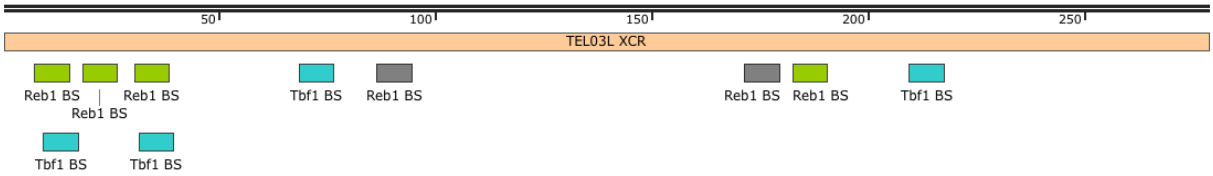

Figure 6: Tbf1 and Reb1 binding sites in TEL03L XCR were mapped by YeTFasCo.
The XCR sequence of TEL03L from the reference genome S288C is depicted, with Tbf1 (blue) and Reb1 (green/grey) binding sites, as identified by the YeTFasCo database. Grey Reb1 binding sites have wild type sequences in pAK007 plasmids/03L-XCRmut$_1$ strains.

Addition of telomeric repeats and integration into S. *cerevisiae*:

Traditional cloning strategies were used to clone DNA fragments with telomeric repeats in plasmids pT3F1 (03L-WT XCR), pRIM2D (03L-XCRmut) and pAK007 (03L-XCRmut$_1$). pEP19A was digested with restriction enzymes NotI and EcoRV to produce a fragment of 356 bp, containing TG$_{1\text{-}3}$ repeats. pT3F1, pRIM2D and pAK007 were linearized by digestion with NotI. Vector and insert DNA were purified on 0.45 % agarose gel by Spin-X ® column and ligated with the T4 Rapid Ligation Kit (NEB). 2 µl of the ligated product was transformed in One Shot ® Stbl3 ® chemically competent E. *coli* bacteria as described above. Plasmid was DNA extracted and verified by sequencing. This produced final plasmids pAK016 (03L-WT XCR), pAK018 (03L-XCRmut) and pAK007T(03L-XCRmut$_1$).

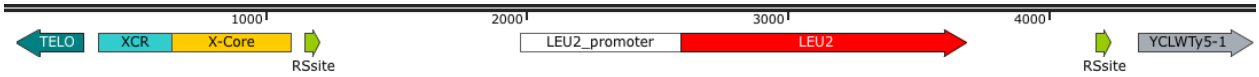

Figure 7: TEL03Lmod linearized plasmids.
Schema of TEL03Lmod integrative plasmid pAK018/pAK016 linearized by EcoR53kI and NsiI. Grey arrow marks an ORF upstream of TEL03L subtelomere.

Cloning TEL01Lmod X-elementΔ, XCRΔ and X-CoreΔ strains

S. *cerevisiae* strains with modified, truncated TEL01L telomeres were constructed by creating intermediate integrative plasmids by 2 fragment Gibson Assembly ®. Four constructs were made for this experiment. All constructs were made by amplifying two fragments with Q5 ® High Fidelity DNA Polymerase (NEB) and assembling them in the

pAK014 vector plasmid, linearized by enzymes NruI and XbaI. Primer pairs and matrices used for each fragment and construct are indicated in table 2. pAK014 is depicted in Figure 8 to show the placement of primer pairs. In X-elementΔ and XCRΔ constructs a constant distance of 1298 bp between telomeric repeats and the URA3 promoter was maintained by replacing X-element or XCR sequences with equal length fragments amplified from *KanMX* in pRS400. TEL01Lmod X-CoreΔ was constructed without replacing the removed sequences with a *KanMX* sequence, leaving a distance of 1106 bp between telomeric repeats and URA3 promoter. A control construct "Short X-element" was made with a wild type TEL01Lmod X-element and a distance of 1106 bp between telomeric repeats and URA3 promoter. Gibson Assembly ® products were transformed into One Shot Top10 chemically competent E.*coli* (Thermo Fisher). Plasmids were extracted from clones and screened by digestion with XhoI and sequencing. Constructs were integrated into W3749 S. *cerevisiae* strains after linearization with BamHI and NotI. Yeast strains were screened by sequencing DNA extracted from multiple clones of each strain. Resulting strains were AKY054 (TEL01Lmod X-elementΔ), AKY055 (TEL01Lmod-XCRΔ), AKY056 (TEL01Lmod X-element short), AKY057 (TEL01Lmod WT XCR X-CoreΔ), AKY058 (TEL01Lmod XCRmut X-CoreΔ) (Table 3).

Table 2: Gibson Assembly layout for modified TEL01L constructs.

		Primer Pairs		
Construct	**Matrix plasmid**	**Fragment 1**	**Fragment 2**	**amplicon length (bp)**
X-element Δ	pRS400	GB8F/GB14R		776
	pAK014		GB1F/GB16R	775
XCRΔ	pRS400	GB5F/GB4R		277
	pAK014		GB1F/GB15R	1230
Short X-element	pAK014	GB10F/GB2R		767
	pAK014		GB1F/GB11R	303
X-CoreΔ WT XCR	pAK014	GB2R/GB12F		302
	pAK014		GB1F/GB13R	765
X-CoreΔ XCRmut	pAK013	GB12F/GB3R		302
	pAK014		GB1F/GB13R	765

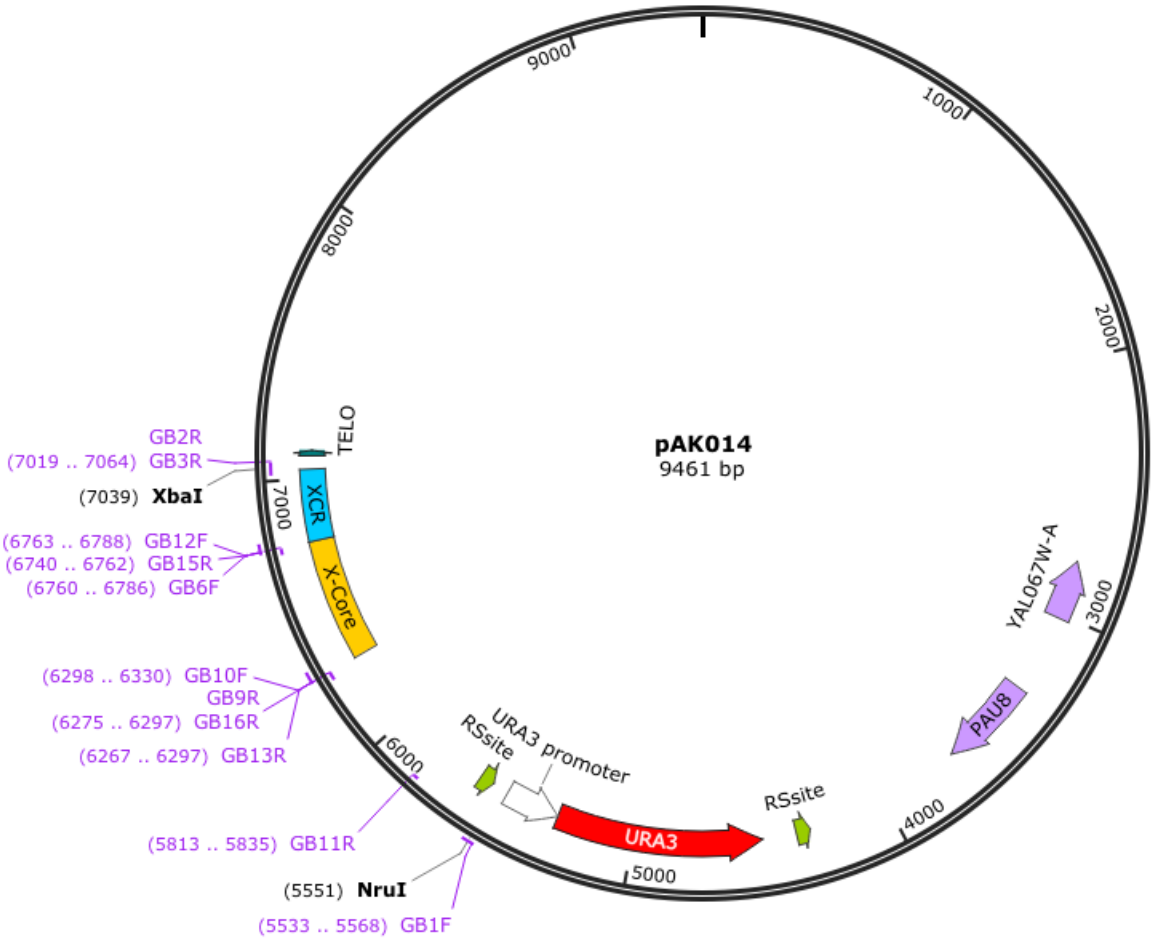

Figure 8: Primer placement on pAK014
Binding sites for primers listed in table 2 amplifying fragments from pAK014 matrix shown in purple. XbaI and NruI restriction sites used for vector linearization are indicated in black. Elements of the TEL01Lmod construct are labelled. Distance from telomeric repeats (TELO) to URA3 promoter in the wild type construct is 1298 bp.

E.*coli* Transformation

50 µl of One Shot Stbl3 chemically competent E. *coli* or One Shot Top10 chemically competent E.*coli* (Thermo Fisher) cells were thawed on ice in 1.7 ml Eppendorf tubes for 20 minutes. 2-5 µl of a ligation reaction, KLD treated PCR product or Gibson Assembly reaction were added, and cells were incubated on ice for 30 minutes. The samples were then heat shocked in a 42 ˚C water bath for 45 seconds and rested on ice for 2 minutes. 1 ml of LB broth was added to the sample before incubation at 37 ˚C for 1 hr with 600 rpm

agitation. The cells were centrifuged for 1 minute at 21,000 x g and 800 µl of supernatant media was removed. The cell pellet was resuspended in the remaining media. 50 µl and 150 µl of the cell mixture were spread with sterile acid washed beads on plates with Luria broth (LB) + ampicillin. The bacteria was grown overnight at 37 ˚C. Colonies selectively grown were transferred to 3 ml liquid LB + ampicillin media and grown once more overnight at 37 ˚C. Plasmid DNA was extracted from 1.5 ml of these cultures using EZ-10 spin column plasmid DNA mini-preps kit (Biobasic), and conserved at -20 ˚C for further use.

Yeast Strains

Yeast strains with slight differences in their genetic backgrounds were used for different studies described here. The originally sequenced S288c strain (Mortimer and Johnston, 1986), was used by Brachman *et al.* (1998) to create, among other, the haploid BY4705 strain, in which non-essential auxotrophic genes are deleted. In this project, yKu70 and 80 were tagged in the BY4705 background. Experiments involving the subtelomere Tbf1 and Reb1 binding sites were conducted in haploid W3749 background strains (Lisby et al., 2004), which is derived from the W303 genetic background. All strains used in this study are described in Table 3.

Table 3: S. *cerevisiae* strains referred to throughout this work.

Yeast Strains used in this project:		
Name	**Genotype**	**Reference**
W37491-A	*MatA can1-100 ura3-1 his3-11,15 leu2-3,112 trp1-1 bar1Δ::LEU2*	Lisby *et al.*, 2004
BY4705	*Mat alpha ade2Del::hisG his3Del200 leu2del0 lys2Del0 met15Del0 trp1Del63 ura3Del0*	Brachmann *et al.*, 1998
EPY06.6b	*MatA can1-100 ura3-1 his3-11,15 leu2-3,112 trp1-1 bar1Δ::KanMX*	E. Pasquier, Wellinger Lab, unpublished
RWY046	*MatA can1-100 ura3-1 his3-11,15 leu2-3,112 trp1-1 tel1Δ::KanMX*	R. Wellinger, unpublished

EPY007	*Matα leu2-3,112 his3-11,15 trp1-1 MN-L1- RAP1 ura3-1 ade2-1 can1-100*	Larcher *et al*., 2016
AKY001	EPY007 *+ TBF1-myc::KanMX*	This work
AKY003	EPY007 + *REB1-myc::HI3S*	This work
EPY109	AKY001 *+ TEL03Lmod-WT XCR*	E. Pasquier, Wellinger Lab, unpublished
EPY110	AKY003 + *TEL03Lmod-WT XCR*	E. Pasquier, Wellinger Lab, unpublished
EPY114	AKY001 + *TEL03Lmod-XCRmut*	E. Pasquier, Wellinger Lab, unpublished
EPY115	AKY003 + *TEL03Lmod-XCRmut*	E. Pasquier, Wellinger Lab, unpublished
AKY036	AKY001 + *TEL01Lmod-WT XCR*	This work
AKY025	AKY001 + *TEL01Lmod-WT XCR*	This work
AKY021	EPY007 + *TEL01Lmod-WT XCR*	This work
AKY018	AKY001 + *TEL01Lmod-XCRmut*	This work
AKY019	AKY003 + *TEL01Lmod-XCRmut*	This work
AKY020	EPY007 + *TEL01Lmod-XCRmut*	This work
EPY116	*MatA leu2-3 trp1-1 can1-100 ura3-1 his3- 11,15 TEL03Lmod-WT XCR*	E. Pasquier, Wellinger Lab, unpublished
EPY117	*MatA leu2-3 trp1-1 can1-100 ura3-1 his3- 11,15 TEL03Lmod-XCRmut*	E. Pasquier, Wellinger Lab, unpublished
AKY116	EPY116 + *sir4Δ::KanMX*	This work
AKY115	EPY117 + *sir4Δ::KanMX*	This work
AKY047	AKY116 + *sir4Δ::KanMX tbf1-453::NatMX*	This work

AKY012	W3749-1A *TEL01Lmod-WT XCR::URA3*	This work
AKY013	W3749-1A *TEL01Lmod-XCRmut::URA3*	This work
AKY046	AKY112 + *tbf1-82::NatMX*	This work
AKY022	*MatA can1-100 ura3-1 his3-11,15 leu2-3,112 trp1-1 TEL01Lmod-WT XCR*	This work
AKY023	*MatA can1-100 ura3-1 his3-11,15 leu2-3,112 trp1-1 TEL01Lmod-XCRmut*	This work
AKY050	AKY022 + *sir4Δ::KanMX*	This work
AKY051	AKY023 + *sir4Δ::KanMX*	This work
AKY027	EPY116 + *yku80Δ::KanMX*	This work
AKY028	EPY117 + *yku80Δ::KanMX*	This work
AKY030	EPY116 + *tel1Δ::KanMX*	This work
AKY031	EPY117 + *tel1Δ::KanMX*	This work
AKY052	AKY022 + *tel1Δ::KanMX*	This work
AKY053	AKY023 *tel1Δ::KanMX*	This work
AKY054	W3749-1A *TEL01Lmod X-elementΔ::URA3*	This work
AKY055	W3749-1A *TEL01Lmod XCRΔ::URA3*	This work
AKY056	W3749-1A *TEL01Lmod X-element short::URA3*	This work
AKY057	W3749-1A *TEL01Lmod WT XCR X-CoreΔ::URA3*	This work
AKY058	W3749-1A *TEL01Lmod XCRmut X-CoreΔ::URA3*	This work
AKY037	BY4705 *MatA bar1::HIS3 YKU70-6xHIS-TEV-3xFLAG::URA3*	This work
AKY038	BY4705 *MatA bar1::HIS3 yor162-163Δ::KanMX YKU70-6xHIS-TEV-3xFLAG::URA3*	This work
AKY039	BY4705 *MatA bar1::HIS3 ylr176-177Δ::KanMX YKU70-6xHIS-TEV-3xFLAG::URA3*	This work
AKY040	BY4705 *MatA bar1::HIS3 yor162-163Δ::KanMX*	This work
AKY041	BY4705 *MatA bar1::HIS3 yor176-177Δ::KanMX*	This work
AKY043	BY4705 *MatA bar1::HIS3 YKU80- 6xHIS-TEV-3xFLAG::URA3*	This work
AKY044	BY4705 *MatA bar1::HIS3 yor162-163Δ::KanMX YKU80-6xHIS-TEV-3xFLAG::URA3*	This work

AKY045	BY4705 *MatA bar1::HIS3 yor176-177Δ::KanMX YKU80-6xHIS-TEV-3xFLAG::URA3*	This work
EVAY01	BY4705 *MatA bar1::HIS3 yku80Δ::LEU2 ade2del::hisG yor162-163D::KanMX*	E. Bouchard, Wellinger Lab, unpublished
EVAY02	BY4705 *MatA bar1::HIS3 yku80Δ::LEU2 ade2del::hisG ylr176-177D::KanMX*	E. Bouchard, Wellinger Lab, unpublished

Yeast Transformation

A 5 ml culture of the desired yeast strain in YEPD liquid media was grown overnight at 30 ˚C. The cells were diluted in 12 ml to an OD_{660} of 0.25 and grown 3-4hrs to an OD_{660} of 0.8-1.0. OD_{660} was measured by a spectrophotometer and can be converted to cells/ml, using a standardized chart (http://www.pangloss.com/seidel/Protocols/ODvsCells.html). The culture was transferred to sterile 15 ml Falcon tubes and spun at 1500 x g for 1 minute. The supernatant was removed, and the cell pellet was washed with 1 ml sterile nano H_20 and transferred to a sterile 1.5 ml tube. The sample was spun 10 seconds at 21,000 x g and all supernatant was removed. The pellet was resuspended in 50 µl 1X TE/1X LiAc. 2-5 µg DNA for transformation (DNA fragment or replicative plasmid) was added along with 5 µl 10 mg/ml herring sperm carrier ssDNA, denatured for 5 minutes at 100 ˚C and 300 µl PEG solution (40 % PEG, 1X TE pH 10, 1X LiAc). The sample was incubated for 45 minutes at 30 ˚C with agitation at 350 rpm before a 20-minute heat shock at 42 ˚C. The sample was centrifuged twice 10 seconds at 21,000 x g in a microcentrifuge, removing all PEG solution after each spin. The cells were resuspended in sterile nano H_20 and 40 µl and 160 µl were plated on selective media, spread by sterile, acid washed glass beads. For transformants containing antibiotic resistance markers, the final cell pellet was resuspended in 1 or 10 ml of YEPD liquid media and incubated with agitation for 2 hours or overnight at 30 ˚C prior to plating 200 µl and 400 µl on antibiotic containing plates. Cells were grown 2-3 days at 30 ˚C.

Tagging proteins in Yeast

Various experiments performed required the tagging of yeast proteins. This was achieved by modifying the yeast genome such that the proteins of interest were expressed in fusion with protein sequences serving as epitopes, C or N terminally. The protein modifications were verified by Western Blot.

Tbf1-myc

Tbf1 was tagged in the strain EPY007 by digesting pTbf1-myc, containing a 13-MYC C-terminally tagged Tbf1 protein, with PvuII and EcoRV to obtain a DNA fragment containing 140 bp of the N-terminal of Tbf1, a 6 amino acid linker, a 13xMYC tag and a kanamycin (*KanMX*) antibiotic resistance cassette with a TEF promoter followed by a 432 bp region of DNA from TBF1+395 bp. This was purified on agarose gel and transformed into the EPY007 strain, to create the strain AKY001 with the *TBF1 13xMYC*::*KanMX* gene locus.

Reb1-myc

Reb1 was C-terminally tagged with 13xMYC by using the PCR Flap method. Plasmids originally derived from the Pringle Labs pFA6a *HisMX6* plasmids (Longtine et al., 1998) contained a 13xMYC tag with a *HIS3* marker. Primers were designed to amplify to the tags and with the selection markers, with flaps of 40 bp containing homologous sequences to the *REB1* DNA locus (Reb1_Tag_F, Reb1_Tag_R). More specifically, the flaps encompass the last 40 bp of the *REB1* gene, excluding the terminating sequence and the first 40 bp after the termination sequence. Tags were amplified and purified by PCR column purification Kit (Biobasic) before transformation into yeast strain EPY007.

Tagging proteins with His-Tev-Flag

yKu70 was tagged with the 6xHIS-TEV-3xFLAG (HTF) tag by Flap PCR method amplifying the HTF tag with *URA3* selection marker from the pBS1539 plasmid obtained from the Granneman Laboratory (Granneman et al., 2009). The flaps added sequence

homology to 50 bp at the end terminal of *YKU70*, and 50 bp directly downstream of the *YKU70*, eliminating the transcription termination sequence. yKu70 was tagged in BY4705 to create AKY037 and then in EVAY01 and EVAY002. The latter two strains are from a *yku80Δ::LEU2* background and contain deletions of intergenic regions *(yor162-163Δ::KanMX* and *ylr176-177Δ*::*KanMX* respectively). They were mated with BY4705 (Matα), sporulated and microdissected. Cells containing the *YKU80* gene were selected for by a lack of growth on YC-LEU medium. This process created the strains AKY038 and AKY039.

yKu80 was tagged by the Flap PCR method described above, with 2 additional rounds of PCR amplification to add a total of 150 bp of homology to the *YKU80* gene locus at the 5' and 3' end of the tagging cassette. The yKu80 protein was tagged in the wild type BY4705 strain, as well as in AKY040 and AKY041 strains. These were derived from the EVAY01 and EVAY02 parental strains, respectively, mated with BY4705 to regain a functional yKu80.

Modification of TEL01L and TEL03L in S. *cerevisiae*

Plasmids pAK013 and pAK014 were linearized with BamHI and NotI (see Fig. 1 for illustration) and transformed into various haploid yeast strains with a W303 background (see transformation protocol below), to obtain 01L-WT XCR::*URA3* and 01L-XCRmut::*URA3* strains. Clones from each strain were screened by extracting DNA and performing PCR and southern blotting. PCR screening was performed with primers QP5-R and Arsdel-F. DNA for southern blotting was digested by SalI and probed with TEL01Lp1. Positive clones were sequenced. This resulted in a final close to native TEL01Lmod construct containing short sequences not present in the wild type subtelomere. Due to the cloning processes outlined above, a 51 bp sequence consisting of 3 bp pBluescript multiple cloning site, 16 bp SK sequencing primer and 32 bp bacterial plasmid DNA was added between telomeric repeats and subtelomere XCR. Recombination was then induced to remove the *URA3* gene and one RS site (see protocol below), leaving behind a 628 bp sequence of

wild type DNA upstream of TEL01L, followed by a 334 bp sequence of residual RS site and plasmid DNA. Integrative plasmids pAK018, pAK007T and pAK016 were linearized with NsiI and Eco53kI (see Fig. 3 for illustration) and transformed into various desired yeast strains in the W303 background. DNA was extracted for screening by PCR and southern blot. Primers QP5-R and SSB1-pRSF were used for PCR screening. DNA was digested by NruI and probed with TEL03Lp1 for southern blotting. Positive clones were sequenced. This produced strains containing 03L-WT XCR::*LEU2* and 03L-XCRmut::*LEU2*. TEL03Lmod contains a sequence of 56 bp between telomeric repeats, consisting of 7 bp pBluescript multiple cloning site, 16 bp SK sequencing primer and 32 bp bacterial plasmid DNA. Directly upstream of the X-Core, TEL03L has a 136 bp sequence of residual non-native sequence after recombination to remove the *LEU2* selection marker (see protocol below).

Site-Specific Recombination

In yeast strains with modified subtelomeres TEL01L and TEL03L, selection markers *URA3* and *LEU2*, respectively, were removed by site-specific recombination, by Recombinase R. Recombinase R recognizes 58 bp RS sites and excises DNA between them when sequences are in the same orientation, creating DNA circles from excised DNA (Gartenberg, 2012). Replicative plasmid pEP21A containing *TRP1* and Recombinase R (RecR) under a galactose (GAL1-10) promoter was derived from the pB3-X plasmid from the Kornberg Lab (Gartenberg, 2012; Griesenbeck et al., 2003). pEP21A was transformed into yeast cells with *RS-URA3-RS* or *RS-LEU2-RS*. Cells were grown on YC-*TRP* + glucose plates at 30 ˚C for 2-3 days. RecR expression was induced by restreaking colonies on to plates with galactose as a carbon source (YC-*TRP* + galactose). After growth on galactose containing media for 2-3 days at 30 ˚C, 2-3 colonies were grown in 3 ml liquid YEPD media overnight at 30 ˚C. The OD of these colonies were measured in order to plate an estimated 100 cells on YEPD plates, which were grown for 2-3 days at 30 ˚C. Successful site-specific recombination was evaluated by growth on selective media. Clones were streaked on selective plates lacking uracil or leucine (depending on what selection marker was removed) and grown for 2-3 days at 30 ˚C. A lack of growth on selective media

indicated successful *URA3* or *LEU2* excision. Clones that had expelled the replicative plasmid during incubation periods in non-selective media (YEPD) were screened for by lack of growth on Yc–TRP selective media for 2-3 days at 30 ˚C.

Serial dilution growth tests on solid plates: "Spot Tests"

Spot tests were used to visualize transcriptional silencing of *URA3* when placed interior to the TEL01L telomere. Cells were taken from YEPD plates and grown to a stationary phase in liquid. An OD_{660} reading was taken and converted to cells/ml, as indicated above. Strains were diluted to 3 x 10^7 cells/ml in 1 ml of sterile nano H_2O. Diluted cells were transferred to a 96-well plate and diluted in 5 serial 1:5 serial dilutions in sterile H_2O. Serially diluted cells were spotted onto YC or YC+ 1mg/ml 5-FoA plates using a replica plater (Sigma-Aldrich) or multichannel pipette. When a multichannel pipette was used, 10 µl of each dilution was plated. Plates were grown for 4-5 days at specified temperatures and pictures were taken using an ImageQuant LAS4000 (GE Healthcare).

PCR mediated Gene Deletions

Multiple strains were created in which genomic loci were replaced with auxotrophic or antibiotic resistance cassettes using PCR generated deletion cassettes. These were amplified from pRS plasmids described by Brachman *et al.* (1998) or from genomic DNA from strains in which the gene was already deleted. Primers for gene deletion can be found in Table 6 (Brachmann et al., 1998).

Mating, Sporulation and Microdissection

Although the experiments done in these projects all involve haploid strains, mating was used in some occasions to facilitate genomic modification of yeast strains. Cells of opposite mating types (Matα; MatA) in liquid YEPD cultures were mixed together in a 1:1

ratio and grown for 3 hours to overnight. The cultures were diluted in 3 ml YEPD and grown overnight. Sporulation of these cells was induced by first pelleting 700 µl of the mated culture. These cells were washed three times in 5 ml sterile nano H_2O and resuspended in 3 ml sterile 0.5 % KAc and grown for 3 days at 23 ˚C. The cells were observed under a light microscope to verify the presence of "tetrads" generated by the two successive cell divisions of meïosis within one cell. 300 µl of the sporulated culture was spun down and washed with 1 ml sterile nano H_2O. The cell wall was digested by resuspending the pellet in 50 µl of zymolase, incubating for 5 minutes at room temperature and slowly adding 300 µl of sterile sorbitol to stop zymolase activity. 20 µl of the digested cells were spread along the edge of a YEPD plate for microdissection. During microdissection, individual spores were separated on the plate and grown for 3-5 days at 30 ˚C. The genotypes of the spores were determined by growth on selective media to evaluate for the selection markers present or absent in each spore.

Yeast Genomic DNA extraction and quantification

3 ml of the desired yeast strains were grown in liquid YEPD or selective media overnight at 30 ˚C to a stationary phase. 1.5-3 ml cells were pelleted, washed once with ddH_20 and transferred to 1.5 ml tubes. Cells were then lysed according to the Fast Prep or Slow Prep method, depending on downstream use of the extracted DNA:

Fast Prep Method Lysis

300 µl lysis buffer (100mM Tris, 50mM EDTA, 250mM NaCl, 1% SDS) and 300 µl acid washed beads were added to the cell pellet, and the tubes were sealed with parafilm. The cells were lysed using a FastPrep (MP Biomedicals) 2x 45 seconds at 4 m/s. The bottom of the 1.5 ml eppendorf tubes were pierced with a hot 23G1 needle and placed into a second tube. The stacked tubes were centrifuged for 1 minute at 400 x g in a microcentrifuge, allowing the lysed cells to pass through the beads into the new tube. 300 µl lysis buffer was added to the lysate.

Slow Prep Method Lysis

Cells were resuspended in 500 µl Winston lysis buffer (2 % Triton-X, 1 % SDS 10 %, 100 mM 5mM NaCl, 10 mM 2 M Tris-HCl pH 8, 1 mM 0.5 M EDTA) and transferred to 5 ml glass tubes. 500 µl acid washed glass beads were added. Cells were lysed by vortexing for 30 seconds and resting on ice 30 seconds, repeated nine times. Lysate was collected from beads with a pipette and transferred to 1.5 ml tubes. Beads were rinsed with 100 µl TE, which was collected again and added lysate. Subsequent steps are as below, using 750 µl phenol-chloroform and chloroform instead of 500 µl.

Extraction continued

DNA was extracted by adding 500 µl phenol-chloroform to the lysate and vortexing and spinning the sample for 5 minutes at 21,000 x g. 550 µl of the upper, aqueous phase was transferred to a new 1.5 ml tube and extracted again with 500 µl phenol-chloroform (vortexed and spun 5 minutes at 21,000 x g). 500 µl of the upper phase was transferred to a new 1.5 ml tube and extracted with 500 µl chloroform. The final 450 µl supernatant was transferred to a new tube and 1 ml -20 ˚C EtOH was added to precipitate DNA either for 20 minutes at -80 ˚C, or minimum 1 hour at -20 ˚C. The DNA was centrifuged for 20 minutes at 16,000 x g at 4 ˚C and the supernatant was removed. The pellet was washed with 1 ml of -20 ˚C 70% EtOH and centrifuged for 5 minutes at 4 ˚C. The EtOH was removed, pellets were resuspended in 500 µl TE/RNase (7.5 mg/ml RNAse in TE pH 8) and heated to 37 ˚C for 30 minutes, vortexing at 5 and 15 minutes. DNA was precipitated again by adding 1 ml cold EtOH, 15 µl 3 M NaOAc pH 5,2 and 1 µl glycogen 10 mg/ml, vortexing, and incubating the tubes for 20 minutes at -80 ˚C, or minimum 1 hour at -20 ˚C. The DNA was pelleted in a microcentrifuge at 4 ˚C for 20 minutes at 16,000 x g, and supernatant was removed. The pellet was washed with 1 ml 70 % EtOH as described previously. Excess EtOH was evaporated from DNA pellets under the fume hood (approximately 30 minutes). DNA was resuspended in 35 µl nano H_20. DNA was quantified (ng/µl) by fluorescence spectroscopy, and the samples were conserved at -20 ˚C.

Yeast total RNA extraction

All buffers and solutions used for RNA extraction were RNAse free. Workspace, pipettes and tube racks were washed with RNAseZap Decontamination spray (ThermoFisher) before beginning experiments.

10 ml of yeast cells were grown in liquid YEPD or selective media to OD_{660} 0.8. Cells were pelleted in 15 ml tubes, washed with 1 ml sterile molecular grade H_20 and transferred to 1.5 ml tubes. Cell pellets were resuspended in 300 µl 1X LETS buffer (see composition of 2X LETS below) and kept on ice from this point. 300 µl acid washed glass beads were added and tubes were sealed with parafilm. Cells were lysed using the MP Biomedicals FastPrep machine 45 seconds at 4 m/s two times, resting cells on ice for 2 minutes between each round. Glass beads were removed by piercing a hole in the bottom of the 1.5 ml tube with a hot 23G1 needle, placing the tube into a new tube and centrifuging at 400 x g for 1 minute. 300 µl 1X LETS buffer was added to the lysate in the bottom tube. The RNA was extracted by adding 500 µl phenol-chloroform-isoamyl (25:24:1), then vortexing and spinning the sample for 5 minutes at 16,000 x g at 4˚C. 550 µl of the upper aqueous phase was transferred to a new tube, and the extraction step was repeated, transferring 500 µl to a new tube after the second spin. 500 µl chloroform-isoamyl (24:1) was added to the sample before vortexing and spinning again for 5 minutes at 16,000 x g at 4 ˚C. 450 µl of the supernatant was transferred to a new 1.5 ml tube, and 1 ml cold EtOH, 30 µl 3 M NaOAc pH 5.2 and 2 µl 10 mg/ml glycogen were added. The sample was vortexed and placed at -80 ˚C for 30-45 minutes or -20 ˚C minimum 1 hour to allow RNA to precipitate. RNA was pelleted in a microcentrifuge for 15 minutes at 16,000 x g at 4 ˚C. The supernatant was removed, and the RNA pellet was washed with 1 ml cold 70% EtOH and spun for 5 minutes at 16,000 x g at 4 ˚C. The supernatant was removed and the pellets were dried. The pellets were resuspended in 10 µl nuclease free H_20 and 1:50 dilutions were quantified using NanoDrop Spectrophotometer (Thermo Fisher Scientific).

DNaseI Treatment of RNA

50 µg of RNA (quantified by Nanodrop), was digested using DNaseI (New England BioLabs), according to the manufacturer's directions. Instead of a heat inactivation of the enzyme, RNA was extracted one time with 500 µl phenol-chloroform-isoamyl (25:24:1) and one time with chloroform-isoamyl (24:1) as described above. RNA was precipitated from solution by adding 1 ml cold EtOH, 30 µl 3 M NaOAc pH 5.2, 2 µl 10 mg/ml glycogen, vortexing and placing at -80 ˚C for 45 minutes or -20 ˚C for minimum 1 hour. The RNA was pelleted for 15 minutes at 4 ˚C at 16,000 x g and washed with 70 % cold EtOH. The pellets were dried and a 1:50 dilution of the sample was quantified using the NanoDrop Spectrophotometer (Thermo Fisher Scientific).

Yeast Rapid Protein TCA Extraction

3 ml yeast culture was grown until OD_{660} 1 and pelleted by centrifugation at 4 ˚C. Cells were washed with 1 ml cold nano H_20 and transferred to 1.5 ml tubes and kept on ice from this point. 100 µl TCA 20 % and 100 µl acid washed glass beads were added to the cell pellet and tubes were sealed with parafilm before lysis using the FastPrep (MP Biomedicals) for 45 seconds at 4 m/s. The bottom of the tube was pierced with hot 23G1 needles, placed in new 1.5 ml tubes, and centrifuged 30 seconds at 900 x g to collect the lysate. After removing the upper, bead-containing tube, the lysate was spun again for 3 minutes at 16,000 x g at 4 ˚C. All TCA supernatant was removed by pipette, and the pellet was resuspended in a mix of 20 µl Laemmli Buffer 1x (4 % SDS 10%, 20 % Glycerol, 120 mM 1 M Tris-HCl, 2.8 ml H_2O), 5 µl 1 M DTT, after which the solution turned yellow. Tris Base 1 M pH 8.8 was added such that the solution changed from yellow to blue (5-10 µl). The sample was incubated for 5 minutes at 100 ˚C and centrifuged at room temperature for 3 minutes at 21,000x g. The supernatant was conserved at -20 ˚C until further use.

Western Blot

Western blots were essentially carried out as described previously (Towbin et al., 1979). Extracted proteins in this project were analyzed on 8 % SDS-PAGE gels. Samples were migrated for 30 minutes at 120 V and approximately 2 hours at 150 V, using the PageRuler Prestained Protein Ladder (ThermoFischer Scientific) as a reference for molecular weight. Proteins were then transferred to Hybond-C nitrocellulose membranes (GE Healthcare) in a BioRad mini Trans-blot Cell apparatus for 90 minutes at 100 V. Membranes were stained with Ponceau S to verify protein quality and transfer efficiency. Membranes were blocked with 5 % m/v powdered milk or BSA dissolved in 1X Phosphate buffered saline (PBS) with 0.1 % Tween, for 1 hour at room temperature with agitation. Then they were washed two times for 15 minutes with PBS-Tween, changing the wash buffer for each wash. The membranes were incubated at 4 ˚C overnight with a 5 ml solution containing primary antibody in 1 % m/v powdered milk or BSA dissolved in 1xPBS. Table 4 depicts antibody concentration and blocking agents (BSA or Milk) for each antibody used in this project. The membranes were washed again as above and incubated for 1 hour with a secondary antibody, peroxidase conjugated anti-mouse at a 1:5000 dilution in 1 % m/v powdered milk or BSA in PBS 1x. The membranes were washed, the proteins were exposed with 300-400 µl Enhanced Chemiluminescence (ECL) (Amersham) and visualized with an ImageQuant LAS 4000 (GE Healthcare). For experiments with yKu70 and yKu80 immunoprecipitation using the anti-TAP or anti-Flag primary antibodies, 200 µl of ECL Plus (Amersham) was used per membrane.

Table 4: Antibodies used in this project.

Antibody	Producer	Dilution	Solution
Monoclonal ANTI-FLAG M2 antibody (mouse)	Merck	1:1000	1 % Milk
TAP Tag Monoclonal Antibody (mouse)	Thermo Fisher	1:500	1 % Milk
		1:1000	1 % BSA
Anti-c-myc (mouse)	Roche	1:1000	1 % Milk
Anti-HA (mouse)	Roche	1:1000	1 % Milk

Southern Blot

In this project, Southern Blots were used to analyze telomere length and to screen for genomic modification of clones in yeast strains. Southern blotting was essentially carried out as described previously (Southern, 1975). After extraction and quantification of yeast DNA, 500 ng -1 µg was digested with restriction enzymes. In experiments measuring telomere length, enzymes XhoI, NruI or SalI were used to analyze global telomere length, TEL03L telomere length or TEL01L telomere length respectively. DNA was migrated on 0.75 % agarose gel in TBE buffer overnight at 35 V, or over day for 3-4 hours at 75 V for screening experiments, and then transferred overnight to a Hybond-XL nylon membrane (GE Healthcare). The membrane was hybridized for a minimum of 6 hours with a radiolabeled probe containing a sequence specific to the DNA fragment to be visualized. Probes obtained by PCR amplification or plasmid digestion were 150-300 bp in length and radiolabelled using Klenow (SPP) random priming labeling procedure. 150 ng of probe was denatured in 9µl ddH20 before adding 11.4µl LS Buffer (see composition below), 1 µl 1 mM dATP dTTP Mix, 1 µl Klenow, 3 µl $dCTP^{32}$, 3 µl $dGTP^{32}$ and incubated for 3 hours to overnight at room temperature. The reaction was stopped by the addition of 25 µl Stop Solution (0.2 % SDS, 50 mM EDTA, Tris pH 8) and heating to 68 ˚C for 10 minutes. Probes were purified with ProbeQuant G-50 columns (GE Healthcare) as per the manufacturer's directions. Probes were denatured for 5 minutes at 100 ˚C before hybridization with a membrane. After hybridization, excess probe was removed by washing the membrane for 20 minutes with 2x SSC (saline-sodium citrate) at room temperature. Hybridized DNA was visualized using a Typhoon FLA9000 (GE Healthcare). Gel Analyzer software was used to determine the band size, using the radiolabelled molecular ladder (1 kb+, Thermo Fischer Scientific) as calibration.

LS Buffer: 50 µl HEPES 1 M pH 6.6, 50 µl TM (250 mM Tris-HCl, 20 mM $MgCl_2$, 50 mM β-mercaptoethanol), 14 µl 2.1 mM Roche Random Hexamers

Northern Blot

All buffers and solutions in used for RNA extraction were RNAse free. Workspace, pipettes and tube racks were washed with RNAseZap Decontamination spray (ThermoFisher) before beginning experiment. Samples of 15 µg of DNAseI treated RNA were diluted to 5 µl in nano H_2O. A mixture of 2 µl MOPS 10 X (Wisent), 2 µl Formaldehyde 37 %, 2 µl RNA dye (see composition below) and 9 µl Formamide were added to each RNA sample. Northern blots for TERRA were carried out as described previously (Pfeiffer and Lingner, 2012). Samples were heated 10 minutes at 60 ˚C prior to migration in a 1.2 % formaldehyde agarose gel for approximately 5 hours at 70 V. The gel was treated through a 20 minute incubation in 50 mM NaOH, and then a 30 minute incubation in 10x SSPE (2.4 M NaCl, 0.3 M NaoAC, 0.2 M KH_2PO_4, 0.2 M EDTA), and transferred overnight to a Hybond N+ membrane (GE Healthcare). RNA samples were crosslinked to the membrane by exposure to 700000 J/cm^2 UV for 2 minutes using the UVP HL-2000 HybriLinker. The membrane was then hybridized overnight with either a radiolabelled DNA fragment (see description for Klenow labeling above) at 65 ˚C, or an oligonucleotide probe, labeled with T4 polynucleotide kinase (New England Biolabs) according to the manufacturer's directions, at 42 ˚C. The membrane was washed 10 minutes at room temperature in 0.1x SCC+ 0.1 % SDS. Hybridized RNA was visualized using the Typhoon FLA9000 (GE Healthcare).

RNA dye: 50 % Formamide, 0.1 % Bromophenol Blue, 0.1 % Xylene Cyanol

Purification of His-Tev-Flag Tagged Proteins

Purification of HTF tagged proteins was carried out as suggested by the Granneman Lab, based on a modified version of the technique used previously (Granneman et al., 2009). Strains with yKu70 and yKu80 tagged with His-Tev-Flag (HTF) and untagged strains were grown in 250 or 500 ml YEPD cultures at 30 ˚C to an OD_{660} of 0.5-0.6. Cells were spun down, washed with 50 ml ice cold PBS and transferred to 50 ml

tubes. Pellets were weighed, frozen in liquid N_2 and conserved at -80 ˚C until lysis and purification. Cells were lysed by adding 1 v/gram pellet TN150 buffer (50 mM Tris-HCl pH 7.8, 150 mM NaCl, 0.1 % NP-40) and 2-3 v/v Zirconia beads to the cell pellet and repeating a cycle of 1 minute vortex and 1 minute rest on ice five times. 3 v/v of TN150 were added, the sample was vortexed and then spun at 4 ˚C for 30 minutes at 4600 x g. The supernatant was transferred to 1.5 ml tubes and spun at 4 ˚C for 20 minutes at 21,000 x g. The supernatant was transferred to new tubes and quantified by Bradford Assay (Bradford, 1976). HTF tagged yKu70 and yKu80 proteins were immunoprecipitated (IP) using 40 µl Anti-Flag M2 Magnetic Beads (Merck) for 2-3 mg total protein. The beads were equilibrated by washing twice with 10 gel volumes of TN150 buffer before adding whole cell extract (WCE) and adding TN150 buffer for a final volume of 1 ml. The proteins were incubated with beads overnight at 4 ˚C with rotation. The beads were collected with a magnet to discard the flow through and washed twice with 20 gel volumes of TN1000 buffer (50 mM Tris-HCl pH 7.8, 1 M NaCl, 0.1 % NP-40) and twice with 20 gel volumes of TN150, inverting tubes several times between each wash. The beads were then resuspended in 100 µl of TN150. Cleavage of the tagged proteins from the magnetic beads was attempted by adding 5-20 u of His-TEV (provided by the Service de Purification de Proteines, UdeS) or AcTEV (Thermo Fisher) and incubating 1-6 hours at room temperature or overnight at 4 ˚C.

Chromatin Immunoprecipitation (ChIP)

ChIP was carried out essentially as described in previous studies, with some modifications (Adam et al., 2001; Larcher et al., 2016). 200 ml yeast culture of strains with untagged, or 13xmyc-tagged Tbf1 or Reb1 proteins were grown at 30 ˚C to OD_{600} 0.5-0.8 in YEPD. 5.6 ml 37 % formaldehyde was added (1 % final concentration) and cultures were incubated for 20 minutes at room temperature, swirling briefly after 5 minutes. 12.5 ml filtered 2 M glycine was added (125 mM final concentration) and cells were incubated 5 minutes at room temperature. The culture was split into 50 ml aliquots and cells were

pelleted at 4 ˚C for 5 minutes at 1600 x g and washed twice with cold TBS (20 mM Tris-HCl pH 7.5, 150 mM NaCl) and spun down at 4 ˚C for 5 minutes at 1600 x g between each wash. Washed pellets equivalent to 50 ml of culture were transferred to 1.5 ml tubes, frozen in liquid N_2, and conserved at -80 ˚C until further use. 1 tube per IP was defrosted on ice and resuspended in 250 µl ChIP lysis buffer (50 mM HEPES-KOH pH 7.5, 140 mM NaCl, 1 mM EDTA pH 8.0, 1 % Triton X-100, 0.1 % Na-deoxycholate, 1 mM PMSF) containing 1X cOmplete Mini Protease Inhibitor (Roche). 250 µl acid washed lysing beads were added and the tube was sealed with parafilm. Cells were lysed with FastPrep (MB Biomedicals) 4 times for 30 seconds at 6.5 m/s, resting cells on ice for 2 minutes between each round of lysis. The tube was pierced with a heated 23G1 needle and placed in a 2 ml tube to collect the lysate by centrifugation for 1 minute at 400 x g. DNA was sheared by sonication 30 times for 1 minute at an amplitude of 100, inverting the tubes and resting on ice for 1 minute after every sonication round. The sample was centrifuged at 4 ˚C for 10 minutes at 19,000 x g and the WCE (supernatant) was conserved. 5 µl 0.4 µg/µl monoclonal mouse anti-c-myc antibody (Merck) were added to 500 µl WCE and incubated overnight at 4 ˚C with rotation. 20 µl WCE was also incubated overnight at 4 ˚C without antibody to serve as the input fraction. 50 µl Pierce Protein A/G Magnetic Beads (Thermo Fisher Scientific) per IP were equilibrated by washing 3 times with 1 ml ChIP lysis buffer. Washed beads were added to tubes containing WCE and antibody and incubated for 1 hour at 4 ˚C with rotation. Beads were washed for 4 minutes with 1 ml of the following cold buffers, and collected with a magnet between each wash:

2 times with ChIP lysis buffer without Protease Inhibitor

2 times with ChIP lysis buffer with 50 mM NaCl final

2 times with ChIP wash buffer (10 mM Tris-HCl pH 8.0, 250 mM LiCl, 0.5 % IGEPAL CA630, 0.5 % Na-deoxycholate, 1 mM EDTA pH 8.0)

1 time with TE pH 8

The IP was eluted from the beads with 50 µl TE pH 8.0 + 0.1 % SDS and an incubation at 65 ˚C with 1200 rpm agitation for 10 minutes. The sample was vortexed after 5 minutes. A second elution was done with 150 µl TE pH 8.0 + 0.1 % SDS for 5 minutes at 65 ˚C with

1200 rpm agitation. Each time, the beads were collected with a magnet. The supernatants were transferred to a new 1.5 ml tube. 180 µl TE pH 8.0 + 0.1 % SDS was added to the input fraction. All samples were incubated at 65 ˚C overnight to reverse the protein-DNA crosslink. The RNA was digested from the sample by adding 195 µl TE-SDS 0.1 %, 3 µl 10 mg/ml RNaseA, 2 µl 20 mg/ml glycogen and incubating 1 hour at 37 ˚C. The samples were centrifuged for 1 minute at 16,000 x g to collect cap condensation, and 7.5 µl 10 mg/ml Proteinase K and 11 µl SDS 10 % were added. Samples were incubated at 50 ˚C for 1 hour. DNA was extracted by adding 400 µl phenol-chloroform and vortexing before centrifugation for 5 minutes at 19,000 x g. 300 µl of the aqueous supernatant was transferred to a new tube and extracted again with 400 µl phenol-chlorofom. Centrifugation was repeated as above and 250 µl supernatant was transferred to a new tube. 400 µl chloroform was added and the samples were centrifuged as described above. 200 µl aqueous supernatant was conserved and NaCl was added to a 200 mM final concentration, in addition to 2 volumes of cold EtOH. DNA was precipitated overnight at -20 ˚C and pelleted at 4 ˚C by spinning for 10 minutes at 19,000 x g. DNA pellets were washed with cold 70 % EtOH, dried under the fume hood and resuspended in 60 µl sterile molecular grade H_20. DNA was conserved at -20 ˚C until used for qPCR reactions.

Quantitative PCR (qPCR)

qPCR in this project was carried out using the KAPA SYBR ® FAST qRT-PCR Master Mix Kit (KAPA Biosystems) as per the manufacturer's protocol, as well as the UdeS RNomics Platform (https://rnomics.med.usherbrooke.ca/fr/welcome). Primer pairs were first tested on genomic DNA extracted from strains to be used in other experiments in order to ensure a good amplification efficiency and target specificity (see results, Chapter I). The geometric efficiency of each primer pair was assessed by evaluating the slope of a standard curve produced by Ct values measured from serial dilutions of amplified target DNA. qPCR was performed with genomic DNA in 5 serial dilutions of 1:8, starting with 10 ng DNA. The slope was converted using an online qPCR Efficiency Calculator provided

by Thermo Fisher (https://www.thermofisher.com/uk/en/home/brands/thermo-scientific/molecular-biology/molecular-biology-learning-center/molecular-biology-resource-library/thermo-scientific-web-tools/qpcr-efficiency-calculator.html). Additionally, a no template control (H_2O) and, when possible, DNA extracted from a negative control strain negative (lacking target locus) were included in each experiment. This allowed for an assessment of primer dimer formation, background amplification levels and non-specific amplification. The qPCRs were performed using either a touchdown qPCR assay (Zhang et al., 2015), TEL77 or TEL80 programs (below). The primer pairs used for all qPCR experiments and their amplification efficiencies are listed below (Table 5).

Program TEL77
95 ˚C 15 seconds
60 ˚C 15 seconds
77 ˚C 30 seconds (Ct measurement)
Repeat steps 40x
95˚C 15 seconds
72 ˚C 15 seconds
Increase to 95 ˚C over 10 minutes
(Ct measurement)
95 ˚C 1 second
60 ˚C 15 seconds
72 ˚C 5 minutes

Program TEL80
95 ˚C 15 seconds
60 ˚C 15 seconds
80 ˚C 30 seconds (Ct measurement)
Repeat steps 40x
95 ˚C 15 seconds
72 ˚C 15 seconds
Increase to 95 ˚C over 10 minutes
(Ct measurement)
95 ˚C 1 second
60 ˚C 15 seconds
72 ˚C 5 minutes

Table 5: Primer Pairs used for qPCR in this project
% amplification efficiency was measured for each primer pair by evaluating the slope of a standard curve produced by Ct values measured from 1:8 serial dilutions of amplified target DNA

Target	Primer 1	Primer 2	% efficiency
TEL01Lmod	Ch2R	TXCRM	90.50
TEL03Lmod	oEP008	QP5R	116.00
TEL06R	6R_F1	6R_R1	93.40
TEL15L	oEP001	oEP002	92.40

TEL10R	oEP005	oEP006	148.46
RTP1	RTP1_For	RTP1_Rev	91.40
PAF1	Paf1B	Paf1B	90.70
HMRE	HMRE-3F	HMRE-2R	90.10

ChIP qPCR

qPCR was performed on DNA extracted from input and IP samples and diluted 1:8 and 1:16 in nano H20, respectively. Each ChIP qPCR included a standard curve with a 4 serial 1:8 dilutions of an input sample for each primer pair used. The percent amplification efficiency of the qPCR reaction with each primer pair was calculated based on the slope of the standard curve of Ct values, as described above. ChIP signals were calculated from Ct values to obtain the percentage of input immunoprecipitated. Experiments with TEL01Lmod strains normalized ChIP signals from tagged strains to untagged strains. ChIP experiments with TEL03Lmod strains were carried out with a no-antibody control sample set to normalize for background signal. The ChIP signals were normalized again to signals produced by negative control loci, as is shown in Results, Chapter I.

Reverse Transcription qPCR

1 µg of DNaseI treated RNA was reverse transcribed with M-MuLV reverse transcriptase (provided by Service de Purification de Proteines, UdeS). The reaction was set up on ice in RNase free conditions, including a reaction without reverse transcriptase (-RT) for each sample. TERRA was targeted for reverse transcription using a CA-primer. Act1 was used as a reference gene and was targeted for reverse transcription by a Random Hexamer Mix (Roche).

RT Mix:
1 µg DNaseI treated RNA
2 µl 60µM Random Primer Mix*
2 µl 10x MRT Buffer
0.2 µl MMuLV RT 200 U/µl / H_2O in -RT
1 µl 10mM dNTP
0.5 µl RNaseI Inhibitor 40 U/µl (SPP, #RI-L)
1 µl 0.5 mM CA primer
20 µl total volume

RT Program
Step 1: 25 ˚C 5 minutes
Step 2: 42 ˚C 1 hour
Step 3: 65 ˚C 20 minutes

* made by dilution of 14.2 µl 2.1mM Roche Random Hexamer Mix in 500 µl H_2O

The complementary DNA (cDNA) produced was diluted 1:5 in nano H_2O. 2 µl of the diluted cDNA was used for qPCR reactions with KAPA SYBR ® FAST qRT-PCR Master Mix Kit or RNomics Platform. Each qPCR reaction included a serial dilution of cDNA (same as above) to ensure adequate amplification efficiency and cDNA quality. Fold change in TERRA RNA expression was calculated by ΔΔCt method (Livak and Schmittgen, 2001), normalizing to Act1 transcription, then comparing normalized values from mutated XCR strains to wild type XCR strains.

Telo-PCR

Telo-PCR was used to amplify individual telomeres for subsequent length measurement by migration on agarose gel. DNA extracted by "Slow Prep" method (see above) was diluted to a 60 ng/µl concentration before C-tailing with TdT transferase (New England Biolabs). 9 µl H_2O was added to 1 µl DNA, heated for 5 minutes at 95 ˚C and cooled on ice. 5 µl 10x Transferase buffer, 5 µl 2.5 mM $CoCl_2$, 1 µl dCTP, 0.1 µl TdT transferase 20 U/µl and 28.9 µl H_2O were added to the 10µl DNA. The solution was heated to 37 ˚C for 30 minutes and then 70 ˚C for 10 minutes. C-tailed DNA was then amplified by PCR using GoTaq Long PCR Master Mix (Promega) as shown below.

PCR Mix

1 µl C-tailed DNA
10 µl GoTaq Long PCR Master Mix 10x
0.5 µl Ars Seq R 20 µM
1 µl YV6_teloPCR_dG 20 µM
7.5 µl H2O

PCR Program

Step 1: 95 ˚C 2 minutes
Step 2: 94 ˚C 20 seconds
Step 3: 65 ˚C 30 seconds
Step 4: 65 ˚C 2.5 minutes
Repeat Step 2-4 40x
Step 5: 72 ˚C 10 minutes

Table 6: Primers used in this project

Name	Sequence 5'-3'
TEL03Lmod plasmid construction	
RS_LEU2_F	TACGTTAATGACGTCATGGTCGCTCTAGAACTAGTGGATCC
RS_LEU2_R	ACTCAATTGCGTATCTATACCATGGTGCACCATATCGACTAGATCC
GB_Ty5_F	GAAGATGACAAGGTAATGCATGCTTTCATCATTCGCGCTG
GB_Ty5_R	ACCATGACGTCATTAACGTAAAAG
GB_X_F	GGTATAGATACGCAATTGAGTGTG
GB_X_R	GGATCCACTAGTTCTAGAGCTCGCGACATGCGGCCGCCCTAACACTAC CCTAACACT
TEL03Lmod XCR Site directed PCR mutagenesis	
tbf1_mut1_F	TAGAGCGGCCGCCGTAACACTACCGTAACACTA
SSb-pRS1-F	GAATAGACCGAGATAGGGTTGAG
tbf1_mut2_F	CAACTTACTCTCCATTAGCCTACCTCTCC
tbf1_mut3_F	GGAGACAGGTAAAATCACGGTTAGAATAGGG
tbf1mut-1b-F	CTACGCTAACACTACGCTATTCTAACCGTGATTTTAC
tbf1mut-1b-R	TGTTAGCGCGGCCGCATGTCG
tbf1_mut_4_F	ACCGCTTAGCCTACCATCGAC
tbf1_mut_4_R	GTGGAGTTGGATACGGGTAG
Reb1mut1F	GTAGTTGGAGCGTAACGGTTATGGTGG
Reb1mut1R	GCGTATCCAACTCCACTACC
Reb1mut2F	CGTAACGAGTGGAGAGGTAG
Reb1mut2R	CTGTCTCATTCAACCGTACC
TEL01Lmod plasmid construction	
TEL01L_GB_F	GCTCCACCGCGGTGGCGGCCGCATGTATGATGCTGGGGAGG
TEL01L_GB_RB	CTTGTTAACTCGAGCTTAAGAGAAGTGACGCATATTCTATACG
TEL01L_GB_FB	TCTTAAGCTCGAGTTAACAAGAACAAGATTGCAGATCAGG
TEL01L_GB_R	GATCCACTAGTTCTAGAGCTCCTAACACTACCCTAACACAG
URA3_NruI_F	TCATTCGCGACAGATTGTACTGAGAGTGCAC
URA3_HpaI_R	CATTGTTAACGTGCGGTATTTCACACCG
RS_URA3_F	TATACTTAAGCGAAAAGTGCCACCTGACGT
RS_URA3_R	TACAGTTAACATAGTTAAGCCAGCCCCGAC

TEL01Lmod XCR Site directed PCR mutagenesis	
TEL01mut1-F	TGGTAGCGTAAGTGGCAGTGGGTTG
TEL01mut1-R	TTACGCTACCATCCACCATGACCTAC
TEL01mut2-F	TGGGTGAGTGGTAGTAAGTAGAG
TEL01mut2-R	CCGTTACGCTCCAATTACCCATATCC
TEL01mut3-F	TGGAGGCAGCGTAATGGAGCGTAAGTTGAGAGACAGG
TEL01mut3-R	CTCGTTACGCTGTCCCATTCAACCATAC
TEL01mut4-F	CGCTGTGTTAGCGTAGTGTTAGGAGCTCTAG
TEL01mut4-R	CCTAATCTAACGCTGGCCAACCTGTC
Sequencing of TEL01Lmod and TEL03Lmod X-elements	
Xel-F	TACGCACACGGATGCTAC
Xel-R	GGTATAGACCGCTGAGGCAAG
Reb1 tagging	
Reb1_Tag_F	TGATTATTTTAGCTCCAATATTTCAATGAAAACAGAAAATCGGATCCCC GGGTTAATTAA
Reb1_Tag_R	TTATTGAGTTTTTCGCTTTCACCAATTATATTTTCCGGAAGAATTCGAGC TCGTTTAAAC
yKu70 tagging	
Ku70_Tag_F	CGATAAAAGAAGAAAAGAAGCCCTTTGATAAAAAGCCGAAATTCAAT ATAGAGCACCATCACCATCACC
Ku70_Tag_R	CTACCAAATATTGTATGTAACGTTATAGATATGAAGGATTTCAATCGTC TTACGACTCACTATAGGG
yKu80 tagging	
yKu80_Tag_F	TGAAGCGCGGTGAACAACACAGTAGGGGAAGTCCAAACAATAGCAAT AATGAGCACCATCACCATCACC
yKu80_Tag_R	CTCTTTAACTGTGGTGACGAAAACATAACTCAAAGGATGTTAGACCTTT TTACGACTCACTATAGGG
Ku80htfTagAmpli2_F	AAACTGAGCTTGAGAGGGAAAAGATCCCGGACCTAGAAACGCTATTG AAGCGCGGTGAAC
Ku80htfTagAmpli2_R	AGTAGTATGACAATTATTTACCCGCTATTTATTTTTTTTTCTCTTTAACTG TGGTGACGA
Ku80htfTagAmpli3_F	ATCAAGAAAGTAGACAAATTAAAACTCGACTCCGAACTAAAAACTGAG CTTGAGAGGG
Ku80htfTagAmpli3_R	GCTAGTGTTCAAAGTTACAAGGTAACAATGCAAATCAGTAGTATGACA ATTATTTACCCG
Gene deletions and amplifications	
yKU80-480 FOR	TTGTTGGCGCAATCGGTAGC
yKU80+472 REV	TCTTTTACACTTTTCAACCCCTGTTTGT
SIR4-348-F	GTATGTGAGTACATATATCCGCAG
SIR4+220_3'-R	GTTCTTGGTATTTGATGGGTTGCTC
TELI-FOR	AACACTAAGTGTGAAGCCTGATC

TELI-REV	AGTTATACGATAACAGAGCTAGC
yKu70F	TGAATAAGCATGATATTAGACGG
yKu70R	GGACCCACAAAGTAATTGTCAGG
tbf1-164	CCTCAATGCTTTGCCCTTCCTTG
tbf+953	CCAACTTTCGCCAATCCTAACAGGA
Construction of probes for Southern Blot	
TEL01Lp1F	CCTTGAAACATCATAAAGTAGCTTTCCGGA
TEL01Lp1R	CAGGTACGAAACGCTAAGAAC
TEL01L P3F	ATCGTATGCATGACGTCTAAGAAAC
TEL01L P3R	TGCATAGTTAAGCCAGCCC
TEL03L-p1F	AGCTTTCATCATTCGCGCTGA
TEL03L-p1R	CGTCAACAGGTTATGAGCCCT
6R_P1_F	GAATTACAAGGGAACAATGAGCAG
6R_P1_R	TGTCTTTAATGATACCGCTTGACTTG
7L_P1_F	CCTGTAAACGACAAAGAACTTTAAATGTG
7L_P1_R	TACAGAGGAATTTTCTGAAGCTATTAATAGAAG
11R_P1_F	TTTTTGAATTTCTATCGATTAAGCTCTATACCAG
11R_P1_R	TAAAAGTAGTGCCACATTTCCTTTGC
13R_P1_F	AAACAAGTAGCAAATCATAGCAAGAG
13R_P1_R	CTATTCCATTTACAGTTACATAAAAAGTTAACC
14R_P1_F	CTTACACCGAAGACGCGG
14R_P1_R	AATTTGCACAAATAAAGAAGTCAGACATATC
Ku70F Probe	ATCGGGGAGAATAAGCCTATACGACT
Ku70R Probe	AACTCGTTGTCAAATGGTTTATCGGC
yKu80 FOR P	CCCTACTGTGTTGTTCACCG
yKu80 REV P	ATCCTCTTAGAATACCCACGGT
PCT300 FOR	TGCCTGCAGGTCGACTCTAG
PCT300 REV	AAACGACGGCCAGTGAATTG
Amplification of specific X-only Subtelomeres (ChIP/ TERRA RT qPCR)	
QP5-R	ACCCACACACTCTCTCACATCTAC
oEP008	GAGAGTAAGTTGGGAGACAGGTAA
TXCRM	ATCTACCTCTACTCTGGGAATTC
Ch2R	GGGAATTCAGATCCACTAGTTCTAGAGCTCC
TEL01L_XCA	AGGTCATGGTGGATGGTAGG
TEL01L_XCMB	TGGCCAACCTGTCTCTCAACT
oEP001	GGGTAACGAGTGGGGAGGTAA
oEP002	CAACACTACCCTAATCTAACCCTGT
oEP005	GGTTATGGTGGACGGTGGATG
oEP006	CCTAACCCTATTCTAATCCAACCCTGATAA
6R_F1	AAATGGCAAGGGTAAAAACCAG
6R_R1	TCGGATCACTACACACGGAAAT

TERRA RT	
Act1F	AACGAATTGAGAGTTGCCCC
Act1R	CAAGGACAAAACGGCTTGGATG
CA TERRA RT	CACCACACCCACACACCACACCCACA
ChIP controls: genomic loci	
HMR-E3f	CGAACGATCCCCGTCCAAGTTATG
HMR-E2r	TCGGAATCGAGAATCTTCGTAATGC
PAF1A	CATACACGCAATGAGAACCCTA
PAF1B	TCATCCAATGTTACAGTCGTCA
RTP1_FOR	AATCAAGGTTACCCGCAGTC
RTP1_REV	AGAAACATGAGGCGGTGATG
Primers tested for qPCR amplification of TEL01Lmod	
TEL01L_Ch_R	ATGGATGGTGGTTCGGAGT
TEL01L_Ch_F	CTCTCTCACATCTACCTCTACTCTGG
TEL1Ch2-F	GGGAATTCAGATCCACTAGTTCTAGAGCTCC
TEL1Ch2-R	TGAGTAGGTCATGGTGGATGGTAG
TEL01LqPCR2F	AGATCCACTAGTTCTAGAGCTCCTAACACTAC
TEL01LqPCR3R	CGGTGGGTGAGTGGTAGTAAGTAGA
TEL01Fhage	CTCCAATTACCCATATCCAA
TEL01Lrhage	ACGATCATTTGTTAGCGTTT
Probes and oligonucleotides for Northern Blot	
TEL03L_TERRA_Plong	TCTCTCACATCTACCTCTACTCTGGGAATTCAGATCCACTAGTTCTAGAGCGGCCG
TEL03L_TERRA_Pshort	TCTGGGAATTCAGATCCACTAGTTCTAGAGCGGCCG
t3TERRA_p1F	ACCCACACACTCTCTCACAT
t3TERRA_p1R	AGTGTTAGcGCGGCC
TLC1-probe FOR	ATCTAAATGCATCGAAGGCAT
TLC1-probe REV	CCATGGGAAGCCTACCATCAC
TeloPCR	
YV6_teloPCR_d G	GGGGGGGGGGGGGGGGGG
QP4-F	CCCTCACTAAAGGGAACAAAAGC
ARS-seq-R	GGGCCTCGTGATACGCCT
Gibson Assembly for silencing constructs (TEL01Lmod)	
GB1F	CTCTCAGTACAATCTGTCGCGAATGACGATTCGGGG
GB11R	AACATATTGGTAGAACACTAACCCCTCAGC
GB13R	GCTAACAAATCTTGTGGTAGCAACACTATCATGGTATCACT
GB9R	GCATAAATTCCTTGTGGTAGCAACACTATCATG
GB16R	CCTTACCCATCTTGTGGTAGCAACACTATCATG

GB10F	GTTAGTGTTCTACCAATATGTTTATGTATTATTGTTGAAAAGTAG
GB15R	GAGGCATAAATTCGATCGTAAATAACACACACGTGC
GB6F	CTTGCCATCATTTGTTAGCGTTTCAATATGGTG
GB12F	CTACCACAAGATTTGTTAGCGTTTCAATATGGTGGG
GB2R	GGGAATTCAGATCCACTAGTTCTAGAGCTCCTAACACTACCCTAAC
GB3R	GGGAATTCAGATCCACTAGTTCTAGAGCTCCTAACACTACGCTAAC
GB4R	GGAATTCAGATCCACTAGTTCTAGCGTCATCAAAATCACTCGCA
GB5F	TACGATCGAATTTATGCCTCTTCCGACC
GB7R	GCTAACAAATGATGGCAAGATCCTGGTATCG
GB8F	CTACCACAAGATGGGTAAGGAAAAGACTCACG
GB14R	GGAATTCAGATCCACTAGTTCTAGTTTTGAAAAAGCCGTTTCTGTAATGAAG

Results Chapter I

Construction of a system to deplete Tbf1 and Reb1 from a subset of subtelomeres

Preamble

A primary objective of this project was to construct a system in which solely the effects of Tbf1 and Reb1 at the chromosomal ends could be observed. Both Tbf1 and Reb1 are essential proteins (Brigati et al., 1993; Chasman et al., 1990), making it impossible to study their function by deleting the respective genes to evaluate potential phenotypic effects. This problem sometimes is bypassed by constructing hypomorphic alleles, which has been done for *TBF1* and *REB1.* Those used in this study and in the Wellinger lab originate from the temperature sensitive (ts) library (Ben-Aroya et al., 2010). However, as both proteins target a multitude of promoters (Bosio et al., 2017; Preti et al., 2010), expression of Tbf1 and Reb1 from hypomorphic alleles could lead to changes in transcription at their targets. This makes it difficult to attribute potential telomeric phenotypes only to the potential impairment of Tbf1 and Reb1 functions at the subtelomere. The phenotype could originate from upstream transcriptional changes in a number of Tbf1 and Reb1 targets. Work done by other groups to characterize the function of these proteins at subtelomeres used the wild type protein alleles, although they worked in systems with heavily modified subtelomeres, or no subtelomeres at all (Arnerić and Lingner, 2007; Berthiau et al., 2006; Fourel et al., 1999; Ribaud et al., 2012). Given the evidence showing that subtelomeres influence telomeric properties (Mak et al., 2009), it is difficult to rule out whether potential phenotypes are merely caused by an alteration of the subtelomeric chromatin. The system constructed in this project circumvents these obstacles by decreasing Tbf1 and Reb1 at two subtelomeres by introducing point mutations into the DNA sequences they are predicted to bind to. Although these modified subtelomeres are not completely wild type, they are minimally modified in attempts to maintain as close to native sequences and chromatin structure as possible. The modifications made to subtelomeres are outlined in this chapter.

Construction of TEL01Lmod and TEL03Lmod strains

The TEL01L and TEL03L telomeres were cloned into bacterial plasmids in order to introduce Tbf1 and Reb1 binding site mutations and re-transformated back into yeast (see Materials and Methods). The potential Tbf1 and Reb1 binding sites at TEL01L and TEL03L were identified using the YeTFasCo database (http://yetfasco.ccbr.utoronto.ca/). Tbf1 and Reb1 have similar binding motif sequences, specifically a 3-cytosine (CCC) repeat sequence (Koering et al., 2000). It is in this CCC sequence to which the point mutation was introduced, exchanging the cytosine for a guanosine (G) nucleotide. The mutations were introduced by "Around the World" PCR (Materials and Methods), using primers designed to span each binding site. After amplification of the plasmid and introduction of the point mutation, the plasmid was transformed into One Shot Stbl3 Chemically competent E.*coli* cells (ThermoFisher). Plasmids were extracted, screened by digestion and sent to be sequencing to ensure that the X-element sequences were successfully mutated. The verified plasmid was then used for a subsequent round of amplification to introduce mutations into additional binding sites. The process of mutation, screening and sequencing was repeated until all predicted Tbf1 and Reb1 binding sites were mutated.

The original plasmid containing the wild type X-element sequence was kept and used as a "wild type" control for all future experiments done with this construct. The modified subtelomere constructs also contained genes *LEU2* and *URA3* used as selection markers for integration into the S. *cerevisiae* genome. These genes were flanked by RS sites, which are recognized by Recombinase R (Gartenberg et al., 2003). The RS sites are utilized to remove selection marker genes after integration into the yeast genome, as one of the benefits of this system is to maintain a close to native structure of the sequences upstream of the subtelomeric repeats. Cloning processes also resulted in some additional sequences upstream of the subtelomere. The native subtelomere and modified subtelomere structures are represented in Figure 9. Two versions of each modified telomere were constructed and transformed into S. *cerevisiae*. 01L-WT XCR (AKY022) and 03L-WT XCR (EPY116) have wild type XCR sequences, but additional sequences of 334 bp

(01L) and 136 bp (03L) upstream of the X-element and 51- 56 bp between the X-element and telomeric repeats. 01L-XCRmut (AKY023) and 03L-XCRmut (EPY117) have the same additional sequences, as well as mutations to the predicted Tbf1 and Reb1 sites in the XCR. Going forward, strains that have gone through this process of telomere modification will be referred to as TEL01Lmod and TEL03Lmod.

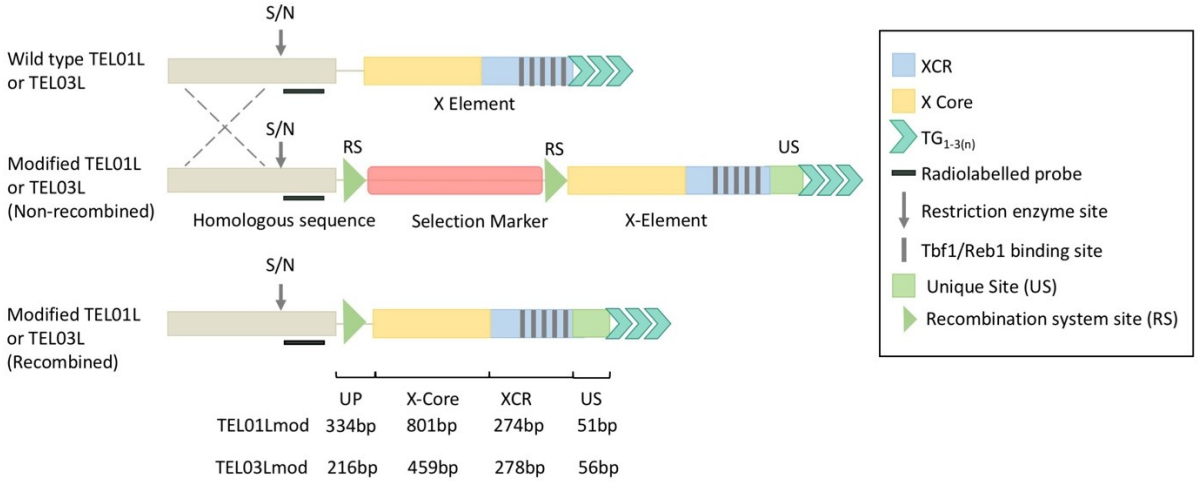

Figure 9: Schema of subtelomeric areas discussed.
Schema illustrating the difference between modified and wild type telomeres. Wild type telomeres are replaced with a modified telomere fragment containing homologous sequences upstream of the X-element, a selection marker (*URA3* or *LEU2*) and wild type or mutated X-elements (indicated with dotted grey lines). Schema labelled "Modified TEL01L or TEL03L (Recombined)" depicts final modified telomere structure after recombinase R targets RS sites to excise the selection marker. Sizes of all elements in the modified subtelomere are indicated below. "UP" marks a sequence added upstream the subtelomere through cloning process. S/N indicates the site cleaved by SalI (S) and NruI (N) restriction enzymes for the visualization of TEL01L and TEL03L, respectively, by southern blots.

Once plasmids were constructed containing TEL01L and TEL03L wild type and mutated X-elements, they were digested and integrated into the genome of a W303 background S. *cerevisiae* strain (strain W3749). The DNA from a number of clones was extracted and used for screening by both PCR and Southern Blot. The size difference between modified and unmodified chromosomal ends allowed us to determine successful integration of the constructs. Shown below is an example of a Southern Blot used to screen for the modified TEL01L subtelomere (Figure 10). The X-element sequence of all

clones were verified once more by sequencing.

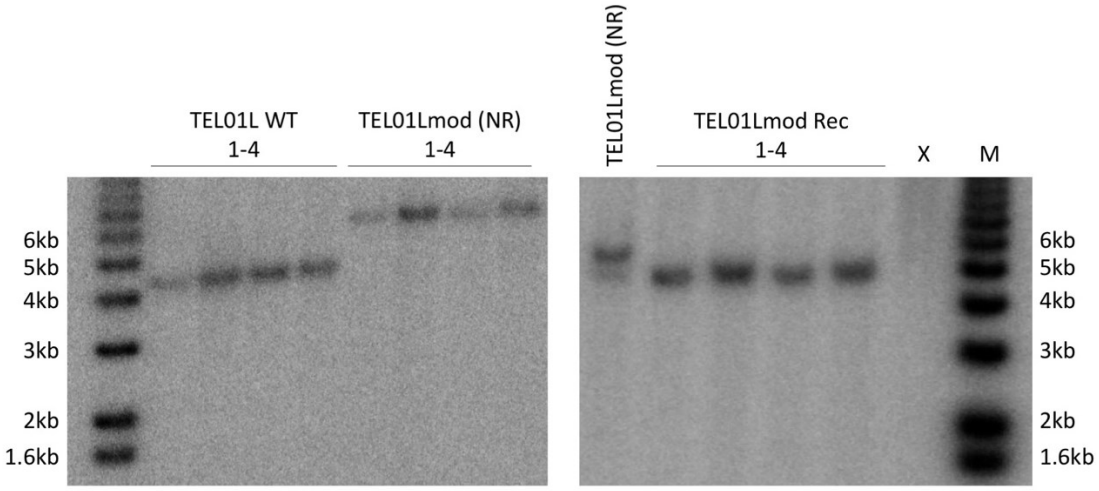

Figure 10: Analysis of integration and recombination of TEL01Lmod subtelomeres. Southern blots with DNA from strains with wild type (WT) TEL01L, not recombined TEL01Lmod (NR) and TEL01Lmod after recombination (Rec) was extracted and digested with SalI. Lane M: Molecular size markers, sizes are indicated on sides of gels. TEL01L WT clones have unmodified TEL01L telomeres, evidenced by the band migration to the expected 4.3 kb (left). TEL01Lmod (NR) clones are from modified, non-recombined telomeres, migrating to the expected length of 5.9 kb. The right blot depicts one TEL01Lmod non-recombined clone with 4 clones of TEL01Lmod after recombination (REC), at 4.7 kb. DNA in lane X was not digested sufficiently.

One of the benefits of constructing this system is that the chromatin structure immediately interior to the subtelomeric repeats remains as close to native as possible. To maintain this chromatin structure, it is also necessary to remove the *URA3* and *LEU2* selection marker genes from their positions interior to the TEL01Lmod and TEL03Lmod subtelomeres, respectively. This was achieved by using recombinase R to target the Recombination System (RS) sites flanking the selection markers (Gartenberg, 2012). The strains were transformed with a replicative plasmid containing recombinase R (RecR) under control of a Gal1-10 promoter and a *TRP1* auxotrophic marker (pEP21A). RecR expression was induced by growing the cells on plates containing galactose as a carbon source. After recombinase induction, the cells were grown in YC medium to allow plasmid expulsion. Clones lacking *URA3* or *LEU2* that had expelled pEP21A plasmids were selected by observing inability to grow on selective medium lacking leucine or uracil and tryptophan. This process reduces the amount of non-native sequence upstream of the

subtelomere from 3200 bp to 136 bp, in TEL03Lmod, and from 2209 bp to 334 bp, for TEL01Lmod. Southern blots performed on these clones demonstrated a decrease in size of the TEL01Lmod and TEL03Lmod fragments. Figure 10 shows the increase in TEL01L size with the integration of the TEL01Lmod, and the decrease after recombination. The final constructs are depicted in Figure 9.

Optimizing amplification of TEL01Lmod

Due to the sequence similarity of different subtelomeres, targeting a single telomere by qPCR requires testing and optimization to ensure that no non-specific amplification of other loci occurs. Multiple primer pairs were tested and optimized to obtain efficiently amplifying primers specific to the TEL01Lmodified locus. The primers were designed such that they did not span any Tbf1 or Reb1 binding sites and produced amplicons of approximately 100-200 bp (Figure 11).

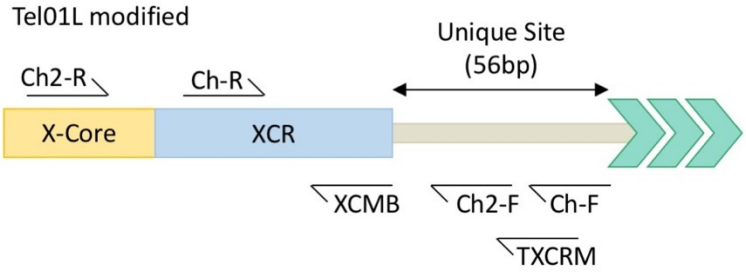

Primer Pair	Amplicon Size (bp)
ChR/ChF	180
ChR/XCMB	92
ChR/TXCRM	171
Ch2F/Ch2R	258
Ch2R/XCMB	196
Ch2R/TXCRM	275

Figure 11: Primer pairs tested for TEL01Lmod ChIP qPCR.
Schema of TEL01L and primer pair sites tested for ChIP qPCR (top). Amplicon sizes are indicated for each primer pair set.

To evaluate primer specificity, each assay included a sample of genomic DNA lacking the TEL01Lmodified construct, which should not generate any PCR products. Additionally, a no template control (H_2O) was included in each experiment to assess primer dimer formation and background amplification levels. Initial tests showed non-specific amplification by primer pairs Ch2F/Ch2R and Ch2R/XCMB. Primer pair Ch2R/TXCRM showed specific amplification of TEL01Lmod DNA, although these assays had high volumes of primer dimer formation and overly high amplification efficiencies (Table 7). These initial assays were done using a touchdown qPCR program (Zhang et al., 2015). Repetition of the qPCR with a program (TEL80, see Materials and Methods) measuring Ct at 80 ˚C improved amplification efficiency, as primer dimers form at a lower temperature and are not detected through this program. The qPCR was further optimized by changing the enzyme from a KlenTaq (SPP) to commercial KAPA SYBR FAST qPCR Master Mix (KAPA Biosystems).

Table 7: The % efficiency of Ch2R/TXCRM primer pair measuring Tel01Lmod by qPCR. Geometric efficiency of Ch2R/TXCRM as assessed by evaluating the slope of a standard curve produced by Ct values measured from serial dilutions of target DNA. qPCR was performed with genomic DNA from 01L-WT XCR and 01L-XCRmut strains, in 5 serial dilutions of 1:8, starting with 10 ng DNA. The qPCR conditions are as indicated.

	% efficiency	
qPCR condition	01L-WT XCR	01L-XCRmut
TD program (KlenTaq)	221	235
TEL80 program (KlenTaq)	143	116
TD program (KAPA)	115	106

Tbf1 and Reb1 ChIP signal is decreased at mutated TEL01Lmod and TEL03Lmod

After mutation of the Tbf1 and Reb1 binding sites at TEL01L, the system was validated by Chromatin Immunoprecipitation (ChIP) qPCR (see Materials and Methods). TEL01L and TEL03L were modified in strains in which the Tbf1 or Reb1 proteins were C-terminally tagged with a 13x*MYC* tag. 01L-WT XCR, 01L-XCRmut, 03L-WT XCR and

03L-XCRmut constructs were integrated into Tbf1-myc (AKY001) and Reb1-myc (AKY003) tagged strains from integrative plasmids (Table 1). Recombination was induced in clones of TEL01Lmod and TEL03Lmod strains to remove the auxotrophic marker genes. ChIP was performed with these strains. Cells were grown to exponential phase and proteins were crosslinked to DNA through the addition of formaldehyde. The cells were lysed and sonicated to shear DNA into ~200 bp fragments prior to Tbf1-myc and Reb1-myc immunoprecipitation (IP) with a mouse anti-myc antibody (Roche) coupled to magnetic IgG beads (Pierce). After isolating precipitated DNA-protein complexes from the rest of the whole cell extract (WCE) through a series of washes, the crosslink was reversed and DNA was extracted. qPCR was performed on these samples, using primer pairs specific for genomic and subtelomeric loci.

As shown in Figure 12A, Tbf1-myc ChIP signal at TEL01Lmod decreased 2.6-fold in strains with mutated XCR sequences. ChIP signals of TEL15L, an X-only telomere with Tbf1 and Reb1 binding sites in the XCR, do not change in 01L-XCR strains. HMRE is a genomic locus that Tbf1 does not bind, serving as a negative control for Tbf1 binding. TEL01Lmod signal in 01L-XCRmut strains is lower than that of HMRE, a negative control locus. Figure 12B shows that Reb1-myc IP efficiency at the mutated TEL01L XCR is decreased 2.52-fold. ChIP signals of TEL015L and RTP1 were measured as a positive controls, as both have binding sites for Reb1 (Bosio et al., 2017). Signals of both positive controls remain consistent in both strains. ChIP signals for 01L-XCRmut is similar to that of HMRE and TEL06R, which have little to no predicted Reb1 binding. The decrease in IP efficiencies of TEL01Lmod with mutated XCR suggests a decrease in Tbf1 and Reb1 binding after mutation of their core binding motifs.

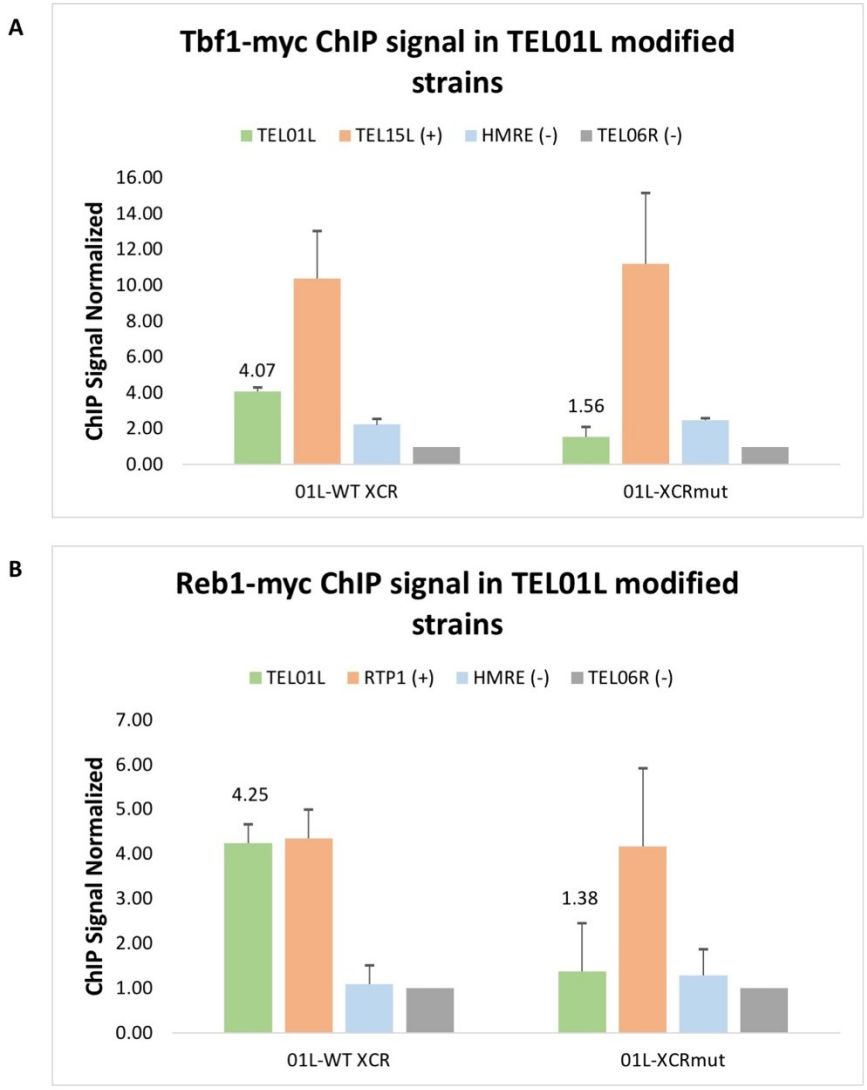

Figure 12: ChIP qPCR of Tbf1-myc and Reb1-myc in TEL01Lmod strains.
ChIP signal was calculated by using qPCR to determine percent of input DNA immunoprecipitated. ChIP signal of Tbf1-myc and Reb1-myc strains was normalized to that of an untagged strain and to ChIP signal from a negative control locus. Cumulative data is represented from 2 independent experiments. **A**. ChIP results for Tbf1-myc, normalized to TEL06R signal. The decrease in ChIP signal in TEL01Lmod strains is significant, with a p-value of 0.00086 generated by a one-tailed T-Test. **B**. ChIP results for Reb1-myc, normalized to signal from HMRE locus. The decrease in ChIP signal in TEL01Lmod strains is significant, with a p-value of 0.0068 generated by a one-tailed T-Test.

Tbf1-myc and Reb1-myc ChIP signal at mutated TEL03Lmod is also decreased when compared to binding at the wild type TEL03L XCR (Figure 13, 14). Figure 13 shows the ChIP signal for Tbf1-myc at subtelomeric and genomic loci. There is a 4.8-fold decrease in Tbf1-myc ChIP signal at TEL03Lmod when the Tbf1 and Reb1 binding sites are mutated. The TEL03Lmod signal in 03L-XCRmut strains is also lower than the signal for PUF6, the negative genomic control. Reb1-myc ChIP signal is decreased 2.46-fold at the mutated TEL03L telomere (Figure 14). The signal for Reb1-myc at 03L-XCRmut is similar to that of PAF1, the negative genomic control. The signal for TEL01L, the positive telomeric control, increases slightly in 03L-XCRmut strains. From these data, we can infer a decrease in Tbf1 and Reb1 binding at TEL03Lmod when predicted binding sites are mutated.

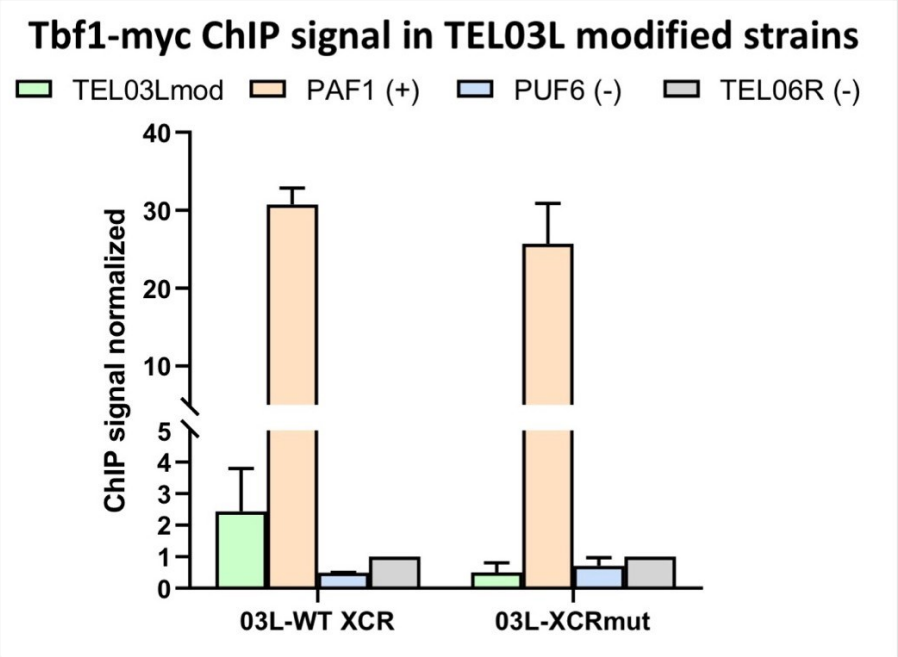

Figure 13: ChIP qPCR of Tbf1-myc in TEL03Lmod strains.
ChIP signal was calculated using qPCR to determine percent of input DNA immunoprecipitated. ChIP signal of Tbf1-myc strains was normalized to no-antibody control experiments and to ChIP signal from TEL06R negative control. ChIP signal for TEL03Lmod is 2.44 for 03L-WT XCR and 0.50 for 03L-XCRmut. Cumulative data is shown from 3 independent experiments. A one tailed T-test comparing fold change in ChIP signal from TEL03Lmod to PAF1 in WT XCR and XCRmut strains results in a p-value of 0.004, indicating a significant difference in fold change.

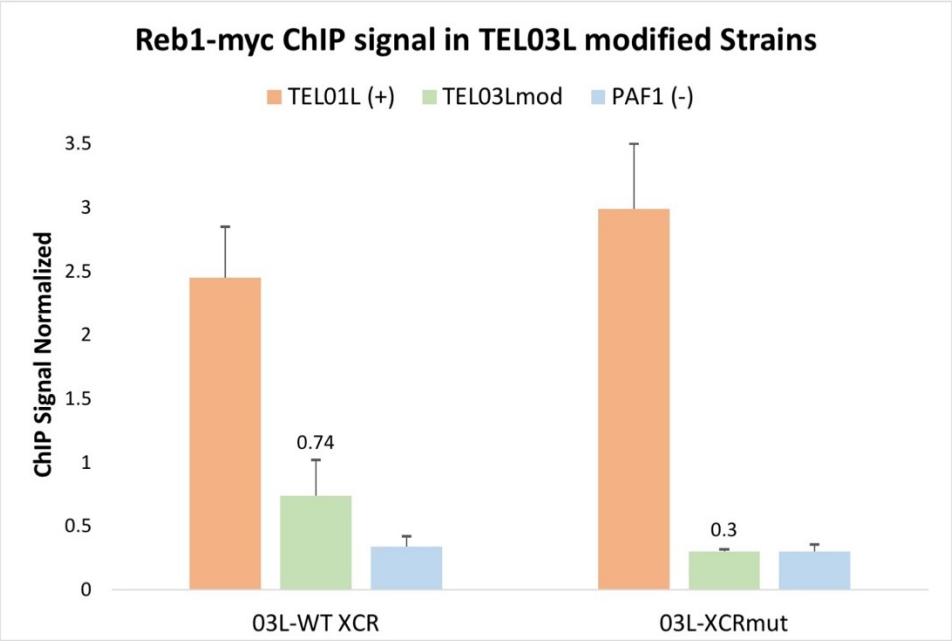

Figure 14: ChIP qPCR of Reb1-myc in TEL03Lmod strains.
ChIP signal was calculated using qPCR to determine percent of input DNA immunoprecipitated. ChIP signal of Reb1-myc strains was normalized to no-antibody control experiments and to ChIP signal from TEL06R negative control. ChIP signal for TEL03Lmod is 0.74 for 03L-WT XCR and 0.3 for 03L-XCRmut. Cumulative data is shown from two independent experiments. A one tailed T-test comparing fold change in ChIP signal from TEL03Lmod to TEL01L in WT XCR and XCRmut strains results in a p-value of 0.026, indicating a significant difference in fold change.

Results Chapter II

Roles of Tbf1 and Reb1 in Telomere Length Maintenance

Preamble

Both Tbf1 and Reb1 are thought to have roles in the regulation of telomere length when bound interior to the telomere repeats (Arnerić and Lingner, 2007; Berthiau et al., 2006). Most experiments done to evaluate the effects of these proteins on telomere length used heavily altered subtelomeres. This makes it difficult to pinpoint whether changes in telomere length observed are due to the presence or absence of the proteins of interest, or because of the changes made to the subtelomere structure. We attempted to clarify the role of Tbf1 and Reb1 in telomere length regulation by measuring telomere length in strains with decreased Tbf1 and Reb1 binding at telomeres with a close to native subtelomere structure.

Global telomere length in TEL03L modified strains

Telomere length was measured by southern blot in strains harbouring the modified TEL03L telomeres (TEL03Lmod), 03L-WT XCR (EPY116) and 03L-XCRmut (EPY117). 03L-XCRmut strains harboured mutations in the Tbf1 and Reb1 binding sites in the TEL03Lmod subtelomere that lead to a significant decrease in Tbf1 and Reb1 binding (see Results Chapter I). Global telomere length was analyzed by Teloblot, a type of Southern Blot for which DNA is digested overnight with the XhoI restriction enzyme and hybridized with a radiolabelled probe that specifically detects fragments with $TG_{1\text{-}3}$ telomeric repeats (called PCT300). The XhoI enzyme cleaves all telomeres with a Y' subtelomere about 900 bp before the start of the telomeric repeats, creating a terminal restriction fragment (TRF) of about 1.2 kb. As these XY' telomeres make up half of the

telomere bulk, the 1.2 kb TRF appears as a thick band on the teloblot and is frequently used to measure bulk telomere length in a population of cells. As expected, Teloblots did not reveal any difference in XY' telomere length between 03L-WT XCR and 03L-XCRmut strains, as seen in Figure 15.

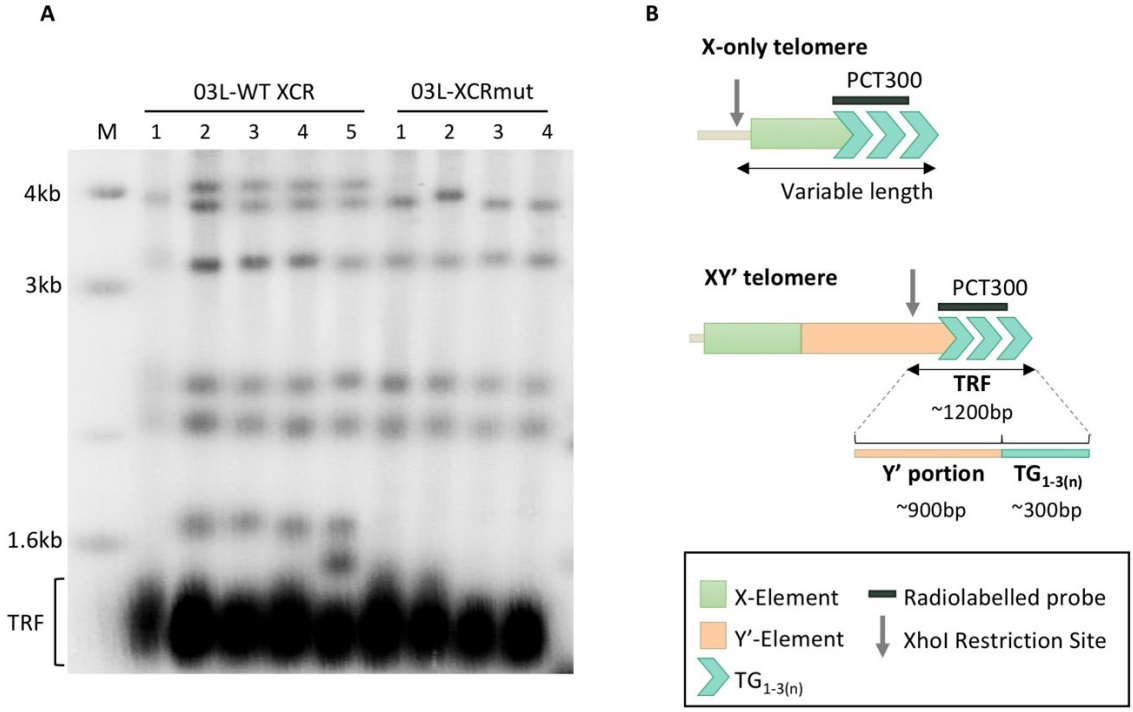

Figure 15: XY' telomere length in TEL03Lmod strains measured by Southern Blot. **A.** Southern blot of DNA from independent clones of 03L-WT XCR and 03L-XCRmut strains (listed at the top), digested with XhoI and hybridized with a PCT300 telomere-specific probe. Molecular marker is marked M. Smear corresponding to TRF is indicated at the bottom left. **B**. Schema of telomeres labelled by PCT300 probe. X-only telomeres migrate to different levels while XY' telomeres migrate as a more uniform smear (TRF).

Lengths of TEL01Lmod and TEL03Lmod telomeres

Specific telomere length of the TEL01L and TEL03L modified telomeres was measured using radiolabeled probes designed to hybridize to DNA sequences of those specific telomeres. Southern blots were run as described above, using DNA digested by different restriction enzymes depending on the telomere analyzed. DNA from 2-7 clones of TEL03Lmod strains was digested with the NruI restriction enzyme and hybridized with

the TEL03Lp radiolabeled probe specific to a DNA sequence upstream of the TEL03L subtelomere (Figure 16A). 03L-WT XCR had no binding site mutations and was used as a control. 03L-WT XCRmut$_1$ had partially mutated XCR sequence with two wild type Reb1 binding sites (EPY118A) and 03L-WT XCRmut had all predicted Tbf1 and Reb1 binding sites in the TEL03L XCR mutated (EPY117). The southern blot shows a variation in the length of the TEL03Lmod telomeres in all clones (Figure 16B). While the length of 03L-XCRmut$_1$ clones only decreases slightly, we observe a significant decrease in telomere length in 03L-XCRmut strains, even when considering the large deviations in telomere lengths of the clones. However, significant shortening of 03L-XCRmut is not observed in subsequent blots (Fig. 20, 23; Table 10, 12). This inconsistency is discussed in further detail in "Discussion of Chapters I-IV". Figure 16 also demonstrates that the TEL03Lmod telomeric repeats are slightly longer than the average expected length of 300 bp, resulting in a TEL03Lmod fragment slightly longer than 2400 bp. This is a phenomenon we observe frequently with the TEL03L telomeres. Telomere lengths for each clone were measured using GelAnalyzer software and are displayed in table 8. The length of TEL03Lmod in different clones varied somewhat, with deviations of 16-43 bp.

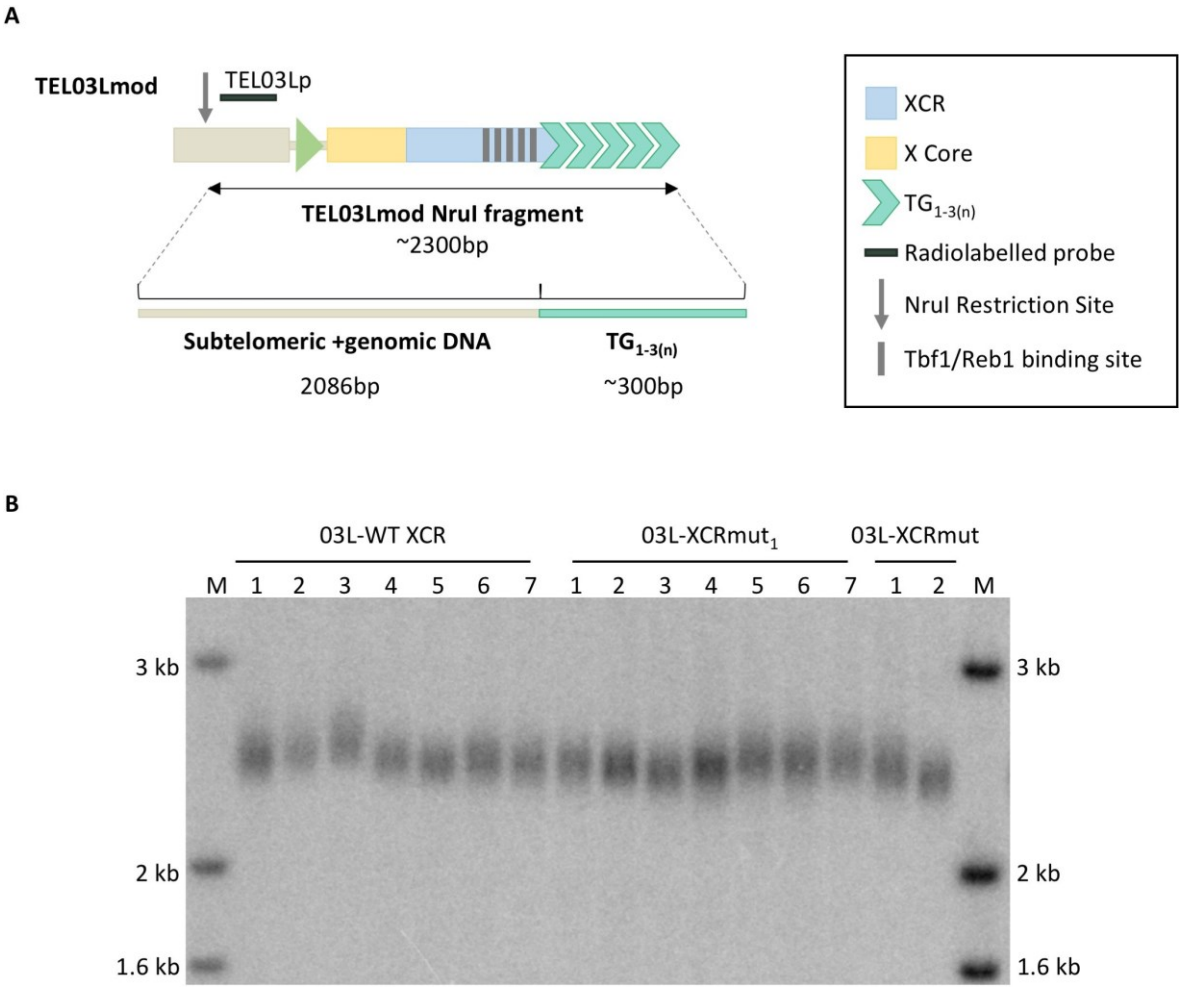

Figure 16: TEL03L telomere length measured by southern blot.
A. Schema of TEL03Lmod telomere labelled with TEL03Lp. **B.** Southern blot of DNA extracted from independent clones of TEL03Lmod strains (listed at top). Molecular marker is marked M. Bands at approximately 2.4 kb correspond to labelled TEL03Lmod fragment digested with NruI restriction enzyme.

Table 8: Average telomere length of TEL03Lmod.
TEL03L length and standard deviations as measured by southern blot, quantified by GelAnalyzer 2010 Software.

Strain	Mean Telomere Length (bp±bp)
03L-WT XCR	2509±43
03L-XCRmut$_1$	2477±25
03L-XCRmut	2432±16

The length of TEL01L modified telomeres was measured in a similar way. DNA of 3 clones of strains of 01L-WT XCR (AKY022) and 01L-XCRmut (AKY023) was digested overnight with the SalI restriction enzyme, creating fragments of the modified TEL01L chromosomal end of approximately 4.7 kb. DNA was hybridized with the TEL01Lp1 radiolabelled probe binding interior to the subtelomere region (Figure 17A). Although some shortening of the 01L-XCRmut clones is visible, it is not significant, as the standard deviations in length are overlapping (Figure 17B, Table 9). Further experiments did not show shortening of 01L-XCRmut telomeres (shown in Fig. 21, Table 10).

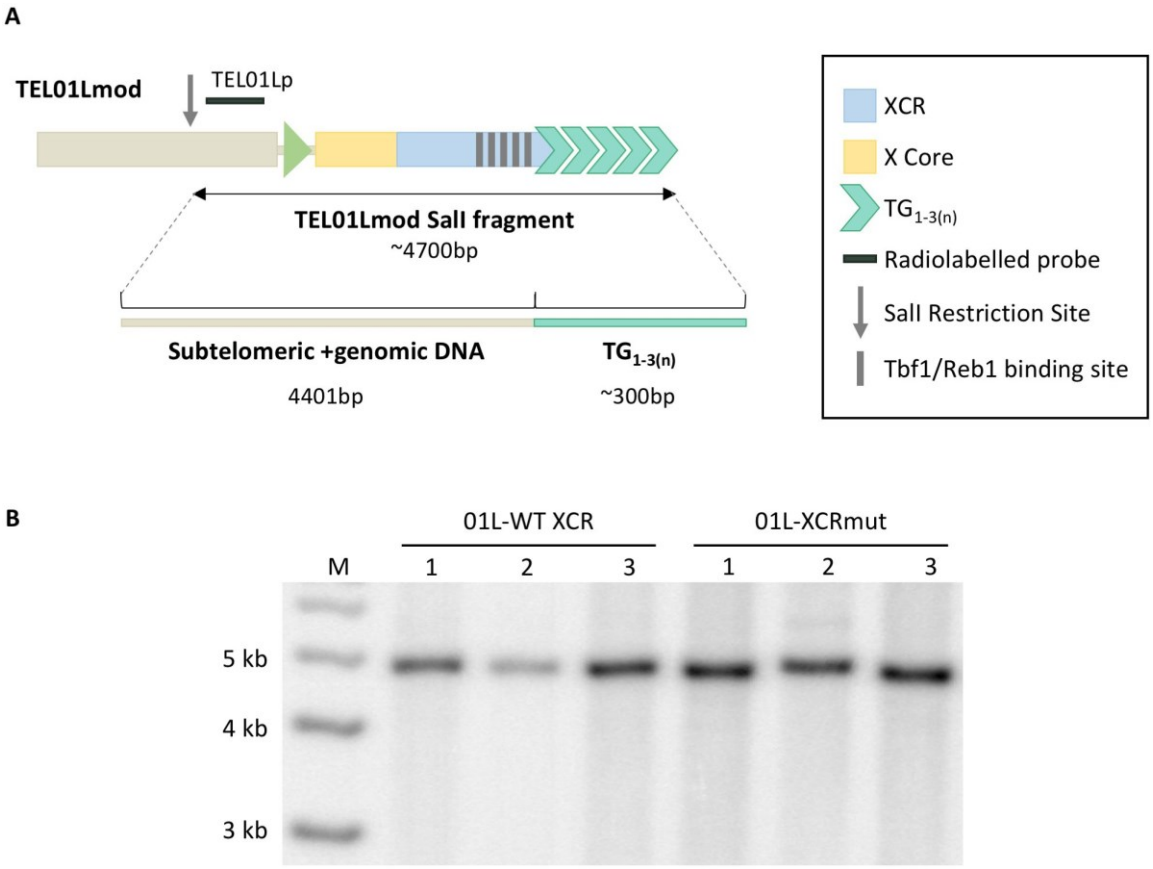

Figure 17: TEL01L telomere length measured by southern blot.
A. Schema of TEL01Lmod telomere labelled with TEL01Lp1. **B.** Southern blot of DNA extracted from independent clones of TEL01Lmod strains (listed at top). Molecular marker is marked M. Bands at approximately 4.7 kb correspond to labelled TEL01Lmod fragment digested with SalI-HF restriction enzyme.

Table 9: Average length of TEL01Lmod.
TEL01Lmod length and standard deviations as measured by southern blot, quantified by GelAnalyzer 2010 Software.

Strain	Mean Telomere Length (bp±bp)
01L-WT XCR	4716±24
01L-XCRmut$_1$	4652±61

Tbf1 and Reb1 as backup telomere length regulators

Tbf1 and Reb1 may have roles as back-up length regulators, maintaining telomere length homeostasis when conventional mechanisms are not fully functioning (Arnerić and Lingner, 2007; Berthiau et al., 2006). Experiments done by both groups were done in strains with a *TEL1* deletion. *TEL1* is important for telomere length maintenance as it recruits telomerase to critically short telomeres, thus *tel1Δ* strains have short, but stable telomeres (Greenwell et al., 1995). We also tested whether Tbf1 and Reb1 have an important role in length regulation when bound at natural subtelomeres in strains with short telomeres. Southern Blots were performed to measure telomere lengths in strains containing the modified TEL01L and TEL03L telomeres in cells with gene deletions causing short telomeres. *TEL1* was deleted in TEL01Lmod and TEL03Lmod strains by integration of a PCR- generated deletion cassette to replace *TEL1* with the *KanMX* antibiotic resistance gene. Clones generated were restreaked once on selective media and two additional times on YEPD plates to allow all telomeres to shorten, grown 3 days at 30 ˚C between streaking. The DNA was extracted and digested with XhoI for subsequent telomere length analysis by Teloblot (Figure 18, 19).

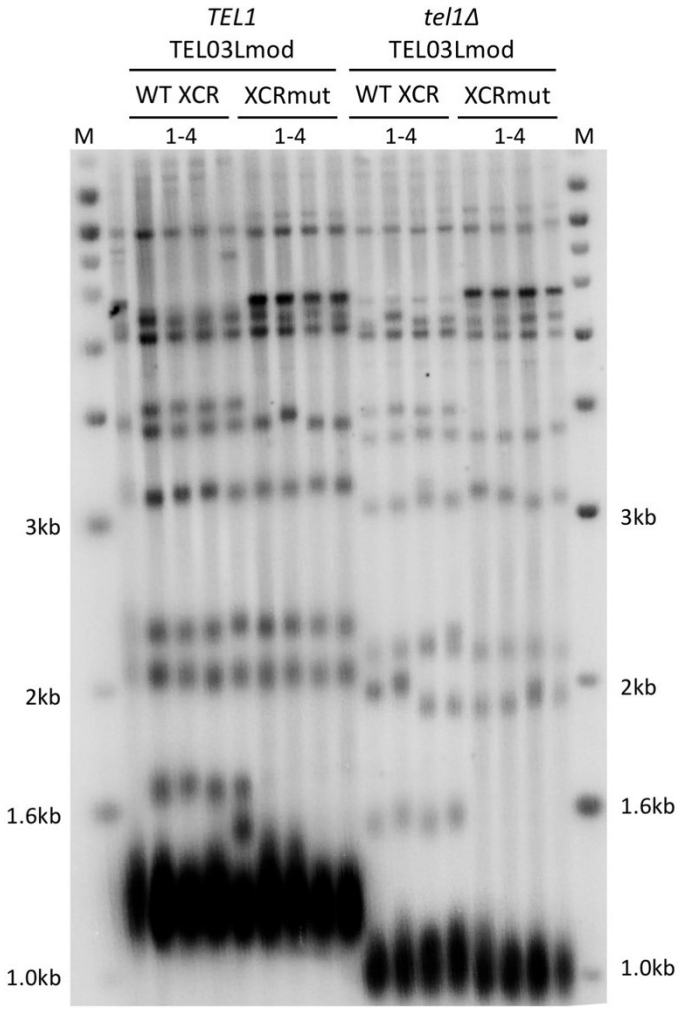

Figure 18: Global telomere length of TEL03Lmod strains with *tel1Δ,* measured by Southern Blot.

Southern blot of DNA from independent clones of genotypes listed at the top, digested with XhoI and hybridized with PCT300 telomeric probe. Molecular marker is marked M.Bottom smear corresponds to TRF and is shorter in *tel1Δ* strains, indicating telomere shortening

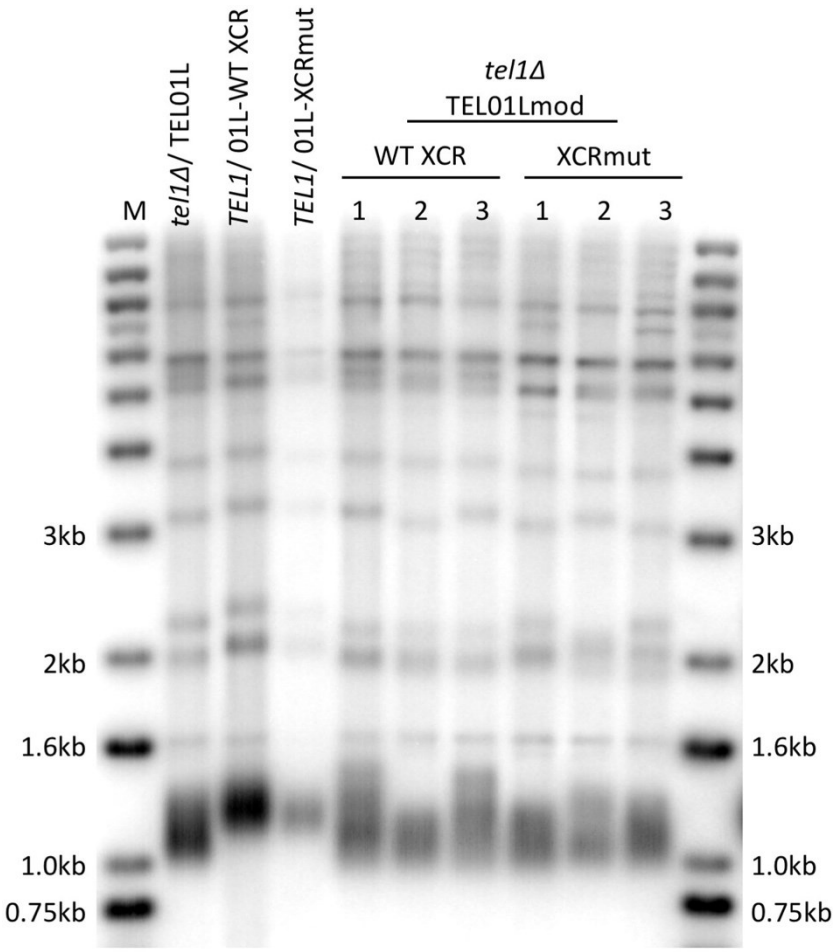

Figure 19: Global telomere length of TEL01Lmod strains with *tel1Δ,* measured by Southern Blot.
Southern blot of DNA from independent clones of genotypes listed at the top, digested with XhoI and hybridized with PCT300 telomeric probe. Molecular marker is marked M. Bottom smear corresponds to TRF. *tel1Δ*/TEL01L is a previously verified strain used as a reference for telomere shortening. *TEL1*/01L-WT XCR and *TEL1*/01L-XCRmut are parental strains with wild type telomere length.

Figure 19 shows that the bulk telomere length in *tel1Δ*/TEL01Lmod strains, as well as the *tel1Δ*/TEL01L reference strain presents as a smear, indicating non-uniform telomere shortening. Clones 2 of the *tel1Δ*/01L- WT XCR and 1 of the *tel1Δ*/01L-XCRmut were selected for use in later experiments as they reached equilibrium in shortening, as indicated by a more compact TRF band. Figure 18 and 19 demonstrate that in a short telomere background, a decrease of Tbf1 and Reb1 at XCR of TEL03Lmod and TEL01Lmod does not influence global telomere length.

We then measured individual telomere length of TEL03Lmod and TEL01Lmod by Southern Blot, using telomere specific radiolabeled probes. TEL03Lmod telomere length in *tel1Δ*/TEL03Lmod strains (AKY030: *tel1Δ*::*KanMX* 03L-WT XCR; AKY031: *tel1Δ*::*KanMX* 03L-XCRmut) were analyzed by measuring the telomere length of 4 clones from each strain (Figure 20). We observe a large variability in TEL03Lmod length in AKY030, as well as slightly longer than average telomeres of 460 bp. In fact, in *tel1Δ* strains, telomeres shorten such that they are closer in length to the average wild type telomere length of approximately 300 bp. Quantification of telomere length with Gel Analyzer 2010 Software determined that there was a shortening of an average of 34 bp in 03L-XCRmut strains in the *tel1Δ* background, when compared to 03L-WT XCR strains (Figure 20, Table 9).

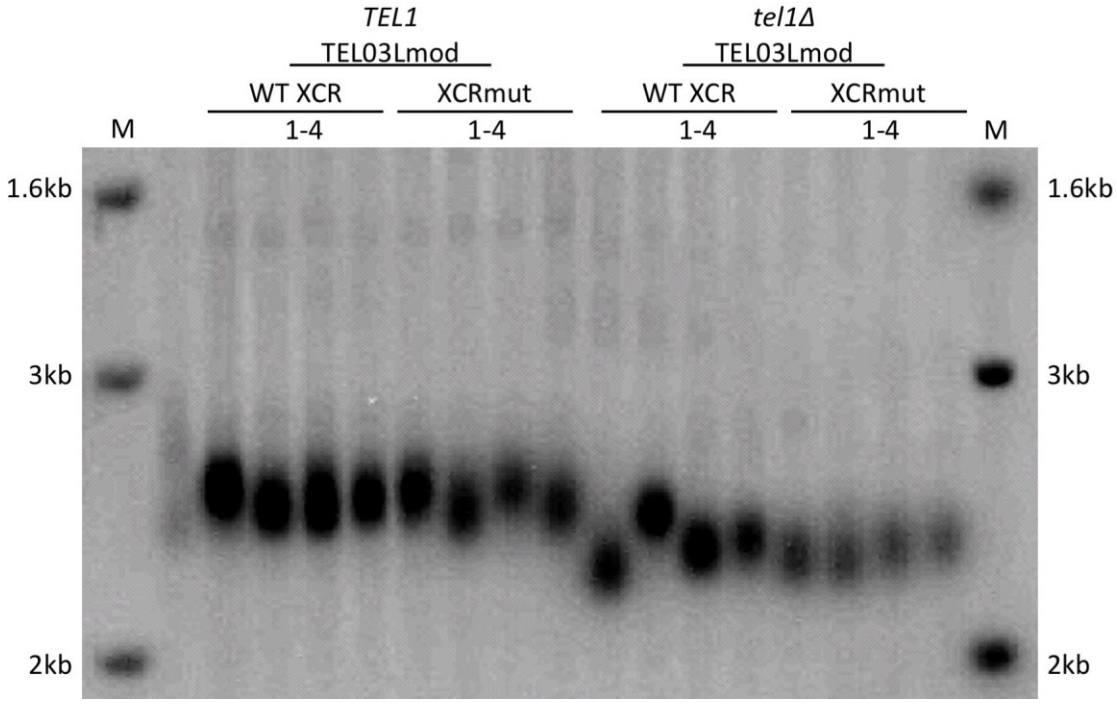

Figure 20: TEL03L telomere length in *tel1Δ background* measured by southern blot. Southern blot of DNA extracted from clones of TEL03Lmod strains (listed at top). Molecular marker is marked M. Bands at approximately 2.3 kb correspond to labelled TEL03Lmod fragment digested with NruI restriction enzyme.

Table 10: Average telomere length of TEL03Lmod in *tel1Δ* strains
TEL03Lmod length and standard deviations as measured by southern blot, quantified by GelAnalyzer 2010 Software.

Strain	Mean Telomere Length (bp ± bp)
TEL1 03L-WT XCR	2540±26
TEL1 03L-XCRmut	2541±34
tel1Δ 03L-WT XCR	2390±70
tel1Δ 03L-XCRmut	2356±35

TEL01Lmod telomere was also measured in a *tel1Δ* background by comparing the telomere length of 3 clones of each strain (AKY022: *tel1Δ*::*kanMX* 01L-WT XCR; AKY023 *tel1Δ*::*kanMX* 01L-WT XCR). Blots previously done to measure the length of the TEL01L modified telomere were executed with DNA digested with the SalI enzyme, producing a TEL01Lmod fragment of ~4.7 kb. The conditions were not ideal for a precise evaluation of change telomere length, as the large band size prevents migration at a high enough resolution to observe small differences in fragment size. We attempted to optimize the conditions for southern blot, first by using High Gel Strength Grade Agarose (BioShop) for low percentage 0.6 % gel, to allow for greater band separation. With these changes only a slight shortening of TEL01Lmod in *tel1Δ* strains could be observed (Figure 21A). We then decreased the size of the DNA fragments by digesting with the XhoI restriction enzyme, such that the fragments were approximately 2 kb, similar to those of TEL03L. As the cleavage site for XhoI on TEL01Lmod is interior to the binding site of the probe used previously, a new probe, TEL01Lp3 was constructed (Figure 21C). These conditions allowed us to observe a decrease of 125-176 bp shortening of TEL01Lmod in *tel1Δ* strains. There was no difference in TEL01Lmod length between 01L-WT XCR and 01L-XCRmut in *tel1Δ* strains. In a *TEL1* background, TEL01L had a higher variability in strains with WT XCR, with a standard deviation of 51 bp, and was, on average, 33 bp longer than TEL01Lmod in 01L-XCRmut.

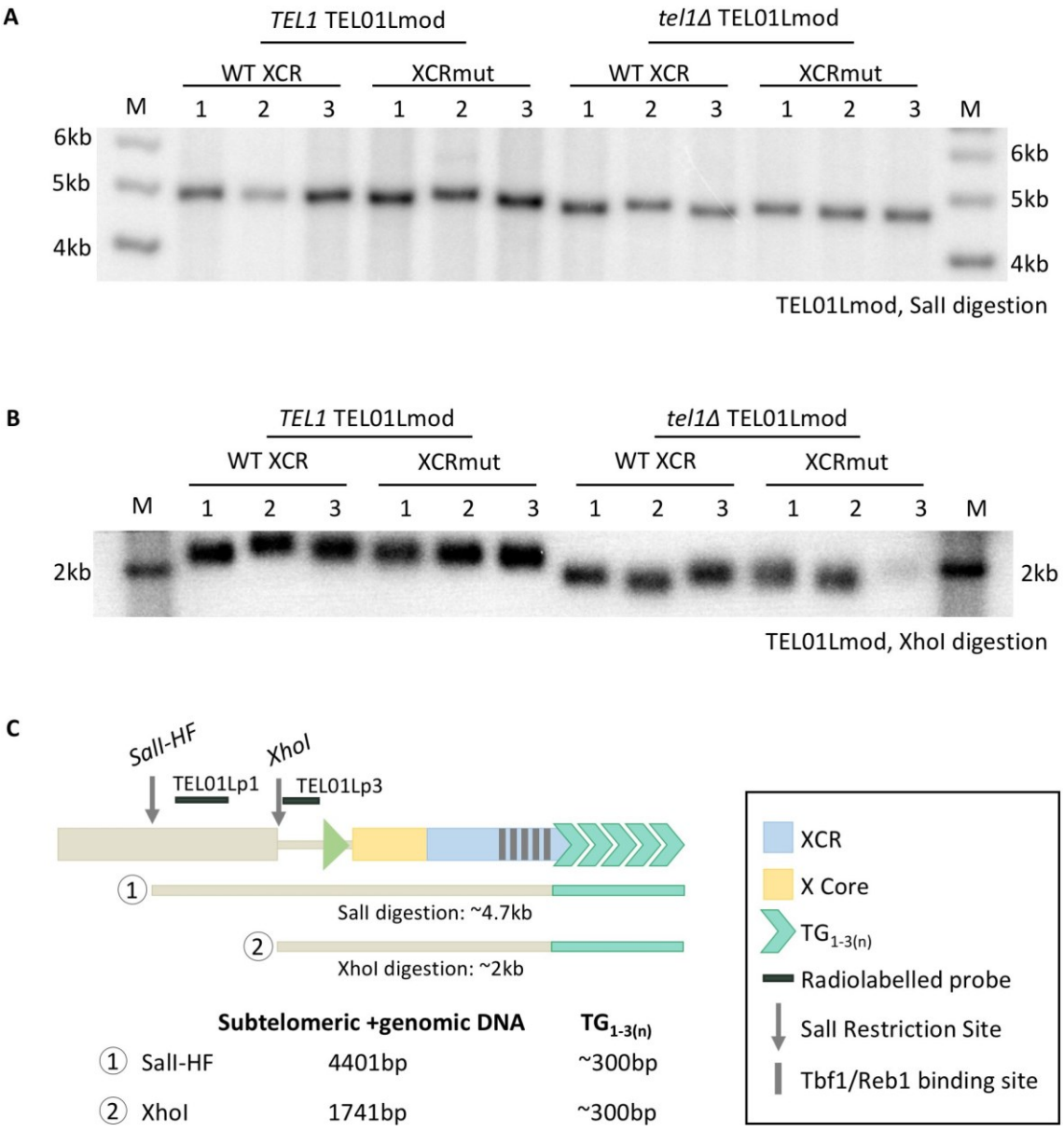

Figure 21: Optimization to measure TEL01Lmod telomere length by southern blot. Southern blot of DNA extracted from clones of TEL01Lmod strains (listed at top of **A**. and **B**.). Molecular marker is marked M. **A**. DNA digested with SalI, hybridized with TEL01Lp1. Band at ~4.7 kb corresponds to TEL01Lmod fragment. **B**. DNA digested with XhoI, hybridized with TEL01Lp3. Band at ~2 kb corresponds to TEL01Lmod. **C**. Schema of TEL01Lmod probe placement, restriction enzyme sites and fragment sizes after digestion.

An alternative approach used to evaluate telomere length of modified TEL01L was Telo-PCR. For this approach, DNA was extracted by Slow Prep method (see Materials and Methods), which produces larger, more homogenous fragments of DNA by lysing cells

through vortexing instead of with a FastPrep machine. The DNA fragments were C-tailed using a TdT transferase (see Materials and Methods). The C-tailed telomeres were amplified with the GoTaq Long PCR kit, using one G-repeat primer (YV216) and one primer binding to the 3'strand of the TEL01L modified subtelomere. The amplicon produced is slightly over 4.8 kb in size, consisting of ~4.5 kb of TEL01Lmod subtelomeric and genomic DNA, ~300 bp of telomeric repeats, and the C-tail. The PCR product was purified by column and digested with XhoI. This produced a telomere repeat-containing TEL01Lmod fragment of approximately 2 kb. Figure 22 shows the migration of digested amplicons. TEL01Lmod length is decreased in all *tel1Δ* strains, but when comparing TEL01Lmod length of 01L-WT XCR and 01L-XCRmut in *tel1Δ,* no change was observed (Table 10).

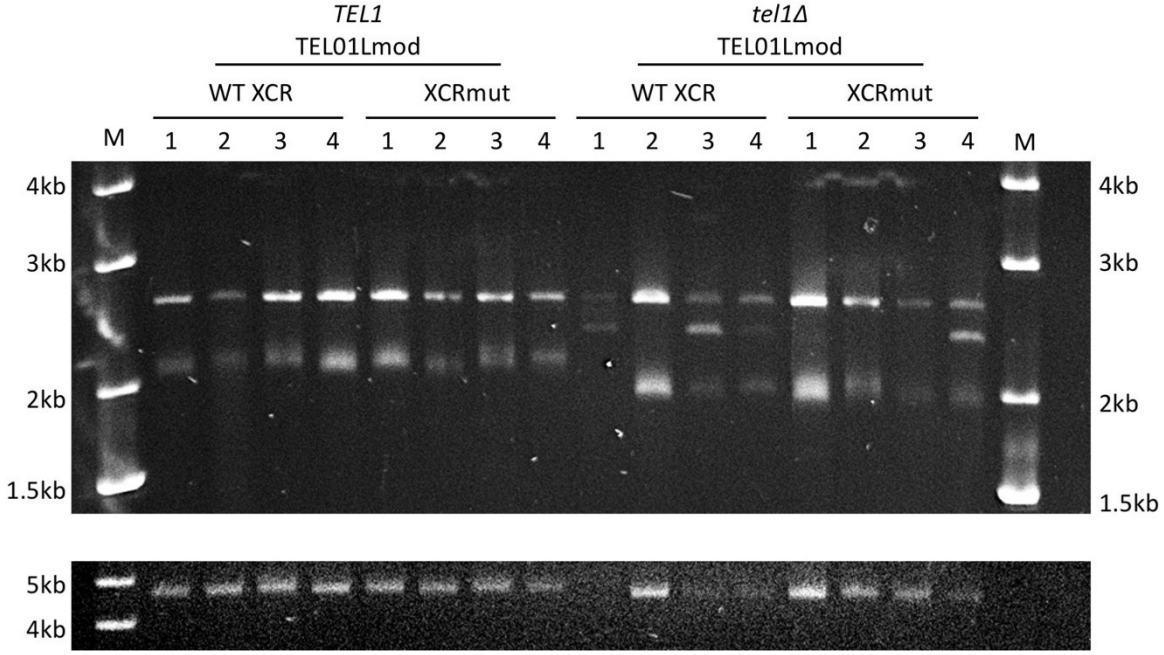

Figure 22: TELO PCR of TEL01Lmod before and after digestion with XhoI.
DNA from clones of TEL01Lmod strains (indicated at top) was extracted by Slow Prep method, C-tailed with TDT transferase, and amplified with TEL01Lmod specific primers. Top gel: amplicons post-XhoI digestion. Upper band corresponds to DNA upstream of the subtelomere, cleaved by XhoI. Lower band contains DNA of TEL01Lmod digested with XhoI (shown in Fig. 14C). Origin of middle bands in clones 1 and 3 of *tel1Δ* 01L-WT XCR and 4 of *tel1Δ* 01L-XCRmut are unknown. Bottom gel: amplicons pre-XhoI digestion at approximately 4.8 kb.

Table 11: Mean telomere length of TEL01Lmod strains measured by Southern Blot and TELO PCR.

TEL01Lmod length and standard deviations as measured by southern blot, quantified by GelAnalyzer 2010 Software.

	Strain	Mean Telomere Length (bp±bp)
Southern Blot	*TEL1* 01L-WT XCR	2076±51
	TEL1 01L-XCRmut	2043±6
	tel1Δ 01L-WT XCR	1909±23
	tel1Δ 01L-XCRmut	1918±17
TELO PCR	*TEL1* 01L-WT XCR	2202±24
	TEL1 01L-XCRmut	2213±20
	tel1Δ 01L-WT XCR	2031±0
	tel1Δ 01L-XCRmut	2022±27

In a study evaluating the roles of Tbf1 and Reb1 in backup telomere length maintenance, telomere length was also measured in *yku70Δ* strains, which also have shortened telomeres (Berthiau et al., 2006; Porter et al., 1996). We proceeded to measure the length of TEL03Lmod in a *yku80Δ* genetic background, which also displays telomere shortening (Askree et al., 2004), to see if Tbf1 and Reb1 presence at the subtelomere affected telomere length maintenance in this short telomere background. *YKU80* was deleted in TEL03Lmod strains by integration of a PCR-generated deletion cassette to replace *YKU80* with the *LEU2* auxotrophic marker. As shown in figure 23 and table 11, TEL03Lmod in *yku80Δ* strains is shorter than wild type. TEL03Lmod of *YKU80* strains has some variation, especially in clones of 03L-XCRmut. This variation is not present in TEL03Lmod of *yku80Δ* strains. Similar to results in *tel1Δ* background, a slight, 41 bp, shortening in TEL03Lmod of clones from 03L-XCRmut strains, can be observed (table 11).

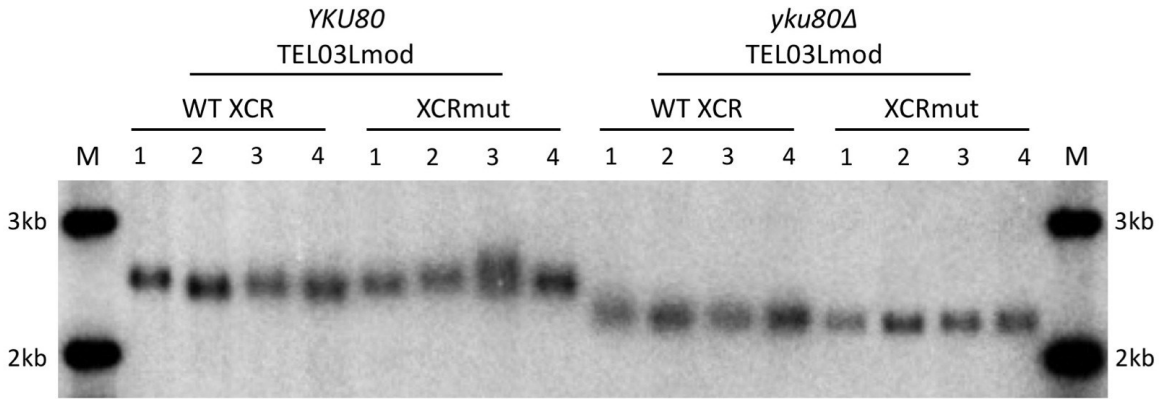

Figure 23: TEL03Lmod in yku80Δ background measured by southern blot.
Southern blot of DNA extracted from clones of TEL03Lmod strains (listed at top). Molecular marker is marked M. Bands at between 2-3 kb correspond to labelled TEL03Lmod fragment digested with NruI restriction enzyme.

Table 12: Mean telomere length of TEL03Lmod strains measured by Southern Blot
TEL03Lmod length and standard deviations as measured by southern blot, quantified by GelAnalyzer 2010 Software.

Strain	Mean Telomere Length (bp±bp)
YKU80 03L-WT XCR	2344±36
YKU80 03L-XCRmut	2387±41
yku80Δ 03L-WT XCR	2100±23
yku80Δ 03L-XCRmut	2062±18

Deletion of *Sir4* can affect the length of X-only telomeres

Working with the modified and unmodified (wild type) TEL03L telomeres, one particular difference in their lengths was observed. As was pointed out from results in figures 9, 13 and 16, clones from TEL03Lmod strains display some variability in the length of telomeric repeats. This is observed to an even greater extent in wild type (unmodified) TEL03L telomeres as well. An additional unique property of TEL03L, is that the tracts of telomeric repeats frequently appear to be longer than 300 bp. This too, is observed at TEL03Lmod telomeres, but to a lesser extent. The phenomenon was previously investigated, when a group performed southern blots to measure telomere length of DNA digested with PvuII instead of XhoI (Vega-Palas et al., 1998). Digestion by PvuII does not create the TRF fragment at approximately 1kb consisting of XY' telomeres. XY' telomeres migrate in larger fragments and remain at the top of the gel, while many of the X-only telomeres migrate between 1.5 and 5 kb. Here too, a large variation in length of some telomeres was observed across clones of the same strain. However, the group observed that in *sir3Δ* strains, telomere length became more consistent amongst the clones and that some telomeres migrated very differently. As this group used a telomeric probe, they were unable to define which telomeres were exhibiting these changes. We performed southern blots with DNA from *SIR4* and *sir4Δ* strains digested with PvuII and hybridized them with probes specific to telomeres TEL11R, TEL06R and TEL03L to specifically measure a change in telomere length and variation in *sir4Δ* backgrounds. Figure 24 shows that TEL11R telomere lengths do not vary from clone to clone, nor strain to strain. TEL03L length of clones in *SIR4* strains varies, although a third clone would have allowed us to determine this more concretely. TEL03L length in *SIR4* strains is above 3.1 kb, although the predicted length is approximately 2.6 kb, which translates to a telomere repeat length of over 500 bp. In *sir4Δ* strains, TEL03L length decreases drastically, such that all clones have a uniform TEL03L length of approximately 2.7 kb. This is observed to a lesser extent in TEL06R telomeres, as they are slightly longer than predicted in *SIR4* strains and decrease in *sir4Δ* strains.

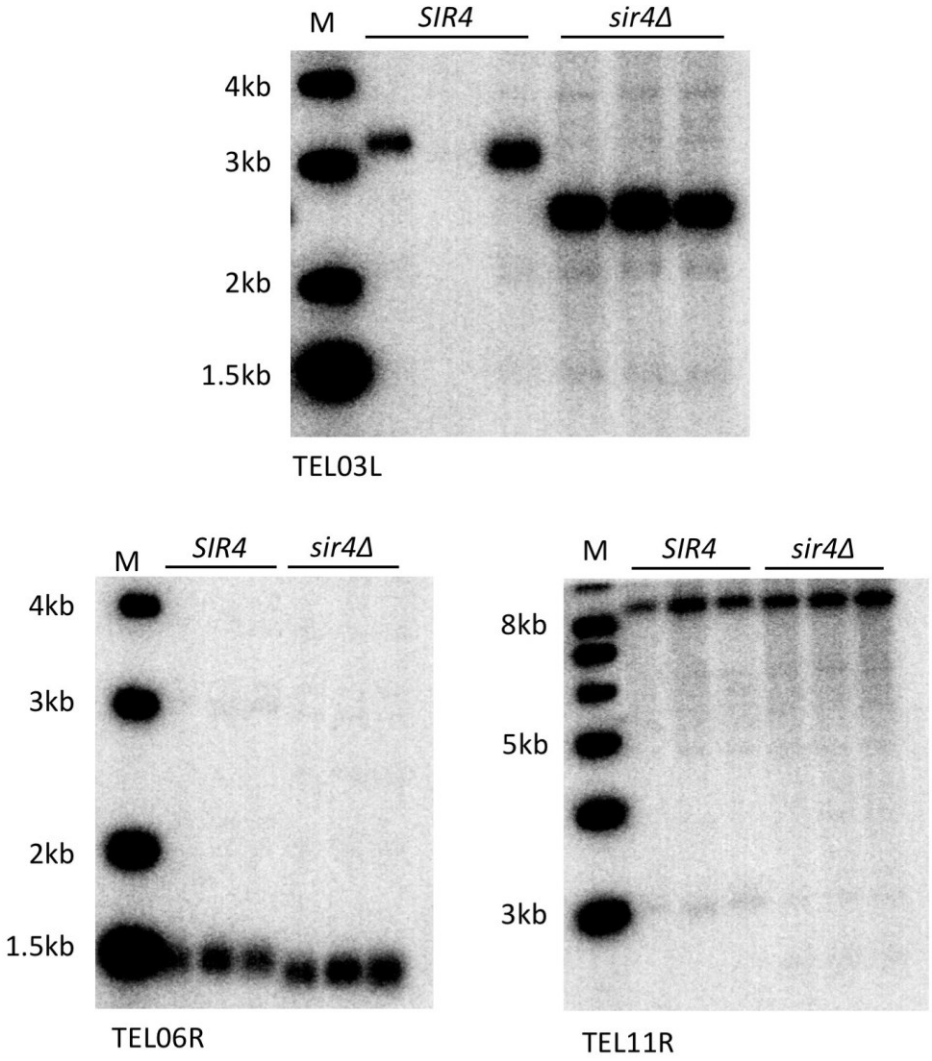

Telomere	Expected Length (bp)
TEL03L	2651
TEL06R	1235
TEL11R	8424

Figure 24: X-Only telomere length measured by Southern Blot.
DNA was extracted from 3 clones of *SIR4* and *sir4Δ* strains (indicated at top) and digested with PvuII. Blots were hybridized with probes for different telomeres (indicated below blot). Molecular marker is marker M. Expected lengths of telomeres detected (assuming 300 bp telomeric repeats) are indicated below blots. Clone 2 of *SIR4* for blots with labelled TEL03L did not appear due to low DNA concentration.

Results Chapter III

Effects of Tbf1 and Reb1 on TPE

Preamble

Tbf1 and Reb1 are described as "anti-silencers", as they bind to STARs (Subtelomeric Anti-Silencing Regions), which have been found to counteract the Telomere Position Effect (TPE) (Fourel et al., 1999). TPE is the repression of telomere proximal genes mediated by the histone de-acetylase components (HDACs) of the Sir complex, which is recruited to the telomeric repeats by Rap1 (Gottschling et al., 1990; Hecht et al., 1995). In addition to the STAR components in the XCR of the subtelomere, the Ars consensus sequence (ACS) of the X-Core was found to contribute to silencing (Power et al., 2011). When both X-Core and XCR regions of the X-element are present, the silencing effect of the X-Core overpowers anti-silencing functions of the XCR region (Fourel et al., 1999; Power et al., 2011). We aimed to use the modified subtelomere system to determine if the depletion of Tbf1 and Reb1 proteins from a native subtelomere structure could influence the spreading of TPE.

Effects of XCR and X-Core on Silencing at modified TEL01L

Similar to previous studies investigating the impacts of subtelomeric elements on TPE, we monitored the propagation of gene silencing by evaluating the expression of a *URA3* reporter gene interior to the subtelomere. The expression of *URA3* on plates containing 5 fluoro-orotic acid (FoA) creates a toxic metabolite resulting in cell death (Boeke et al., 1987). Thus, all cells able to grow on Yc-5-FoA are presumed to possess a silenced *URA3* gene.

Silencing experiments were done in modified TEL01L strains, constructed as described previously. *URA3* was used as a selection marker to integrate the modified

TEL01L fragment into the genome. For the gene silencing experiments, the step inducing recombination was omitted to retain *URA3* as a reporter gene. This resulted in an initial construct with a wild type subtelomere structure and a total distance of 1.5 kb from the beginning of the *URA3* promoter to the telomeric repeats (AKY012).

We then constructed truncated TEL01L telomeres, using Gibson Assembly to replace the whole X-element or only the XCR with sequences of a *KanMX* gene. This was done to maintain a consistent distance between *URA3* promoter and telomeric repeats, as TPE dissipates with increased distance from the telomere repeats (Gottschling 1990). The *KanMX* gene was chosen as it is not a native gene in S. *cerevisiae* and is expected to have a lower probability of interacting with additional proteins that could affect chromatin organization of the area. To further minimize the chance of the DNA of the *KanMX* gene having effects on silencing, the promoter sequence was not added to any contruct. The strains constructed for this experiment were 01L-X-elementΔ (AKY054) and 01L-XCRΔ (AKY055) and 01L-WT XCR (AKY012), which contains the entire wild type X-element (Figure 25C).

The spot tests in Figure 25B were performed with two verified clones of each construct. Cells from each strain were grown overnight in liquid YEPD medium at 30 ˚C, serially diluted 1:5, and then spotted with a multichannel pipette onto 5-FoA plates to test *URA3* silencing, and YC plates. TPE was observed in all strains containing *URA3* at TEL01Lmod, demonstrated by their ability to grow on YC+ 5-FoA plates (Figure 25A bottom). Strains containing constitutively expressed wild type genomic *URA3* were unable to grow, while *ura3Δ* strains were able to grow without hindrance (Figure 25A, top). Individual colonies grown on 5-FoA and YC-complete medium were counted. The growth of each strain on YC+5-FoA was normalized to the strains' growth on YC medium to quantify the resistance of each strain to 5-FoA (FoA^R). The fold change in 5-FoA resistance of each strain was calculated by comparing the FoA^R of cells from strains with subtelomeric deletions in TEL01L (AKY054; AKY055) to that of strains with wild type TEL01L subtelomeres (AKY012). 01L-X-elementΔ (AKY054) clones had a decreased silencing ability, as they grew 0.8-fold less than 01L WT-XCR (AKY012) clones on

YC+ 5-FoA. 01L-XCRΔ (AKY055) clones possessing only the X-Core portion of the subtelomere grew slightly better on FoA, demonstrated by a 1.2-fold higher FoA^R than WT (Figure 25). Given the standard deviations obtained, it remains unclear whether there really is a difference between these situations.

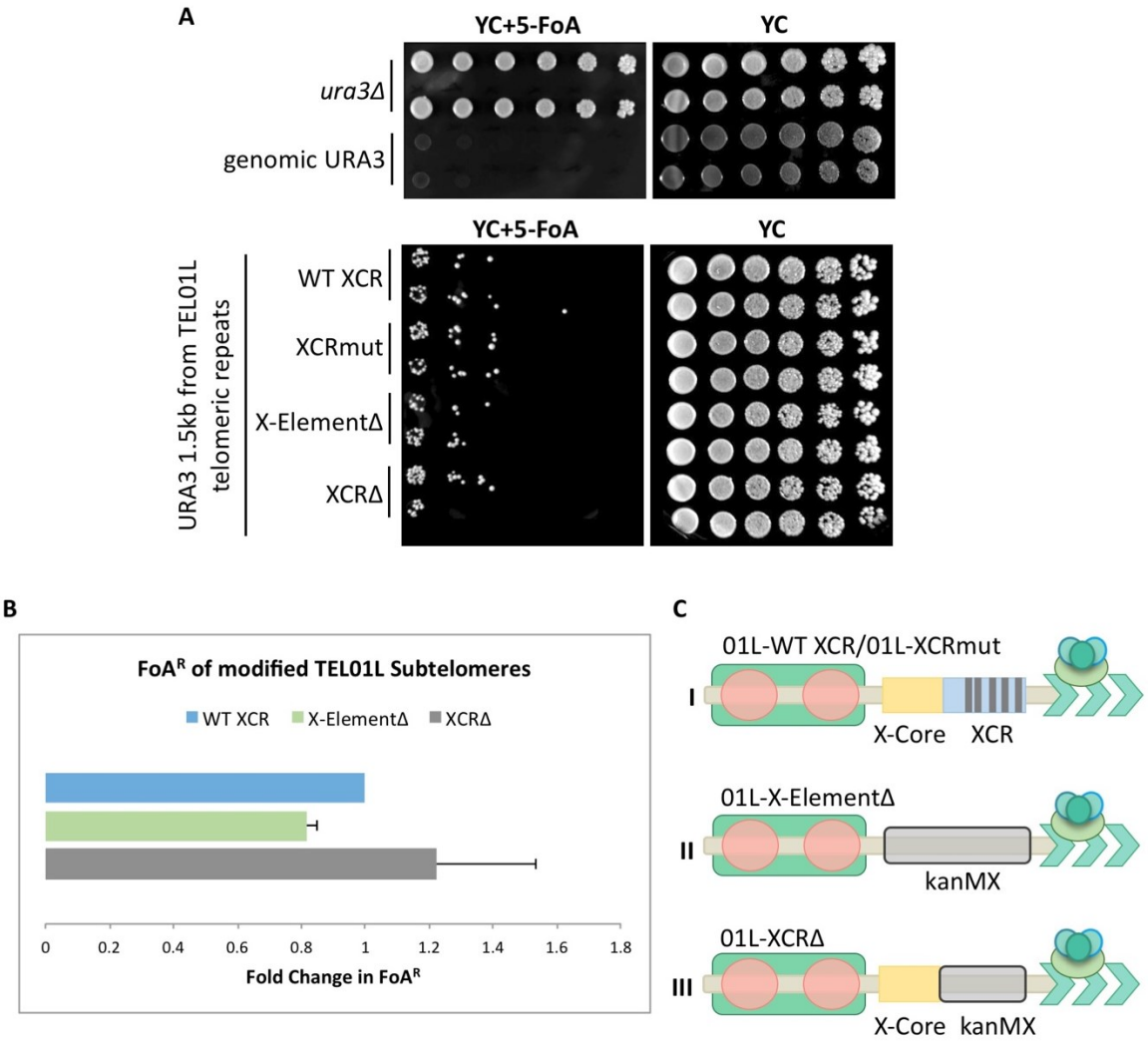

Figure 25: Quantification of serial dilution growth tests of cells with *URA3* at 01L-WT X-element, 01L X-elementΔ and 01L-XCRΔ.

A. Cultures of cells with indicated genotypes were diluted to a uniform concentration of 3 x 10^7 cells/100 µl and then serially diluted (1:5). 10 µl of each dilution was pipetted on YC and YC+ 1 mg/ mL 5-FoA plates and grown for 4 days at 30 ˚C. The experiment was done with 2 independent clones for each genotype. The spot tests shown are representative of one plating of 5-6 done. **B**. Fold Change in FoA^R was calculated by counting colonies grown on each YC+5-FoA plate and normalizing to growth (colony number) on YC plates. FoA^R of 01L-X-elementΔ and 01L-XCRΔ were compared to 01L-WT XCR for Fold Change. **C**. Schema of constructs used for this experiment. *URA3* (green box),

covered with nucleosomes (red circles), is 1.5 kb from telomeric repeats (green arrows). I. WT X-element with X-Core and XCR containing Tbf1 and Reb1 binding sites (grey lines), which have point mutations on 01L-XCRmut. II. X-element is replaced by a 776 bp fragment of the *KanMX* gene. III. The XCR is replaced by a 277 bp fragment of the *KanMX* gene.

Tbf1 and Reb1 have no major effects on silencing at native subtelomere

Figure 26 shows a spot test of TEL01Lmod strains containing a WT XCR (01L-WT XCR; AKY012) and XCR with mutated Tbf1 and Reb1 binding sites (01L-XCRmut; AKY013). The spot tests were done by serially diluting cells (1:5) and spotting with a 96- pinner, which does not allow for quantification of FoA^R, as the exact volume released is not known. Visually, the same TPE effect was observed for the 01L-WT XCR as the 01L-XCRmut, as both were able to grow similarly on YC+5-FoA. A second set of serial dilution growth tests were done using a multi-channel pipette (Figure 25A) in order to be able to calculate the FoA^R of each strain and quantify the silencing in more detail. In this assay, the average percentage of colonies with FoA resistance was 5.1 x 10^{-3} in strains with WT XCR, and 5.5 x 10^{-3} in strains with mutated XCR, demonstrating that there is little, if any, change in TPE effect in the absence of Tbf1 and Reb1.

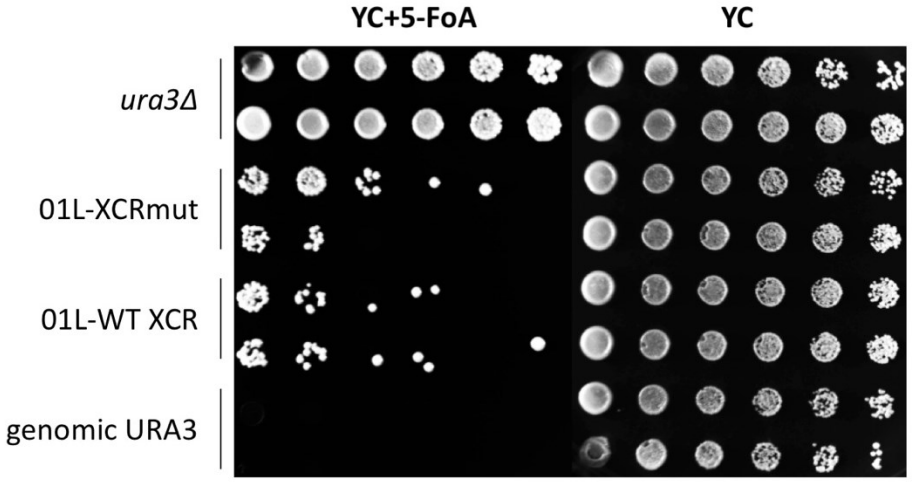

Figure 26: Serial dilution growth test of cells with URA3 at 01L-WT XCR and 01L-XCRmut. Cultures of cells with indicated genotypes were diluted to a uniform concentration of 3 x 10^7 cells / 100 µl and then serially diluted (1:5). Cells were spotted on YC plates and YC + 1mg / mL 5-FoA and grown at 30 ˚C for 4 days.

X-Core deletion decreases TPE at TEL01L

It has been observed in this project and previous studies, that X-Core has a strong silencing effect (Fourel et al., 1999; Power et al., 2011). It has also been shown previously, that the presence of the X-Core results in a weakening of the anti-silencing properties of the XCR (Fourel et al., 1999, 2001). To test the anti-silencing properties of Tbf1 and Reb1 in the absence of the X-Core, the X-Core was deleted in plasmids containing 01L-WT XCR and 01L-XCRmut sequences. Two 01L-X-CoreΔ constructs were created. 01L-X-CoreΔ WT XCR contained a wild type WT XCR sequence (AKY057). 01L-X-CoreΔ XCRmut contained an XCR with mutations in the Tbf1 and Reb1 binding sites (AKY058). To simplify the cloning, the X-Core was not replaced with *KanMX*, yielding constructs with a distance of 1.1 kb between the *URA3* promoter and the telomeric repeats, instead of the 1.5 kb distance in the constructs used previously (explained in further detail in Materials and Methods). To control for the difference in distance from the *URA3* promoter to the telomeric repeats, a control construct was made containing the wild type TEL01Lmod subtelomere, with a distance of 1.1 kb between the telomeric repeats and promoter (AKY056).

Figure 27 shows spot tests plated with a multichannel pipette grown 4 nights at 30 ˚C. Clones of all 01L-X-CoreΔ strains display decreased growth on FoA plates. Clones of 01L-X-CoreΔ WT XCR strains show a 7-10-fold decrease in FoA^R, although growth seems to vary between clones (Figure 27B). Both clones of 01L-X-CoreΔ XCRmut strains display an approximate 10-fold decrease in FoA resistance. Thus, even in the absence of the X-Core, Tbf1 and Reb1 do not have major effects on anti-silencing effects at TEL01Lmod.

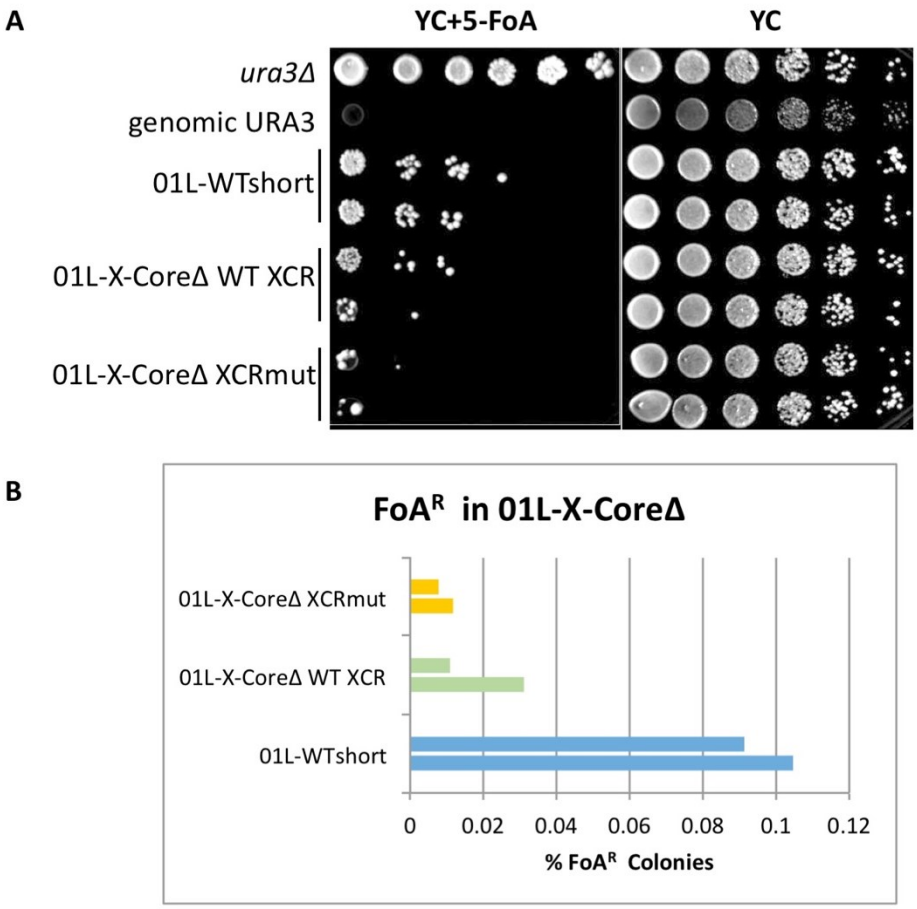

Figure 27: Quantification of serial dilution growth tests of cells with *URA3* at 01L-X-CoreΔ WT XCR, 01L-X-Core XCRmut and 01L-WTshort.
A. Cultures of cells with indicated genotypes were diluted to a uniform concentration of 3 x 10^7 cells / 100 µl and then serially diluted (1:5). 10 µl of each dilution was pipetted on YC and YC + 1 mg / mL 5-FoA plates and grown for 5 days at 30 ˚C. The experiment was done with 2 independent clones for each genotype. The spot tests shown are representative of one plating out of 5-6 done.

TPE decreases in *tbf1-82* mutant with decreased DNA binding

TPE was also tested in strains expressing the *tbf1-82* heat sensitive allele, which has decreased binding at genomic and telomeric targets (Bonnell and Wellinger, unpublished data). Strains containing the 01L-WT XCR construct with *URA3* gene (AKY012) were transformed with a PCR generated fragment containing *tbf1-82*::*NatMX* to construct AKY046 (01L-WT XCR/*tbf1-82*). Two independent clones for each strain were spotted.

Cells were grown for 4 days at the temperatures indicated in Figure 28. As expected, cells expressing *tbf1-82* grew on YC at 30 ˚C, but not at 37 ˚C (Figure 28). We observed TPE again in clones expressing wild type Tbf1 in strains with *URA3* at TEL01Lmod. However, in both clones of 01L-WT XCR/*tbf1-82,* TPE was no longer observed, as the cells were completely unable to grow on FoA plates.

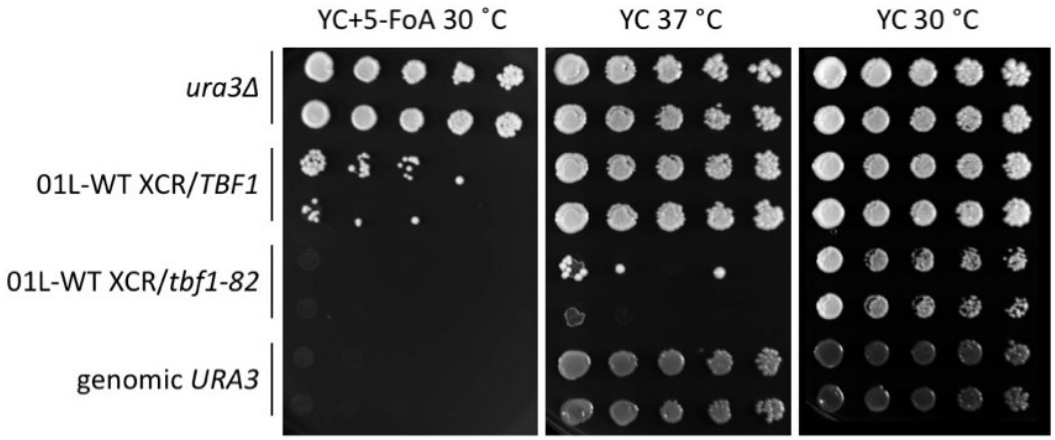

Figure 28: Serial dilution growth tests of cells expressing *TBF1* or *tbf1-82* and *URA3* at 01L-WT XCR.
Cultures of cells with indicated genotypes were diluted to a uniform concentration of 3 x 10^7 cells/ 100 µl and then serially diluted (1:5). Cells were spotted on YC plates and YC+ 1 mg / mL 5-FoA with a 96-pinner and grown at the indicated temperature for 4 days.

Results Chapter IV

Effects of Tbf1 and Reb1 on TERRA

Preamble

Both Tbf1 and Reb1 are essential general regulatory factors when bound at genomic targets (Bosio et al., 2017; Fourel et al., 2002; Preti et al., 2010). The proteins often have overlapping targets, as both are important for creating nucleosome free regions and fine-tuning transcription. Reb1 is also important for regulating the termination of RNA polymerase II transcription and suppressing ectopic transcription at its targets (Challal et al., 2018; Colin et al., 2014). Telomeres are also transcribed into long non-coding RNA called TERRA (telomeric repeat containing RNA), with a transcriptional start site located in the subtelomere (Pfeiffer and Lingner, 2012). Telomeric transcription is conserved across species and TERRA function is thought to have important effects on telomere length regulation in human cells (Arora et al., 2011). Due to the importance of Tbf1 and Reb1 at genomic promoters, we wondered if they retained their function as transcription factors at their subtelomeric locations, in the form of regulators of TERRA transcription.

Measuring TERRA from TEL03Lmod in *sir4Δ* by Northern Blot

Given that TERRA is found in extremely low abundance in yeast cells, we chose to work in genetic backgrounds in which TERRA abundance is increased. At X-only telomeres such as TEL01L and TEL03L, the Sir complex is important for regulating TERRA transcription (Iglesias et al., 2011), presumably by propagating chromatin deacetylation. We used a PCR generated gene deletion cassette to replace *SIR4* with a *KanMX* antibiotic resistance marker in strains with modified TEL03L and TEL01L telomeres. This produced strains AKY016 (*sir4Δ::KanMX* 03L-WT XCR), AKY015 (*sir4Δ::KanMX* 03L-XCRmut), AKY050

(*sir4Δ::KanMX* 01L-WT XCR) and AKY051 (*sir4Δ::KanMX* 01L-XCRmut), which were used to measure TERRA expression. In order to detect TERRA specifically transcribed from TEL03Lmod telomere, a probe was developed to bind the unique sequence inserted between the subtelomeric element and telomeric repeats (Figure 29A). Figure 29 shows that of the two probes developed, TERRA pShort probe was specific to TEL03Lmod sequences. The 36 nt oligonucleotide probe did not show any non-specific binding elsewhere in the genome, contrary to the 56 nt TERRA pLong probe (Figure 29 B, C).

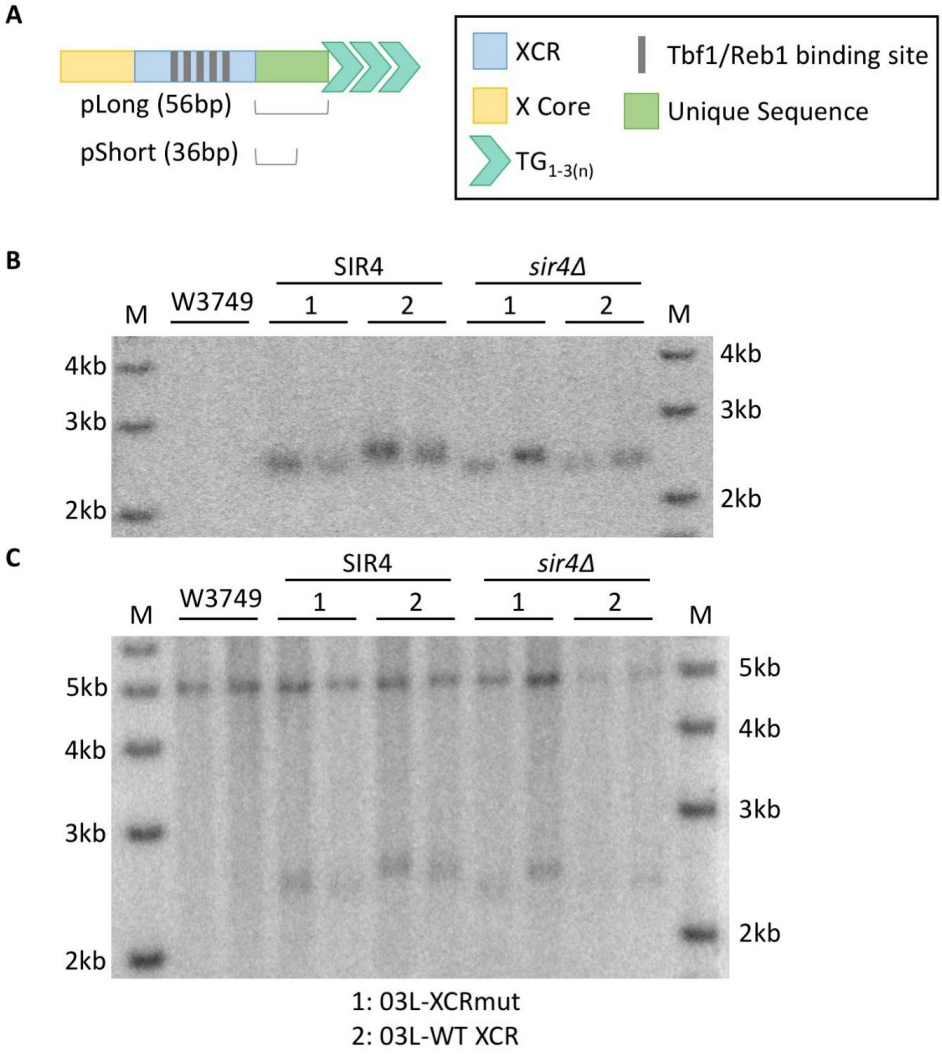

Figure 29: Probes developed to specifically detect TEL03Lmod
A.Schema of two probes tested by southern blot. **B**. DNA of strains (indicated at top) digested by NruI and hybridized with TERRA pShort probe in a southern blot. No bands are visible in W3749 lanes, indicating probe specificity to TEL03Lmod sequence. **C**. DNA of

strains digested by NruI and hybridized with TERRA pLong probe in a southern blot. Non-specific (upper) band is detected in all strains.

RNA was extracted from the strains EPY116, EPY117, AKY015, AKY016 and W3749 and treated with DNase I. 10-15 µg RNA was run in a Northern Blot as described in Materials in Methods. The □-ATP labelled oligonucleotide probe (TERRA pShort) was hybridized with the membrane overnight at 42 ˚C and then washed twice for 10 minutes. The membrane was exposed in a phosphor-cassette for 4 nights. The resulting blot showed cross hybridization between the probe and the 25S and 18S ribosomal RNAs (Figure 30), presumably due to the large quantity of RNA on the membrane. Aside from this cross hybridization, there was no indication of TERRA detection by Northern Blot.

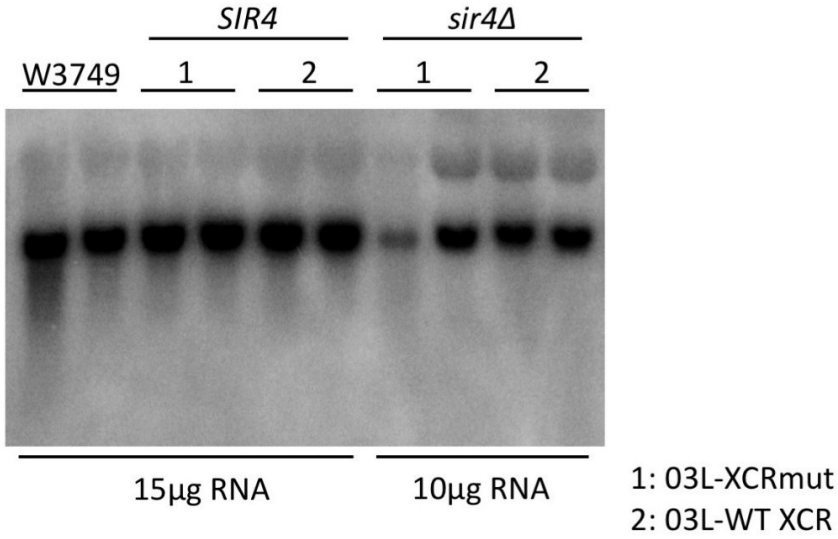

Figure 30: Northern Blots hybridized with TERRA pShort probe.
RNA of 2 clones of each TEL03Lmod strains (indicated at top) run on northern blot and hybridized with TERRA pShort. RNA amounts loaded are indicated below. Dark lower band could correspond to 18S ribosomal RNA.

As the inability to detect TERRA from TEL03L was likely due to its low abundance, several attempts were made to increase the specificity and strength of the probe. However, these attempts were not successful, as we were never able to detect TERRA by Northern Blot. From these tests, we concluded that it was not possible to assess the

TERRA levels of TEL03Lmod by Northern Blot, even in the *sir4Δ* background with increased TERRA abundance.

TERRA levels increase when Tbf1 and Reb1 are depleted from subtelomeres

According to research by other groups, TERRA originating from a single telomere can be measured by RT qPCR (Iglesias et al., 2011). We performed reverse transcription on RNA extracted from various strains with the *sir4Δ* background using random hexamer primers (Roche) and a $C_{1\text{-}3}A$ TERRA RT primer to target telomeric repeat sequences for reverse transcription. TERRA transcribed from different telomeres was then quantified by qPCR with primer pairs targeting subtelomeres of chromosomal ends TEL06R TEL15L, TEL10R, TEL01Lmod and TEL03Lmod. The telomeres at which TERRA levels were evaluated were all X-only telomeres. The subtelomeric region of TEL06R consists of only the X-Core and has only 1 predicted Reb1 binding site and no Tbf1 binding sites (YetFasCo:http://yetfasco.ccbr.utoronto.ca/).

RT qPCR was done on two clones each of *sir4Δ* strains with either TEL03Lmod or TEL01Lmod. By RT qPCR of TEL03Lmod TERRA in *sir4Δ*, we measured a 29.8-fold increase in TERRA levels from 03L-XCRmut compared to 03L-WT XCR. However, the abundance of TERRA from other X-only telomeres did not change in this strain (Figure 31). A similar trend was observed in strains with TEL01Lmod. TERRA abundance from modified 01L-XCRmut was increased 3.7-fold. Little to no change in TERRA levels from other X-only telomeres was measured in clones from the same strain. These experiments indicate that the depletion of Tbf1 and Reb1 at one telomere causes an increase in TERRA abundance in *cis*, although the magnitude of the increase in seems to differ from telomere to telomere.

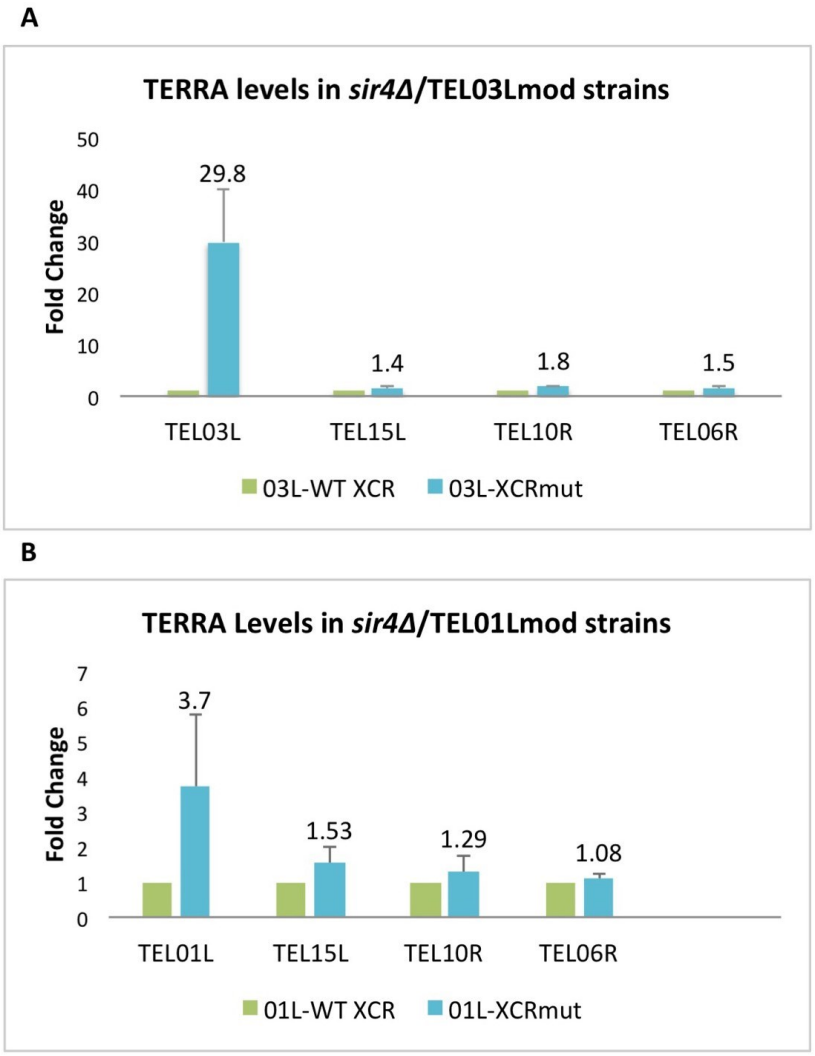

Figure 31: TERRA measured from X-only telomeres in *sir4Δ* strains
RT qPCR of RNA extracted from 2 clones of each indicated *sir4Δ* strains. TERRA signal was normalized to Act1. Fold change was calculated by ΔΔCt method, comparing TERRA from XCRmut strains to WT XCR strains. Data labels indicate fold changes. Each RT-qPCR was repeated 5 times from new RNA extracts. **A**. Fold change in TERRA transcription in *sir4Δ* TEL03Lmod strains. **B**. Fold change in TERRA transcription in *sir4Δ* TEL01Lmod strains.

We then examined TERRA expression in strains expressing the *tbf1-453* cold sensitive allele, which has a decreased binding affinity to DNA (Bonnell and Wellinger, unpublished). The strain constructed (AKY046) contained *sir4Δ*::*KanMX tbf1-453*::*NatMX* and 03L-WT XCR. Thus, this experiment measured TERRA from multiple X-only telomeres with decreased Tbf1 binding, but wild type Reb1 binding. As seen in Figure 32A, expression of *tbf1-453* resulted in an increase of TERRA originating from telomeres

TEL03Lmod, TEL10R and TEL15L. The TERRA levels of TEL06R did not change significantly, which is expected as it does not have any predicted Tbf1 binding sites. With the *tbf1-453* decreasing Tbf1 presence at all telomeres, we observe again that TEL03Lmod has the highest increase in TERRA abundance compared to other telomeres.

To verify if this was due to a difference in number of predicted Tbf1 binding sites at TEL03L, we used YetFasCo to map all predicted binding motifs for Tbf1 and Reb1 at telomeres 03L, 01L, 15L, 10R and 6R (Table 12). This showed, that although TEL03L had fewer predicted Tbf1 binding sites than TEL01L and TEL10R, it had similar amounts to TEL15L. In *tbf1-453 sir4Δ* strains, TEL15L TERRA increases 3.3-fold, while that of TEL03Lmod is increased 8.7-fold, indicating that the number of predicted binding sites does not necessarily impact TERRA abundance. It must be noted that a predicted binding site does not confirm that Tbf1 must be bound, simply that it may bind.

A

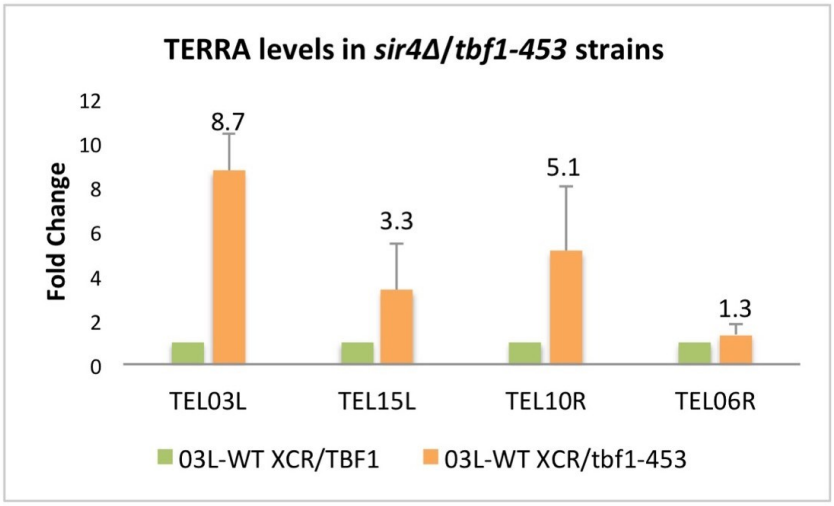

B

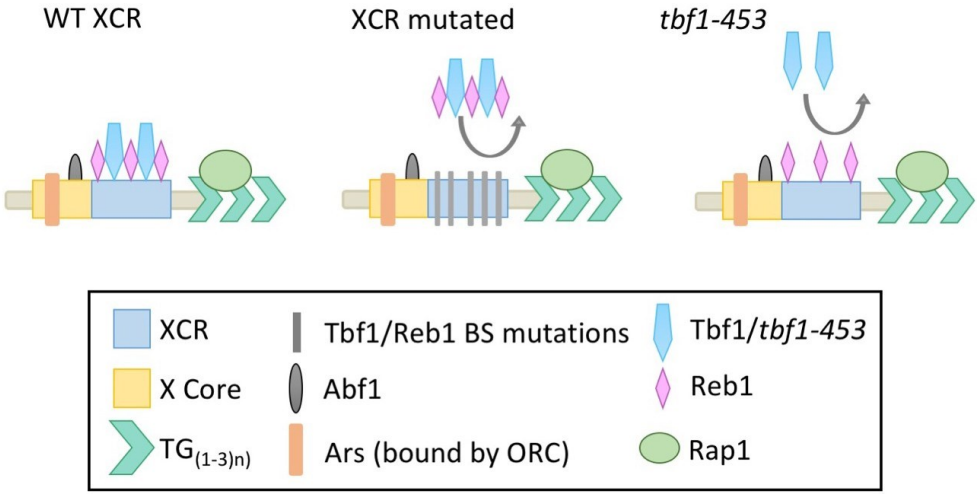

Figure 32: TERRA measured from X-only telomeres in *sir4Δ tbf1-453* strains.
A.RT qPCR of RNA extracted from 2 clones of each indicated *sir4Δ* strains. TERRA signal was normalized to Act1. Fold change was calculated by ΔΔCt method, comparing TERRA from *tbf1-453* strains to TBF1 strains. Data labels indicate fold changes. Each RT-qPCR was repeated 5 times from new RNA extracts. **B.** Schema of Tbf1 and Reb1 binding at subtelomeres throughout RT qPCR experiments. "XCR mutated" depicts 01L and 03L-XCRmut, while "*tbf1-453*" represents all X-only telomeres in *tbf1-453* strains. Rap1 bound at telomeric repeats recruits Sir complex, from which Sir4 has been deleted.

Table 13: Predicted Tbf1 and Reb1 binding sites at X-only telomeres.
Sequences of indicated telomeres were scanned by (http://yetfasco.ccbr.utoronto.ca/) to determine number of predicted Tbf1 and Reb1 binding sites, with a minimum of 75 % maximum score.

	Number of predicted sites	
Telomere	**Tbf1**	**Reb1**
TEL01L	9	10
TEL03L	5	9
TEL06R	0	1
TEL10R	10	10
TEL15L	6	8

Results Chapter V

Purification of yKu70 and yKu80

Preamble

The yKu complex is known to bind telomeric DNA, genomic DNA and the TLC1 RNA, which is part of the telomerase RNP (Peterson et al., 2001). However, chromatin immunoprecipitation (ChIP) experiments by previous lab members R. Stephen MacDonald and Isabelle Dionne suggest that yKu80 also may co-transcriptionally bind two other RNA transcribed from intergenic regions (IGRs). ChIP-sequencing (ChIP-seq) data indicates that this yKu80-RNA interaction is independent of Sir4 but depends on yKu80 directly binding the nucleic acids (Dionne and Wellinger, unpublished). One of the sites identified in the yKu80 ChIP-seq is found on chromosome XII and is the 5' UTR (untranslated region) for the verified ORF RFX1 (Yassoura et al., 2009), a transcriptional repressor of DNA damage regulated genes (Emery et al., 1996). We refer to this IGR as YLR176/177, as it is transcribed from the IGR of the *YLR176* and *YLR177* (uncharacterized) ORFs. The second site is the IGR of *YOR162C* and *YOR163W* on ChrXV. These are verified ORFs for proteins Yrr1 and Dop1 respectively. Yrr1 is a Zn2-Cys6 zinc-finger transcription factor which activates genes involved in drug resistance (Cui et al., 1998) and Dop1 is a protein involved in the Golgi networks vesicular transport (Cui et al., 1998; Gillingham et al., 2006). Preliminary experiments were done to test whether yKu80 was binding to DNA or RNA transcribed from the IGRs. yKu80-myc was immunoprecipitated by ChIP technique and samples were treated with RNase, followed by qPCR of the IGRs and *TLC1*. Some of these experiments yielded a decrease in IP signal after treatment with RNase (McDonald and Wellinger unpublished).

In order to determine the RNA binding capabilities of the yKu complex on all potential cellular RNA, we aimed to perform a cross-linking and analysis of cDNA

sequencing (CRAC-seq) experiment in collaboration with the Granneman Laboratory. In the CRAC technique, proteins of interest are tagged with a HIS-TEV-FLAG tag for a modified tandem affinity purification and they are crosslinked to total cellular RNA in living cells by UV irradiation (Granneman et al., 2009). The protein-RNA complexes are immunoprecipitated on beads, cleaved from the beads by tobacco etch virus (TEV) protease and purified by nickel affinity purification under denaturing conditions. The RNPs are partially digested by RNase, radioactively labelled and resolved on a gel to select the protein of interest based on relative molecular mass. The proteins are then digested in order to amplify the purified RNA by RT PCR for sequencing. Preliminary experiments were done to construct strains and controls designed for the CRAC technique.

yKu70 and yKu80 were tagged with His-TEV-Flag

yKu70 and yKu80 were each C-terminally tagged with the HTF tag as described in Materials and Methods. In addition to tagging the proteins in the wild type BY4705 strain, the proteins were also tagged in control strains containing deletions of the intergenic regions (*yor162-163Δ::KanMX*; *ylr176-177Δ::KanMX*, see Table 14).

Table 14: Strains constructed for this project.
yKu70 and yKu80 were tagged with 6xHis-TEV-3xFlag. Schema of tag below.

Name	Genotype
AKY037	*YKU70-HIS-TEV-FLAG::URA3*
AKY038	*yor162-163Δ::kanMX YKU70-HIS-TEV-FLAG::URA3*
AKY039	*ylr176-177Δ::kanMX YKU70-HIS-TEV-FLAG::URA3*
AKY043	*YKU80-HIS-TEV-FLAG::URA3*
AKY044	*yor162-163Δ::kanMX YKU80-HIS-TEV-FLAG::URA3*
AKY045	*ylr176-177Δ::kanMX YKU80-HIS-TEV-FLAG::URA3*

yKu70-HTF: 76.6 kDa
yKu80-HTF: 77.2 kDa

All strains were first tested by growing them in YEPD until OD_{660} of ~1.0 and extracting proteins by TCA preparation for a Western blot using the monoclonal anti-FLAG mouse M2 antibody (Sigma Aldrich) diluted 1:5000 in 1 % milk. The blots were exposed with 200 µl ECL plus (Amersham). The Western blots confirmed the presence of tagged yKu80 and yKu70 proteins (Figure 33). In addition to the bands corresponding to the tagged proteins, a non-specific (NS) band was visible in many strains. The first blot done with strains containing the yKu70-HTF protein showed that this band was present in all tagged and untagged strains (Figure 33A). Subsequent blots done to test yKu80-HTF tags also revealed a second band at the same size as in Figure 33A present in only tagged samples. The control strains AKY037 and *yor162-163Δ::KanMX* used in Figure 27B were from the same TCA extracts as in the previous blot, though they did not have a NS band in Figure 33B. The parental BY4705 strains and a W3749 strain from the W303 genetic background were newly extracted to be tested for the presence of the second band by extracting proteins from newly streaked out strains. None of the new extracts presented with the NS band.

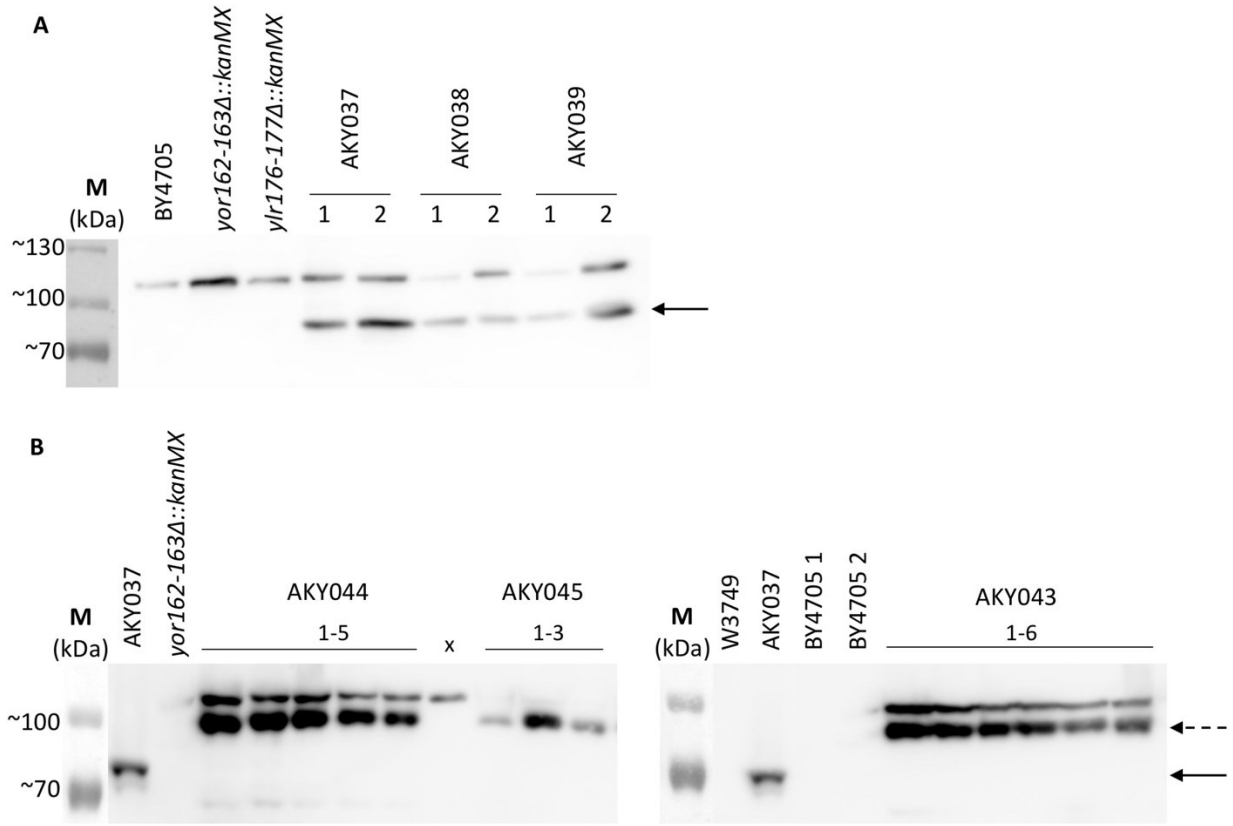

Figure 33: Testing yKu70-HTF and yKu80-HTF Flag tags by Western Blot.
Western blots detecting HTF tagged proteins with anti-FLAG antibody. Molecular ladder is marked M. Solid arrows indicate bands representing yKu70-HTF while dashed arrow indicates yKu80-HTF bands. **A**. yKu70-HTF tagged in wild type, *yor163-163Δ::KanMX* and *ylr176-177Δ::KanMX* backgrounds (lower band). Band above 100 kDa in all strains is non-specific (NS). **B**. Band below 100 kDa indicated yKu80HTF tagged in wild type, *yor163-163Δ::KanMX* and y*lr176-177Δ::KanMX* backgrounds. AKY037 and *yor163-163Δ::KanMX* extracts were rerun (left) and did not show NS band. Wild type strains of W303 (W3749) and S288C (By4705) background did not display NS band. NS band at 100 kDa present in all clones of tagged strains except AKY045. X marks a lane with an unsuccessfully tagged clone of the AKY044 strain (discarded).

Tagging yKu70 with His-TEV-Flag does not impact telomere length

As the deletion or impairment of yKu70 leads to telomere shortening (Porter et al., 1996), we verified telomere length of tagged protein to ensure telomere functions of a tagged yKu complex were not impaired. We performed teloblots with yKu70-HTF tagged proteins (Figure 34) and found that telomere length was only slightly shorter than in wild type strains, thus we could continue working with tagged yKu70-HTF.

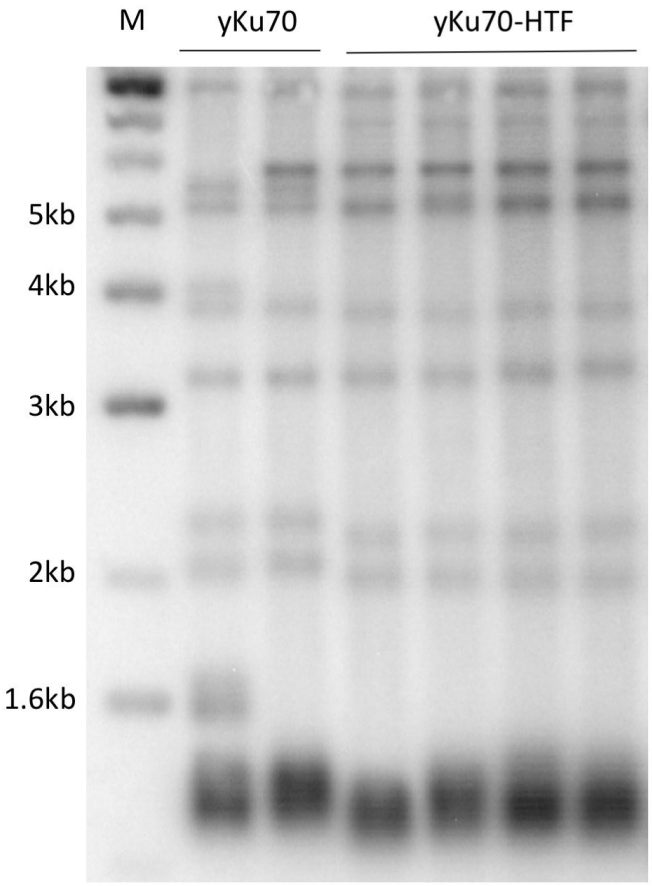

Figure 34: Teloblot of yKu70 and yKu70-HTF strains.
DNA was extracted from strains with yKu70 and yKu70-HTF (indicated at top) and subjected to teloblot. Molecular marker is labelled M. Bottom band is TRF representing global telomere length.

Immunoprecipitation of yKu70-HTF and yKu80-HTF

To prepare for the CRAC-seq protocol, each element of the His-TEV-Flag tag was tested to ensure its compatibility with the proteins of interest. The protein purification is described in detail in Materials and Methods. Briefly described, the cells were grown in 250-500 ml YEPD cultures to OD_{660} ~0.6, pelleted, weighed and frozen with liquid nitrogen. The pellets were resuspended in TN150 buffer and lysed by the addition of zirconia beads and vortexing 5 times for one minute. The cell debris and beads were pelleted by centrifugation and the supernatant containing the proteins was transferred to new tubes. After a second round of centrifugation, the proteins were quantified by

Bradford Assay (Bradford 1976). 1 g cell pellet typically yielded a concentration of 7-10 mg total protein/ml.

The proteins were immunoprecipitated with anti-FLAG M2 magnetic beads (Merck). In order to determine the optimal amount of anti-FLAG beads necessary for the IP, 2 mg of total protein extract was incubated overnight with 20 µl, 40 µl and 60 µl anti-FLAG magnetic beads previously equilibrated with 10 V TN150 buffer. The beads were washed twice with TN1000 wash buffer and heated to 65 ˚C for 5 minutes with agitation at 1200 rpm to elute proteins. The input, flow through, IP/elution and bead fractionswere loaded in an 8 % acrylamide gel in a 1:1:12:12 ratio. The IP of yKu80-HTF proteins was done without an elution step and the beads still bound to the protein were loaded directly on to the gel. The Western Blot was done with the same anti-Flag antibody as described above. The IP showed that both yKu70-HTF and yKu80-HTF could be immunoprecipitated with anti-FLAG magnetic beads (Figure 35). We also see that the optimal volume of beads was between 40 µl and 60 µl per 2 mg total protein extract. The NS band persisted in all fractions of both tagged and untagged strains. 40 µl was chosen to be the preferable volume of beads for IP as the signal from the tagged proteins was stronger than that of the NS band in this condition.

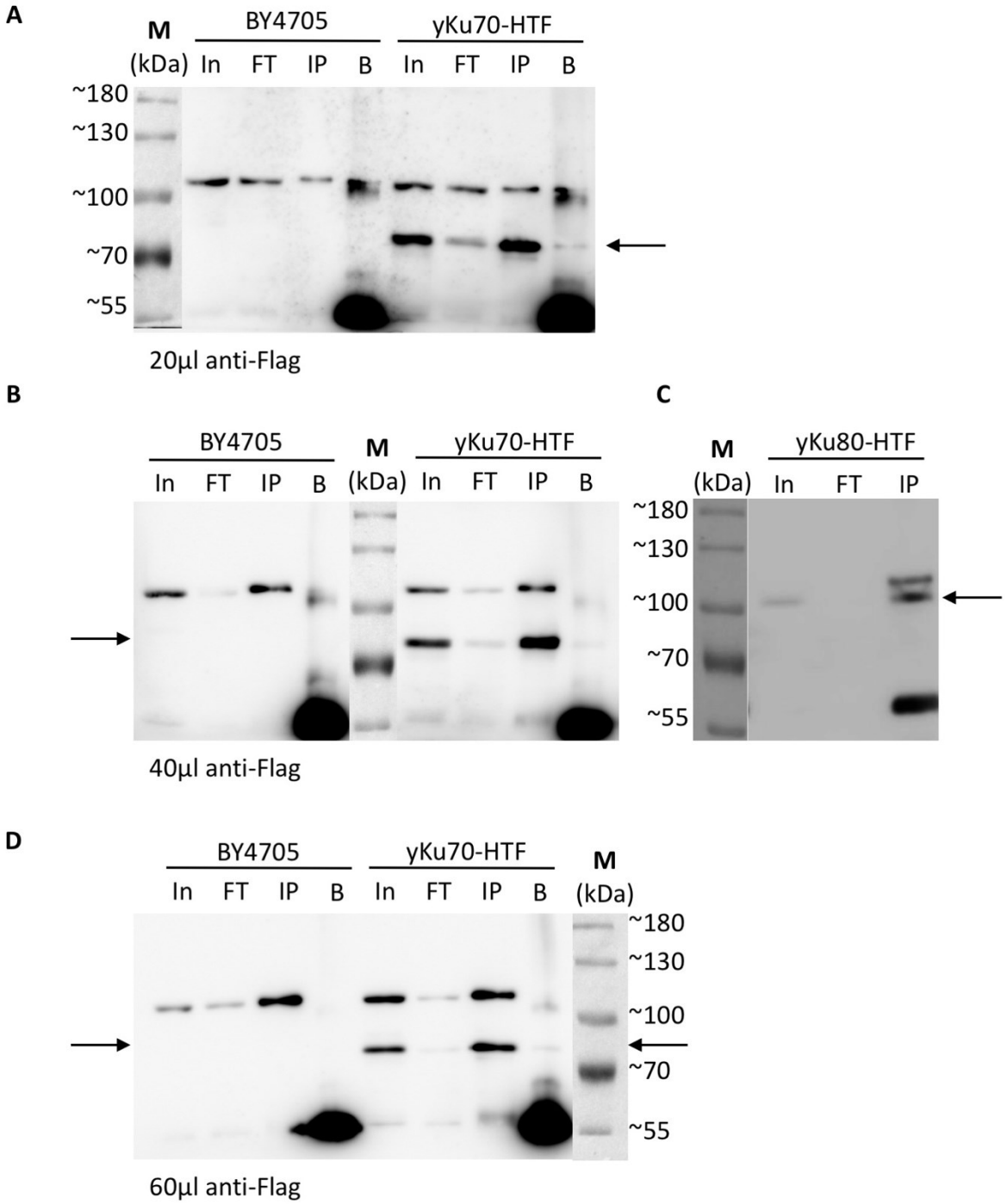

Figure 35: Optimization of the IP of yKu70-HTF and yKu80-HTF
2 mg protein extract was immunoprecipitated with 20 µl **(A),** 40 µl (**B, C**) and 60 µl **(D)** anti-FLAG magnetic beads. Black arrows indicate migration of proteins of interest. Input (IN), flowthrough (FT), Immunoprecipitation (IP) and bead (B) fractions were migrated in 8 % polyacrylamide gels in 1:1:12:12 ratios. All fractions of all strains presented with the NS band (above ~100 kDa). Bead fractions also showed IgG proteins (~55 kDa) from magnetic beads. yKu80-HTF IP fraction **(C)** also has bead fractions as IP on beads were loaded

without elution step.

TEV cleavage for the elution of protein of interest

In order to elute the purified protein from the anti-Flag magnetic beads, TEV protease is used to specifically cleave the ENLYFQG sequence between the 6xHis and FLAG portions of the HTF flag. Before proceeding with the CRAC seq experiment, the TEV cleavage site on the yKu70-HTF and yKu80-HTF proteins was tested by performing test TEV cleavage experiments. TEV was added to whole cell extracts (WCE) or IP's of the protein of interest and incubated 1 hour to overnight. Aliquots were removed at multiple timepoints. Eluates were collected by separating the magnetic beads from the supernatant by magnet and transferring the supernatant to a fresh tube. All fractions were analyzed by Western blot to evaluate the depletion of the protein of interest from the bead fraction. Since the FLAG epitope was to be cleaved off by the TEV protease, a mouse TAP Tag monoclonal antibody (ThermoFisher Scientific) was used in a 1:500 dilution in 1 % milk to detect proteins after cleavage.

The TEV protease was purified by Bruno Lemieux at the *Service de Purification de Protéines* (SPP) at Université de Sherbrooke. Cleavage efficiency was tested by adding a gradient (10 u, 5 u, 2.5 u, 1.25 u) of TEV protease to 2 mg of a control substrate protein (also provided by SPP) and incubating at 4 ˚C with rotation. Aliquots were removed at 1 hr, 3 hrs and after overnight incubation. Western blot showed that the addition of 2.5 u completely cleaved 2 mg of substrate protein during an overnight incubation, while 10 u cleaved 2 mg substrate protein within a 1 hr incubation period at room temperature (data not shown). As the TEV protease contained a 6xHis tag that would interfere with the Nickel purification in the next step, we chose to begin testing with the minimal amount of 2.5 u of TEV in the following experiments.

An IP was done with 4mg of yKu70-HTF and yKu80-HTF. After the overnight incubation, the beads were resuspended in 100 µl TN150 before the addition of 2.5 u TEV protease. A 20 µl aliquot was removed after a 3 hours incubation at 4 ˚C. The magnetic

beads were collected and resuspended in 20 µl TN150 to remove them from the eluate in the supernatant. The same was done at the second timepoint after an overnight incubation. IN, FT and IP as well as the beads and eluates from each time point were analyzed by Western blot using the anti-TAP antibody (Figure 36). The blot shows that although the IP of both proteins was efficient, the bead fractions of both timepoints (T_{1B}, T_{2B}) still contain the proteins of interest, without any band shift to indicate a cleavage. There are no bands visible in the eluate fractions (T_1, T_2), indicating that the TEV cleavage in these experiments was not successful.

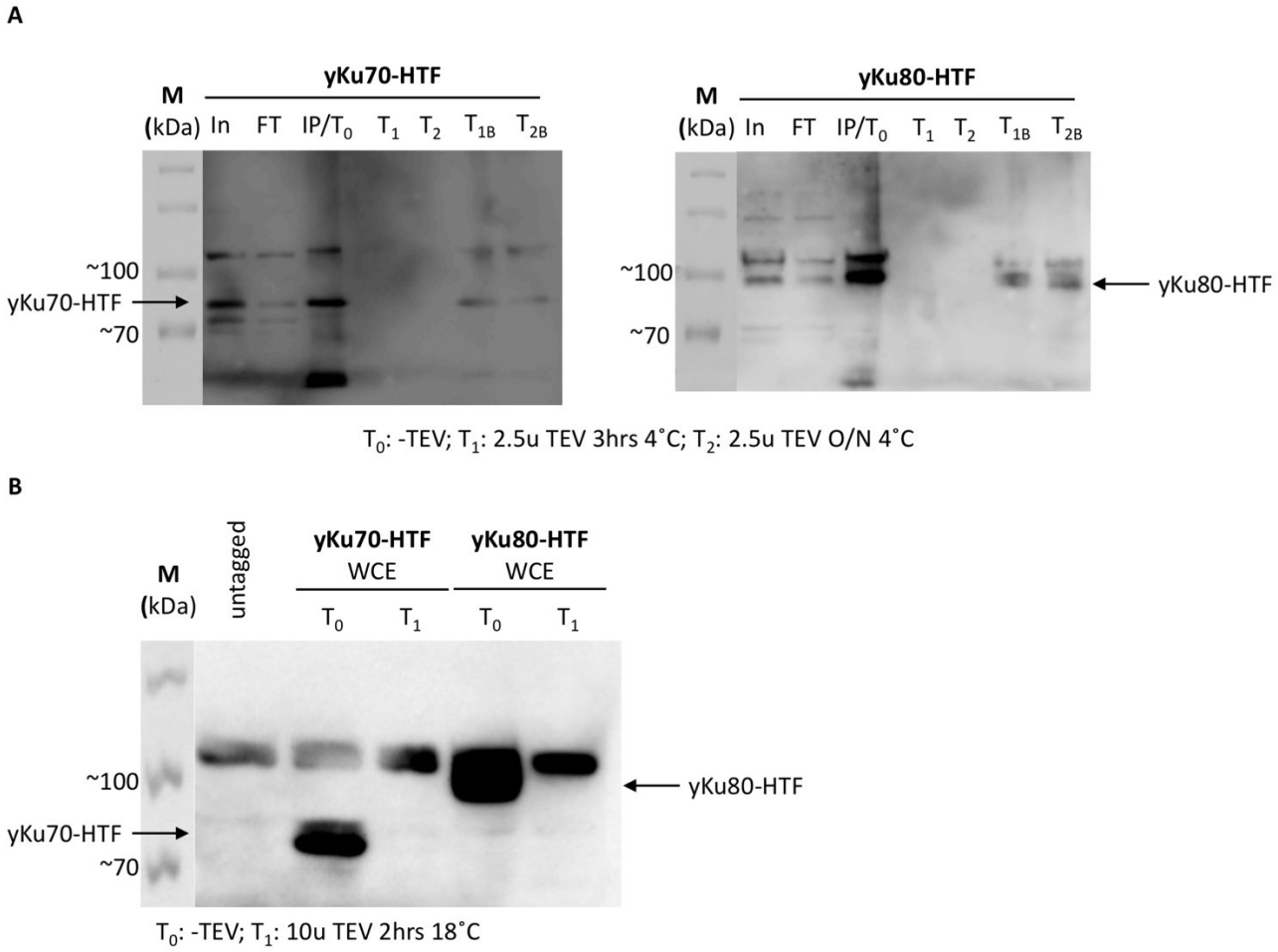

Figure 36: TEV cleavage of yKu70-HTF and yKu80-HTF from beads and in whole cell extract.

A. Western blot with anti-TAP to detect yKu70-HTF (right) and yKu80-HTF (left) IP and cleavage fractions. IP, T_1, T_2, T_{1B} , T_{2B} fractions were loaded in a 10:1 ratio compared to IN and FT fractions. Arrows indicate bands corresponding to yKu70-HTF and yKu80 HTF present in bead fractions without a shift in size. **B**. Western blot with anti-TAP showing WCE of tagged proteins before (T_0) and after incubation with 10 u TEV for 2 hrs at 18 ˚C

(T_1). NS band (above 100kDa) is visible in all lanes. Arrows indicate tagged proteins visible in T_0 lanes, while only NS band is visible after TEV incubation. BY4705 was included as an untagged strain (leftmost band).

We then tested the cleavage of the proteins of interest without the presence of the anti-Flag magnetic beads, in case the TEV protease was sterically hindered by their presence. Whole cell extracts (WCE) of AKY037 (*yKu70-HTF::URA3*) and AKY043 (*yKu80-HTF::URA3*) were incubated with 10 u of TEV at 18 ˚C for two hours. The amount of TEV protease was increased to account for additional proteins in the WCE potentially inhibiting or competing for TEV protease. A downward shift in the band after incubation with TEV would indicate a cleavage of the protein of interest. However, as can be observed in Figure 36B, both proteins of interest disappear after the 2 hour time point, although they are clearly visible at T_0. Meanwhile, the NS band was present before and after incubation with TEV. This indicated that the proteins of interest were degraded during the incubation period. In order to rule out degradation by proteases present in the WCE, we resumed experiments testing the cleavage of the yKu70-HTF and yKu80-HTF from beads.

In order to be able to detect cleavage of smaller amounts of proteins from the beads, the experiments were repeated on a larger scale. An IP of 7 mg of yKu70-HTF and yKu80-HTF protein was done with 100 µl anti Flag magnetic beads. The IP of yKu70-HTF was resuspended in 150 µl and incubated with TEV for 2 hours at room temperature (T1) and then transferred to 4 ˚C for an overnight incubation. A new TEV protease, commercial AcTEV protease (ThermoFisher Scientific) was used for the cleavage of yKu80-HTF from and anti-FLAG beads. The beads were resuspended in a mixture of 10 units of AcTEV, 1.5 µl 0.1 M DTT, 75 µl 2x TEV filled to 150 µl H_20. The incubation time points were the same as for the cleavage of yKu70-HTF from beads by the original TEV protease. The western blots in Figure 37A show bands corresponding to both proteins of interest in the bead fractions of all timepoints. However, the elution fraction of the second timepoints for both proteins of interest revealed bands corresponding to yKu70 and yKu80. Furthermore, there is a downward shift in the eluted yKu70 protein. Although there is no

visible shift in the yKu80 eluted protein, this could be because of a lack of resolution, as it migrates higher on the gel. The NS band is also present in both the bead and eluate fractions.

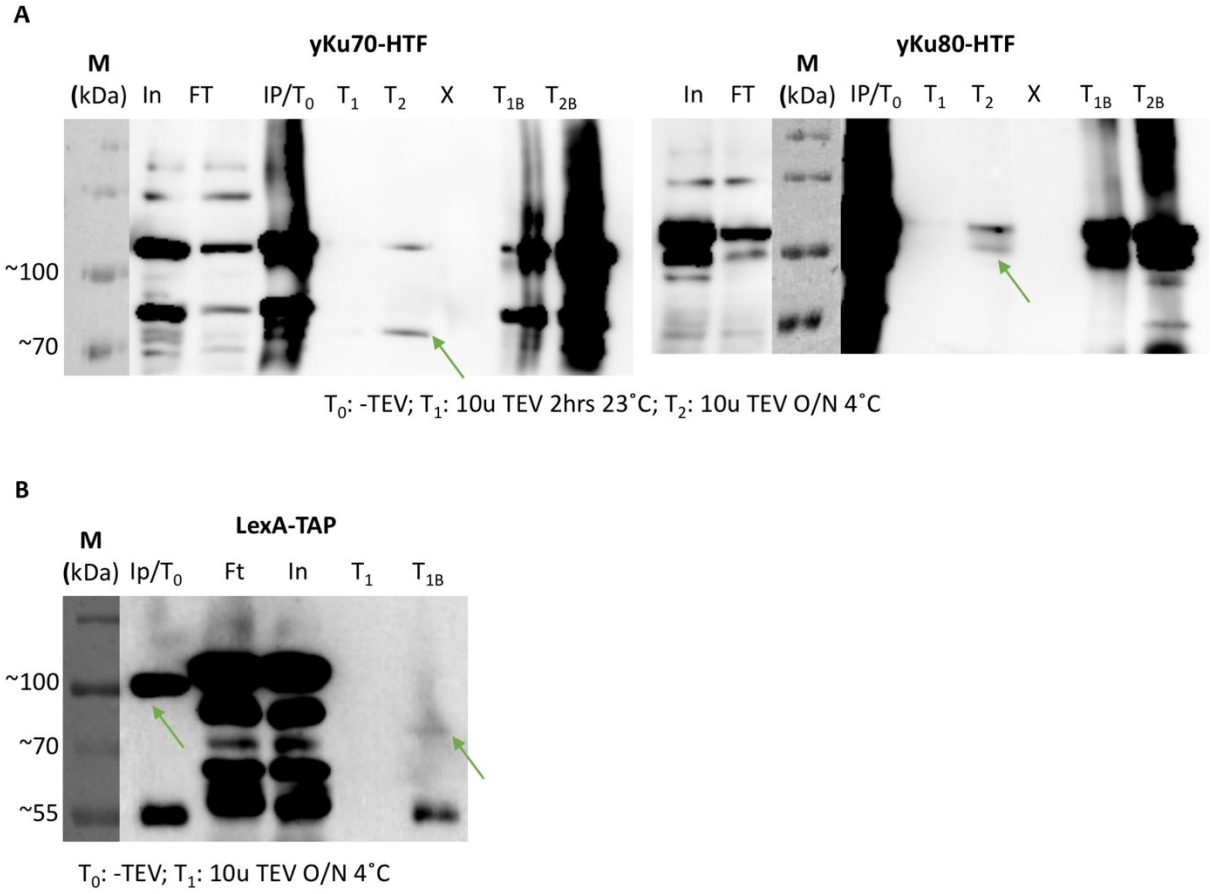

Figure 37: Cleavage of proteins of interest and control protein LexA-TAP by TEV Western blots of proteins immunoprecipitated with magnetic beads incubated with 10 u TEV. **A**. yKu70-HTF and yKu80-HTF IP and cleavage timepoints were detected with the anti-TAP antibody. Molecular ladder is marked M. The lane X was not loaded. Loading ratios were 1:10:20 IN, FT: IP, T_1, T_{1B}: T_2 ,T_{2B}. Green arrows indicate the proteins of interest in the T_2 elution fraction after O/N incubation with TEV. There is a downward band shift of yKu70-HTF in T_2 fraction (left). NS band is also visible in both T_2 elution fractions. **B**. LexA-TAP IP and cleavage detected with anti-TAP antibody. Loading ratios were 1:1:10:20 IN: FT: IP: T_1, T_{1B}. Molecular ladder is marked M. Green arrow indicates LexA-TAP is in the IP fraction at ~100 kDa. T_{1B} shows NS band at 55 kDa and green arrow indicates faint band at ~70 kDa (size of cleaved LexA-TAP).

The TEV protocol was then tested by using control strain EPY06.3b with a LexA-TAP tagged protein (~100 kDa), which had previously been successfully cleaved with TEV. An IP of 15 mg of the LexA-TAP protein was done by incubating the WCE (extracted as

described above) with 40 µl magnetic beads coupled with rabbit IgG (Dynabeads Antibody Coupling Kit, ThermoFisher Scientific) equilibrated with TN150 buffer, for 1 hour at 4 ˚C. The beads were washed twice with TN1000 with a two minute rotation at 4 ˚C between each wash. The beads were then resuspended in 100 µl TN150 and incubated with 20 u TEV overnight at 4 ˚C. The beads were removed from the elution fraction with a magnet. Figure 37B shows the resulting western blot done with anti-TAP antibody (1:1000 dilution in BSA). There is a successful IP of the LexA-TAP protein (~100 kDa), in addition to a non-specific band (~55 kDa). No proteins are detected in the elution fraction (T_1). The bead fraction (T_{1B}) still contains the non-specific band, as well as a very faint signal at approximately 72 kDa, which is the migration size of the cleaved protein. No signal is detected corresponding to the uncleaved protein. This indicates some cleavage or degradation of the protein is occuring, but that the protein is no longer detectable after an overnight incubation with the TEV protease in the TN150 buffer. In order to continue with the remaining steps of the CRAC seq experiments, more research is necessary to uncover the problem in the TEV cleavage step and test the compatibility of the yKu70 and yKu80 proteins with the HTF tag.

Discussion of Chapters I-IV

Roles of Tbf1 and Reb1 at subtelomeres

Previously, the functions of essential proteins Tbf1 and Reb1 have been investigated using hypomorphic alleles and through the insertion of artificial binding sites at various locations within the genome and at chromosomal ends. Tbf1 and Reb1 were found to have somewhat overlapping functions as general regulatory factors when bound at a multitude of promoters. Studies investigating the roles of Tbf1 and Reb1 at subtelomeres have implicated these proteins in telomere length maintenance and anti-silencing. We have created a system in which the phenotypic effects of the reduction of Tbf1 and Reb1 at native structure subtelomeres can be observed. Through this system, we observed that Tbf1 and Reb1 at native structure subtelomeres may have a less pronounced roles in telomere length maintenance and anti-silencing than previously suggested. These experiments also uncovered a previously unknown role for Tbf1 and Reb1 at the subtelomeres – repression of TERRA transcription.

System constructed for the study of Tbf1 and Reb1 at subtelomeres

In order to observe the effects of decreasing Tbf1 and Reb1 solely at the subtelomere, we modified the subtelomere regions of X-only telomeres TEL01L and TEL03L. The choice to work with X-only telomeres was based on two factors. Firstly, the X-element is present at all telomeres and contains the binding sites for Tbf1 and Reb1 in telomere proximal regions of the XCR, while the Y' elements are only present at approximately half of telomeres, although they too possess telomere proximal binding sites for Tbf1 and Reb1 (Koering et al., 2000). Secondly, working with telomere-specific Y' elements would be technically difficult, due to their sequence homology. As we aim to target specific telomeres by radioactive probe or qPCR assays, the homology of Y'

elements across different chromosomes would prove a less than ideal system to work with.

As is visible in the schema of the modified subtelomere constructs (Figure 9, Results section), our system is a close to native structure, with some additional sequences not present in the wild type subtelomere. The presence of non-native sequences has been minimized where possible, through the use of the Recombinase R system targeting 58 bp RS sites to excise the selection markers used to integrate the constructs into yeast strains (Gartenberg, 2012). The final constructs contain ~55 bp sequences between the XCR and telomeric repeats. Upstream of the subtelomere, TEL01Lmod has a wild type sequence stretch of 628 bp, followed by a 334 bp stretch containing the remaining RS site and residual plasmid sequence. TEL03Lmod has a 136 bp sequence of plasmid DNA and RS site directly adjacent to the subtelomeric element. In order to account for any potential effects these alterations could have on subtelomere properties, a control is used in every experiment. Wild type modified telomeres were constructed the same way as mutated modified telomeres, aside from the mutation of the Tbf1 and Reb1 binding sites. In this way, we accounted for the modifications of the subtelomeres and ensured that observed phenotypes were only due to the mutations of the Tbf1 and Reb1 binding sites.

Predicted Tbf1 and Reb1 binding sites were mutated by switching a single G or C nucleotide in the core binding motifs to a C or G nucleotide, respectively. These point mutations are advantageous as they maintain an X-element with as close to native structure as possible. Substituting the G or C nucleotide with a C or G nucleotide, disrupts the GGG or CCC core binding motifs for Tbf1 and Reb1, while still maintaining a native G/C rich DNA structure. The efficacy of these binding site mutations was evaluated by ChIP qPCR experiments (Results, Chapter I). These experiments showed a 2.6-fold decrease in ChIP signal from Tbf1-myc and 2.52-fold decrease ChIP signal from Reb1-myc IP of 01L-XCRmut as compared to 01L-WT XCR. The decreases in ChIP signal were significant, as shown by p-values generated by one tailed T-tests. The ChIP signal from Tbf1-myc and Reb1-myc IP of TEL03Lmod were also decreased. ChIP with Tbf1-myc resulted in a 4.8-fold decrease in TEL03L XCRmut ChIP signal, while Reb1-myc signal of 03L-XCRmut was

decreased 2.46-fold. The fold changes in Tbf1-myc and Reb1-myc ChIP signal of 03L-XCRmut and 03L-WT XCR were significant, according to p-values generated by a one tailed T-test. From this data, we can infer that the mutations in the Tbf1 and Reb1 binding sites lead to a decrease in Tbf1 and Reb1 binding. Furthermore, in many of these experiments, ChIP signals of mutated subtelomeres are close to those of negative control sites, indicating a background level of Tbf1 or Reb1 binding at mutated XCRs. However, it is noted, that the ChIP signals are only decreased approximately 2-5-fold from mutated subtelomeres, indicating that Tbf1 and Reb1 may still bind these sites. Thus, we speak of a decrease to minimum half of the wild type Tbf1 and Reb1 presence at mutated subtelomeres, not an abolishment.

Weak roles of Tbf1 and Reb1 at native subtelomeres

Previous research suggests that Tbf1 and Reb1 both have functions in counteracting the telomere position effect (TPE) and telomere length maintenance in a short telomere background (Arnerić and Lingner, 2007; Berthiau et al., 2006; Fourel et al., 1999; Hediger et al., 2006). However, these roles were inferred from experiments using constructs with altered or absent subtelomere regions. Our aim was to use the modified telomere system to research the roles of Tbf1 and Reb1 when bound at a native subtelomere. In general, we have found that these proteins play a less important role in native conditions than has been observed in previous experiments with artificial subtelomeres.

Telomere Length Maintenance

Analysis of modified telomere length showed that the mutation of Tbf1 and Reb1 binding sites trended in a slight decrease in telomere length of TEL03Lmod in TEL1, *tel1Δ* and *yku80Δ* strains. However, high standard deviations in length make it difficult to discern significant differences in telomere length. In a wild type background, one

southern blot assay showed that TEL03Lmod length appears to decrease progressively with the mutation of Tbf1 and Reb1 binding sites (Figure 16). However, this was not consistently visible in all experiments (Tables 10,12). This inconsistency may partly be explained by the smaller number of clones of the 03L-XCRmut strain used for the southern blot in Figure 16, indicating that the short 03L-XCRmut telomere may be an outlier. Indeed, subsequent blots (Figures 20, 23), using 4 clones of two independently constructed strains, for each genetic background, do not show significant shortening of 03L-XCRmut telomeres. The mutated TEL03Lmod telomeres are decreased in length by 40 bp in *yku80Δ* and 34 bp in *tel1Δ* backgrounds, again with high deviations of 20-70 bp in clones of the same strains (see Tables 11, 12). Analysis of the TEL01Lmod telomeres in *tel1Δ* background did not show any significant difference in length between WT XCR and XCRmut strains.

Previous experiments have implicated Tbf1 and Reb1 in telomere length regulation in *tel1Δ* strains (Arnerić and Lingner, 2007; Berthiau et al., 2006). The Tel1 kinase is important for the recruitment of telomerase specifically to short telomeres in a Rap1-dependent manner (Sabourin et al., 2007). Telomeres lacking a subtelomere area in *tel1Δ* strains are no longer preferentially elongated (Arnerić and Lingner, 2007). However, the presence of the subtelomere, or tethering of GBD-Tbf1N to the subtelomeric area restores the preferential elongation of short telomeres in *tel1Δ* backgrounds, indicating a Tel1- independent back-up mechanism for this function. Another study suggests that Tbf1 is important in recruiting telomerase to short T_2AG_3 tracts at double stranded breaks, but protecting long T_2AG_3 tracts, from further elongation (Ribaud et al., 2012). This is consistent with the idea that Tbf1 could play a role in preferential elongation of short telomeres, but also suggests an additional role in capping of long telomeres. Similarly, a further study implicates both Tbf1 and Reb1 in inhibiting telomere elongation in *tel1Δ* backgrounds (Berthiau et al., 2006). From these studies, it seems that Tbf1 and Reb1 can affect telomere length in a system similar to the Rif complex, where small amounts of the proteins encourage preferential elongation, while increasing amounts inhibit it.

However, these studies were also done using tracts of T_2AG_3 repeats as Tbf1

binding sites or tethering Tbf1 and Reb1 to subtelomeric areas. Thus, perhaps when Tbf1 or Reb1 are the only proteins present in large numbers interior to the telomere repeats, without the presence of the subtelomeric element structures, they have the potential for a more robust effect on telomere length. By decreasing Tbf1 and Reb1 from a native subtelomere, we can see that their effects on telomere length are in fact much less impactful. These results indicate that the main role of Tbf1 and Reb1 at the subtelomere may not be in telomere length maintenance. On the other hand, if Tbf1 and Reb1 do have a small role in preferential elongation of short telomeres, the phenotype at 01L-XCRmut and 03L-XCRmut may be too subtle to detect by Southern blot, as this measures the bulk length of all TEL01Lmod or TEL03Lmod telomeres in a population of cells, rather than individual telomeres. Sequencing of multiple individual modified telomeres in mutated XCR and WT XCR strains would give a more accurate detection of telomere length and telomere elongation and could be done in the future.

Anti-Silencing

Contrary to what was expected based on the literature, we could not observe a difference in TPE between TEL01Lmod strains with wild type or mutated Tbf1 and Reb1 binding sites (Figure 26), (Fourel et al., 1999). As Tbf1 and Reb1 bind STARs (subtelomeric anti-silencing regions) in Y' elements and XCR portions of X-elements, the proteins are thought to be partially responsible for the anti-silencing properties of these regions (Fourel et al., 1999; Koering et al., 2000). The direct effects of the proteins as anti-silencers, or insulators, have also been observed in experiments in which Tbf1 or Reb1 were situated between a *URA3* or *TRP1* gene and telomeric repeats (Fourel et al., 1999, 2001). In these configurations, genes were still transcribed, indicating a protection from TPE. However, the same studies showed that anti-silencing properties of the XCR were greatly reduced in the presence of the X-Core. Similarly, we observed a slight decrease in *URA3* silencing in a construct completely lacking an X-element, compared to one possessing a wild type TEL01Lmod subtelomere, indicating the X-Core has a stronger influence on the expression of *URA3* than the XCR.

The role of the X-Core as a silencing element is not surprising, as the Sir proteins have been found to associate to it, at sites where ORC and Abf1 are also localized (Ellahi et al., 2015; Louis, 1995; Zhu and Gustafsson, 2009). We then hypothesized that the strong silencing functions of the X-ore were masking potential weaker functions of Tbf1 and Reb1 as anti-silencers, making them unobservable by spot testing on plates. Thus, we conducted experiments with constructs of the TEL01Lmod subtelomere lacking the X-Core, containing either the wild type or mutated TEL01Lmod XCR (Figure 27). We observed a clear increase in *URA3* expression in strains containing only an XCR. However, due to a large variation in 5-FOA resistance between clones of the wild type XCR strain, we cannot conclude that there is a difference between the anti-silencing of WT or mutated XCRs.

Curiously, we observed a loss of TPE at TEL01Lmod in strains expressing the *tbf1-82* heat sensitive allele, which has decreased DNA binding at several predicted sites tested by ChIP qPCR (Figure 28)(Bonnell and Wellinger, unpublished data). The loss of resistance to 5-FOA in *tbf1-82* strains is surprising, as the loss of Tbf1's predicted anti- silencing function would be expected to result in an increase in TPE (Fourel et al., 1999, 2001). As Tbf1 is a general regulatory factor and binds many promoters of coding and non-coding RNA throughout the genome, we cannot rule out that this change in 5-FOA resistance results from a change in transcription of one of Tbf1's many targets (Koering et al., 2000; Preti et al., 2010). Indeed, it has been observed before that this assay is not compatible with certain genetic mutants, as they cause a sensitivity to the 5-FOA drug itself (Rossmann et al., 2011). Furthermore, the mere reduction of Tbf1 from the subtelomeric area was not expected to have such a large effect, as Reb1 still binds the subtelomere. Since Reb1 has a been shown to have significantly higher capacities in anti- silencing, a reduction in Tbf1 binding at the subtelomere should not be able to induce such a large change in TPE (Fourel et al., 1999, 2001). This all points to the change in TPE being related to upstream transcriptional changes rather than changes to the subtelomeric areas and underlines the importance of working with wild type Tbf1 and Reb1 alleles to fully understand their functions at subtelomeres.

These experiments do not show any clear changes in TPE when Tbf1 and Reb1 are decreased at the X-only telomere, TEL01Lmod. Of course, we cannot rule out that residual binding of Tbf1 and Reb1 in TEL01L-XCRmut strains are enough to maintain anti-silencing properties of the XCR, as we do observe a slight increase in 5-FOA resistance in strains with a deletion of the entire XCR. Alternatively, additional proteins may be recruited to the XCR in the absence of Tbf1 and Reb1, as it was observed that other proteins with transcription activation domains can also act as insulators (Fourel et al., 2001). Another study similarly reported inconsistencies in TPE that suggest that the subtelomeric elements are not the only determinants of TPE properties of each telomere (Mondoux and Zakian, 2007). Here, it was found that although the X-element of TEL06R was an effective proto-silencer at its native chromosome, transplanting it to TEL07L^{tr} resulted in a slight decrease, rather than increase in silencing. This indicates that the roles of the subtelomeric elements can differ slightly according to the surrounding DNA structures of a specific telomere, for example the chromatin structure of upstream DNA (Mondoux and Zakian, 2007). TPE has also been suspected to be related to the nuclear localization of individual telomeres, as they are found clustered at the nuclear periphery, which is largely thought to be a region where silent chromatin is localized (Andrulis et al., 1998; Bourgeois et al., 1985; Gotta et al., 1996). Indeed, it was observed that tethering telomeres to the nuclear periphery slightly increased TPE at these telomeres (Mondoux and Zakian, 2007). Although localization to the nuclear periphery does not replace the need for the Sir complex, it has been shown that interference with some proteins important for nuclear tethering also has effects on silencing (Mondoux et al., 2007; Poon and Mekhail, 2012). In summary, there seem to be multiple factors involved in regulating TPE and the complete mechanism is not yet fully understood. Although Tbf1 and Reb1 have the capacity to act as insulators when tethered in subtelomeric areas, this may be an artifact from their roles as general regulatory factors at promoters throughout the genome, and not their main purpose at the subtelomeres (Fourel et al., 1999, 2001; Koering et al., 2000).

Tbf1 and Reb1 regulate TERRA abundance

In light of the functions of Tbf1 and Reb1 as transcriptional regulators of a multitude of coding and non-coding genes, we hypothesized that they could play a role in regulating the transcription of the long non-coding RNA, TERRA, which is transcribed from the subtelomeres into the telomeric repeats (Bosio et al., 2017; Koering et al., 2000; Luke et al., 2008). By RT qPCR, we observed that indeed, the decrease of Tbf1 and Reb1 from TEL03Lmod and TEL01Lmod resulted in an important increase in TERRA levels *in cis* in *sir4Δ* backgrounds. While TERRA levels from 01L-XCRmut increased 3.7-fold, they increased 29.8-fold from 03L-XCRmut, as compared to 01L-WT XCR and 03L-WT XCR, respectively (Figure 31). We tested the ability of Tbf1 alone to regulate TERRA abundance through the use of the *tbf1-453* mutant allele, which is cold sensitive and has decreased DNA binding abilities (Bonnell and Wellinger, unpublished data). In a *tbf1-453 sir4Δ* double mutant, we also observed a 3.3 - 8.7-fold increase in TERRA from all three telomeres measured, except TEL06R (Figure 32). As TEL06R lacks an XCR and has only one predicted Reb1 binding site in its X-Core, its TERRA levels were not expected to vary in *tbf1-453 sir4Δ* strains.

Further investigation is necessary to uncover what factors determine the degree to which TERRA abundance increases with the decrease of Tbf1 and Reb1, which is quite variable among different telomeres. The number of predicted Tbf1 and Reb1 binding sites do not seem to correlate with the increase of TERRA levels in *tbf1-453 sir4Δ* (Table 12). For example, while both TEL03Lmod and TEL15L have 5-6 predicted binding sites for Tbf1, TERRA from TEL03Lmod increases over 8-fold compared to 3-fold from TEL15L in *tbf1-453 sir4Δ*. The increase in TERRA levels from TEL03Lmod in *tbf1-453* is not as great as in 03L-XCRmut and we are unable to distinguish if this is due to a difference in degree of decrease of Tbf1 binding at the subtelomere, or if it is due to the continual presence of Reb1 at the subtelomere. Indeed, Reb1 has roles in the termination of RNA polymerase II transcription (Colin et al., 2014; Roy et al., 2016). Furthermore, Reb1 has been reported to repress ectopic transcription at its target promoters and could potentially retain this

function at subtelomeres (Challal et al., 2018). In light of the results shown here, Tbf1 may share these functions in repressing ectopic transcription.

Experiments involving TERRA were all conducted in *sir4Δ* strains in order to increase TERRA transcription, which allows for easier detection by qPCR. However, preliminary results suggest that the effect of the XCR mutations combined with the deletion of *SIR4* are cumulative, as neither the *sir4Δ* nor the 03L-XCRmut strains have TEL03Lmod TERRA levels as high as in the strains with combined mutations (data not shown). This suggests that Tbf1 and Reb1 could act in a pathway separate from the Sir proteins in ensuring TERRA transcription is limited. As the transcription start site for TERRA has been mapped to the X-Core, where Sir proteins are known to associate, Sir4 may help regulate transcription start at the TSS and at the telomeric repeats (Ellahi et al., 2015; Pfeiffer and Lingner, 2012). Providing the XCR is indeed an insulator, as has been suggested in multiple studies as well as this project, regulation by Sir proteins may not be effective in this region, creating a need for Tbf1 and Reb1 to regulate transcription there (Fourel et al., 1999, 2001). Thus, the removal of both regulatory systems would allow the complete derepression of TERRA transcription, while leaving either Sir4 or Tbf1 and Reb1 in place could partially repress transcription. In order to further investigate the interactions between Tbf1, Reb1 and Sir proteins, an RT qPCR protocol must be optimized to allow more accurate measurements of even lower abundance transcripts.

Although Tbf1 and Reb1 are both known for their roles in regulating transcription when bound at promoter regions, we are not able to conclude that they regulate TERRA abundance at a transcriptional level (Bosio et al., 2017; Koering et al., 2000; Preti et al., 2017). The increases in TERRA levels may not be due to an increase in transcription, but due to defects in transcription termination or RNA degradation. Indeed, Reb1 has the potential to be involved in the termination of TERRA transcription (Colin et al., 2014; Roy et al., 2016). In some cases, when RNA polymerase II encounters Reb1-bound DNA, termination of transcription is triggered, and the resulting RNA transcript is degraded. Thus, it is possible that the increases in TERRA levels from mutated subtelomeres are due to a defect in the Reb1 termination pathway targeting TERRA transcripts for degradation.

However, not all Reb1 binding sites are known to cause termination of RNA polII transcription (Roy et al., 2016). Until now, studies have shown that TERRA degradation pathways involve Rat1 exonuclease and RNase H proteins (Graf et al., 2017; Luke et al., 2008; Misino et al., 2018). Interestingly, it was also observed that deleting Trf4 in a *rat1-1* strain also resulted in a slight increase of TERRA abundance and length (Luke et al., 2008). This is of particular interest as Trf4 is involved in the same pathways as Reb1 mediated termination of RNA polII (Colin et al., 2014). RNA transcripts terminated due to a Reb1 roadblock are polyadenylated by Trf4 and subsequently degraded (Colin et al., 2014). Thus, TERRA abundance may be regulated *via* multiple degradation pathways. In order to assess the role of Reb1 in transcription termination at subtelomeres, we attempted to measure the length of TERRA transcripts by Northern blot. Unfortunately, this was not possible as we were unable to generate a specific probe sensitive enough to detect the low abundance RNA. In summary, despite the observed increase in TERRA levels from mutated subtelomere constructs, it is unclear how Tbf1 and Reb1 repress TERRA levels. As it has been shown that Tbf1 is not involved in the termination of RNA polII transcription, it may not have a role in terminating the transcription of TERRA (Roy et al., 2016). However, Tbf1 is known to have roles in the regulation of transcription at many of its binding sites throughout the genome (Bosio et al., 2017; Koering et al., 2000; Preti et al., 2010). Furthermore, experiments with *tbf1-453 sir4Δ* strains show that the decrease of Tbf1 from subtelomeres is sufficient to increase TERRA levels (Figure 32). Thus, it is conceivable that Tbf1 regulates TERRA from a transcriptional side, while Reb1 has a role in termination of transcription and RNA degradation.

Unfortunately, these observations do not provide a complete picture of the roles of Tbf1 and Reb1 at telomeres, as the role of TERRA in S. *cerevisiae* is not yet completely understood. One study suggests that the increase in TERRA transcription *via* inducible GAL promoter leads to telomere shortening in *cis* (Pfeiffer and Lingner, 2012). This observation conflicts with our results, as we did not observe changes in telomere length of telomeres with mutated XCRs. However, as mentioned, further experiments could be done to better assess telomere length of modified telomeres, particularly in a *sir4Δ* background. Other

studies suggest that TERRA is involved in telomere length regulation, either by recruiting telomerase in T-Recs to its telomere of origin, or alternative elongation of telomeres in telomerase negative cells (Cusanelli et al., 2013; Graf et al., 2017; Misino et al., 2018). Cell death and senescence can be avoided in some telomerase negative "survivor" cells, by maintaining telomere length *via* BIR, a homologous repair pathway triggered by DNA-RNA hybrids called R-loops (Balk et al., 2013; Lydeard et al., 2007). TERRA, when found in increased abundance in telomerase negative cells, can form such R-loops by base pairing with the subtelomere it is transcribed from (Graf et al., 2017; Misino et al., 2018). If a decrease in Tbf1 and Reb1 leads to an increase in TERRA levels and TERRA is indeed involved in recruiting telomerase to short telomeres, this could be a reason for the discrepancy in observations in telomere length in this project and previous studies. As studies investigating the effects of Tbf1 and Reb1 on telomere length were conducted without the presence of a subtelomeric element, thus lacking the X-Core with TSS for TERRA, the effect of TERRA at short telomeres would not have been observed (Berthiau et al., 2006). In support of this, it was observed that preferential elongation of short telomeres occurred at telomeres with an intact subtelomere region, but not at those lacking a subtelomere (Arnerić and Lingner, 2007).

Although TERRA may be useful for telomere maintenance in the absence of telomerase, increased telomeric transcription or increases in R-loops at telomeres may increase the vulnerability of telomeric DNA to replication fork stalling, which could lead to telomere breaks and genome instability (Gan et al., 2011; Maicher et al., 2012). Thus, despite TERRA's potential role in maintaining telomere length, TERRA levels must be tightly regulated in order to avoid genomic instability. These negative effects of increased TERRA transcription have indeed been reported (Maicher et al., 2012). In strains without functional telomerase or HDR as telomere maintenance pathways, accelerated senescence was observed when increased telomeric transcription was induced long-term *via* a galactose inducible system. Moreover, while the mere induction of telomeric transcription lead to telomere shortening, which has been previously reported (Pfeiffer and Lingner, 2012), premature senescence was only observed in cells allowed to pass the

DNA-replication phase (S phase) (Maicher et al., 2012). This experiment suggests that either the act of increasing telomeric transcription, or the increased abundance of TERRA, leading to R-loops that cannot be resolved in the absence of HDR machinery, could lead to replication fork stalling or collapse (Graf et al., 2017; Maicher et al., 2012). Thus, telomeric transcription and TERRA levels must be tightly regulated in order to avoid genomic instability. Previous results from the Wellinger lab implicate Tbf1 in telomere maintenance, as accelerated senescence has been observed in telomerase negative strains expressing the *tbf1-453* allele (Bonnell and Wellinger, 2020; in preparation). These results, along with the observation that TERRA levels are increased in *tbf1-453 sir4Δ* strains, provide a link between Tbf1, TERRA and senescence. It was also observed that telomere shortening was only induced when transcription proceeded into the telomeric repeats, where R-loops are more likely to occur (Maicher et al., 2012). This further supports the idea of Reb1 as an important transcription terminator, reducing transcription of the telomeric region in order to maintain genome stability.

Thus, we propose that the roles of Tbf1 and Reb1 at the subtelomeres are to regulate TERRA levels in order to maintain chromosomal end integrity. Their depletion from the subtelomere leads to an increase in TERRA, which could result in chromosomal ends being more vulnerable, especially when conventional telomere maintenance mechanisms are compromised. This vulnerability may be simply due to the act of transcription, the increase of TERRA R-loops, or a combination of the two. In order to gain a better understanding of what roles TERRA, Tbf1 and Reb1 have at telomeres, we aim to sequence the telomeric repeats of modified subtelomeres. In addition to providing a more accurate reading of telomeric length, this would allow us to monitor increases in instances of telomere breaks and repairs through homologous recombination. Furthermore, the mechasisms by which Tbf1 and Reb1 repress TERRA levels must be further studied in order to determine how these proteins function at the chromosomal ends. This new link between Tbf1, Reb1 and TERRA transcription may allow a new avenue to research the roles of TERRA in S. *cerevisiae*.

Telomeric properties vary at different chromosomal ends

In multiple experiments in this study, the chromosomal ends seemed to vary in their telomeric properties. One aim of subtelomere research is to clarify how the subtelomeric elements can influence telomere properties and determine whether they are the cause for the variability observed. TEL01Lmod and TEL03Lmod vary both in the average lengths of telomeric repeats and variability in lengths (see Results, Chapter II). While TEL01Lmod seems to consistently have approximately 330 bp of TG_{1-3} repeats in a wild type background, the number of repeats at TEL03Lmod are much longer, with an average of over 400 bp. They are also much more variable, with deviations of up to 70 bp between clones. When measuring the length of unmodified TEL03L in SIR4 and *sir4Δ* strains, we observed that this long telomere phenotype was even stronger, with TG_{1-3} repeats over 500 bp long. As we always compared WT XCR and XCRmut in TEL03Lmod strains to evaluate effects of Tbf1 and Reb1, we were not concerned by this difference in TEL03L and TEL03Lmod telomeres. However, the TEL03L telomere continued to be of interest, as its length showed a particular sensitivity to the deletion of Sir4, along with TEL06R, to a lesser extent. In addition, it had a much higher increase in TERRA transcription in TEL03L-XCRmut *sir4Δ* strains. Whether the high increase in TERRA and telomere shortening are related remains to be determined. Curiously, a Southern blot done with a short migration period to test the specificity of the TEL03Lmod TERRA probes did not show consistent shortening in TEL03Lmod (Figure 29). This may be explained by the fact that the TEL03Lmod telomere seems to have a less pronounced “long telomere” phenotype than wild type TEL03L. However, repeating this experiment with a longer migration time and including more clones of each strain would provide more accurate information. The ability of the Sir proteins to affect the length of some telomeres, but not others, has been observed previously (Vega-Palas et al., 1998). By developing probes specific to subtelomeric areas, we were able to determine that in addition to TEL03L, TEL06R also shortened slightly after deletion of the Sir function (Figure 24). This

experiment showed that both telomeres were slightly longer than the expected 300 bp and that the deletion of Sir4 reduced the telomeres to their expected lengths.

A closer look at other studies comparing the properties of chromosomal ends revealed that, unlike most telomeres, TEL03L has a large upstream region silenced by the Sir complex (Ellahi et al., 2015). Just 80 bp upstream of the X-element of TEL03L lies the non-functional *YCLWTY5-1* transposon, which contains the three genes silenced by the Sir complex. The TY5 transposon has long been reported to localize to silenced chromatin, particularly near HMR and subtelomere regions (Zou et al., 1995). Interestingly, it has also been found that the machinery used to target TY5 to heterochromatin is also able to induce gene silencing (Xie et al., 2001). TEL03L also contains the silent mating type HML locus within approximately 11 kbp from the chromosomal end, which is still considered a "subtelomeric" region. Notably, TEL03L is the only telomere at which a large subtelomeric domain (almost 20 kbp) is silenced by hypoacetylation through the Sir2 deacetylase (Ellahi et al., 2015). As the Sir proteins can spread to form silent chromatin, perhaps the presence of multiple areas able to nucleate silencing in the larger subtelomeric area results in the creation of the large segment of hypoacetylated chromatin at TEL03L (Oppikofer et al., 2013).

This does not explain the Sir4-dependent difference in telomere length observed. Interestingly strong Sir2-dependent silencing has been observed at TEL06R as well (Ellahi et al., 2015; Mondoux et al., 2007). The *YFR057W* gene, 200 bp upstream of the TEL06R X-Core, is also under Sir mediated transcriptional regulation, providing a link between the two telomeres. Although TEL03L and TEL06R are not the only two telomeres with Sir-mediated silencing of upstream genes, only 8 out of 32 other telomeres also demonstrated these properties. Investigating the lengths of these 8 additional telomeres may provide more links between the Sir complex and telomere length. If other telomeres with increased Sir mediated silencing also show increased telomere length, this could indicate a local increase in Sir proteins outcompeting Rif1 and Rif2 for binding to Rap1 (Paolo Moretti et al., 1994; Wotton and Shore, 1997). As Rif1 and Rif2 negatively regulate telomere length, their decrease at certain telomeres would allow them to become

elongated more than the average 300 bp (Wotton and Shore, 1997).

Discussion of Chapter V

Purification of yKu70 and yKu80

ChIP sequencing evidence from the Wellinger lab suggests that the yKu complex may have a role binding RNA other that TLC1. Given that one of the functions of yKu is the retention of TLC1 RNA in the nucleus, confirmation that the yKu complex binds to additional transcripts could lead to the discovery of a new role for this complex (Gallardo et al., 2008; Peterson et al., 2001; Stellwagen et al., 2003). Perhaps the yKu complex binds to several non-coding RNAs in order to retain them in the nucleus and protect them from degradation, as it seems to do with long non-coding RNA TLC1. Performing a CRAC seq would not only confirm the binding of the yKu complex with two IGR transcripts but may also reveal additional binding partners for the protein complex. Preliminary data also suggests that the yKu association with the IGR transcripts is independent of the Sir proteins, hinting that the complex may interact with the RNA by encircling it with its ring-like structure, as it does with TLC1 (Pfingsten et al., 2012). This is a further indication that there may be similarities in roles of yKu binding TLC1 and other RNAs.

Although the tagging of yKu70 and yKu80 was successful and did not cause impairment of the functions of the yKu complex, the steps to purify either of the proteins were unsuccessful. Based on the experiments and controls done, it seems as though the proteins were never efficiently cleaved from the anti-Flag magnetic beads they were immunoprecipitated with (Figure 36, 37). The apparent cleavage in Figure 37 was later attributed to a long incubation time, where the proteins of interest may have gradually disassociated from the beads and were then cleaved. This conclusion is partly made due to the appearance of the non-specific band in the elution fraction, which should not be cleaved by the sequence specific TEV protease. Furthermore, the elution fractions contain very small amounts of protein, while the majority of the proteins seem to remain in the bead fraction. Thus, the tagged proteins may be sterically hindering the access by the TEV

protease when bound by the anti-Flag magnetic beads. Experiments were done to test the cleavage of the proteins of interest without interference of the magnetic beads, by incubating WCE with TEV protease (Figure 36B). However, rather than a band shift, which would indicate successful protein cleavage, we observed a disappearance of the bands representing yKu70-HTF and yKu80-HTF. This indicated that TEV cleavage could not be done without protein purification from the WCE, which could contain additional proteases responsible for the degradation of the proteins of interest during the incubation time. Performing IPs with different sets of beads and antibodies, using agarose or sepharose beads coupled with an anti-Flag antibody, would help determine whether different bead and anti-body combinations facilitate more efficient TEV cleavage. A control experiment using TAP tagged LexA protein, which has been previously successfully cleaved with TEV in the Wellinger laboratory, also showed some protein degradation, even when working with the purified LexA-TAP protein. As the TAP tag does not contain an epitope for the anti-Flag beads, the IP was done with magnetic beads coupled with IgG antibody. As we see only a slight signal for LexA-TAP in the bead fraction after TEV cleavage (Fig. 37B), while the non-specific signal persists, it is possible that the cleavage of the protein from the magnetic IgG beads is successful. This indicates that by changing the type of beads or antibodies used for the IP could indeed improve TEV efficiency. However, the lack of signal in the elution fraction indicates that some other form of protein degradation is taking place. Altering the buffers used during the IP and TEV cleavage steps could help rule out any incompatibilities or contaminants in the TN150 buffer that could lead to protein degradation after cleavage.

Performing a CRAC-seq with the yKu70 and yKu80 proteins could confirm new RNA binding partners for the yKu complex and lead to the discovery of interesting new roles for yKu. It is clear from the experiments done thus far, that there is an incompatibility with the proteins of interest and the HTF tag, or other materials used in these experiments. As the CRAC-seq experiments are to be done in collaboration with the Granneman laboratory, where proteins of interest are purified *via* the HTF tag with the materials tested here, alternate buffers and bead types were avoided thus far. However,

in light of the unfavourable results obtained, it would be valuable to begin testing purification with alternate buffers and bead types in order to proceed with efficient yKu70 and yKu80 purification.

Conclusions and Perspectives

For this project, a system was constructed in which telomeric phenotypes could be observed when Tbf1 and Reb1 were reduced from native subtelomere structures, without compromising the functions of either protein when bound elsewhere. Through this system, we observed that the roles of these main subtelomeric proteins as insulators or as direct regulators of telomere length may not be as important as previously indicated. Furthermore, we have uncovered a previously undocumented role for these proteins in the regulation of the telomeric transcript TERRA. As the transcriptional start site for TERRA is located within the subtelomeric sequences, this property may have been overlooked when working with truncated or heavily altered subtelomere structures. This underlines the importance of working with native subtelomere structures in order to develop a more complete and accurate understanding of these areas.

After observing the increase of TERRA abundance at telomeres with decreased Tbf1 and Reb1 presence, we can ask what this means for genome stability and telomere maintenance, and how important Tbf1 and Reb1 are for these functions. Multiple studies indicate that TERRA could play a role in telomere maintenance in the absence of telomerase. Perhaps Tbf1 and Reb1 are involved in this by associating to the subtelomeres in a cell cycle or stress related manner. On the other hand, as increased telomeric transcription and R-loops are known to cause genomic instability through replication fork stalling and collapse, perhaps the sole role of Tbf1 and Reb1 are to limit TERRA in order to decrease telomeric vulnerability. In either case, it is important to research these possibilities further in order to fully understand events that could increase genomic instability or evade cellular senescence.

References

Abdallah, P., Luciano, P., Runge, K. W., Lisby, M., Géli, V., Gilson, E., Teixeira, M. T. (2009). A two-step model for senescence triggered by a single critically short telomere. *Nature Cell Biology,* 11: 988-993. https://doi.org/10.1038/ncb1911

Adam, M., Robert, F., Larochelle, M., Gaudreau, L. (2001). H2A.Z Is Required for Global Chromatin Integrity and for Recruitment of RNA Polymerase II under Specific Conditions. *Molecular and Cellular Biology*, 21(8): 6270-9. https://doi.org/10.1128/mcb.21.18.6270-6279.2001

Andrulis, E. D., Zappulla, D. C., Ansari, A., Perrod, S., Laiosa, C. V., Gartenberg, M. R., Sternglanz, R. (2002). Esc1, a Nuclear Periphery Protein Required for Sir4-Based Plasmid Anchoring and Partitioning. *Molecular and Cellular Biology*, 22(23): 8292-8301. https://doi.org/10.1128/mcb.22.23.8292-8301.2002

Andrulis, Erik D., Neiman, A. M., Zappulla, D. C., Sternglanz, R. (1998). Perinuclear localization of chromatin facilitates transcriptional silencing. *Nature*, 394: 592-5. https://doi.org/10.1038/29100

Arnerić, M., Lingner, J. (2007). Tel1 kinase and subtelomere-bound Tbf1 mediate preferential elongation of short telomeres by telomerase in yeast. *EMBO Reports*, 8(11): 1080–5. https://doi.org/10.1038/sj.embor.7401082

Arora, R., Brun, C. M. C., Azzalin, C. M. (2011). TERRA: Long Noncoding RNA at Eukaryotic Telomeres. In: Ugarkovic D (eds) Long Non-Coding RNAs. *Progress in Molecular and Subcellular Biology*, 51. Springer, Berlin, Heidelberg. https://doi.org/10.1007/978-3-642-16502-3_4

Askree, S. H., Yehuda, T., Smolikov, S., Gurevich, R., Hawk, J., Coker, C., Krauskopf, A., Kupiec, M., McEachern, M. J. (2004). A genome-wide screen for Saccharomyces cerevisiae deletion mutants that affect telomere length. *Proceedings of the National Academy of Sciences of the United States of America*, 101(23): 8658-8663. https://doi.org/10.1073/pnas.0401263101

Azzalin, C. M., Reichenbach, P., Khoriauli, L., Giulotto, E., Lingner, J. (2007). Telomeric repeat-containing RNA and RNA surveillance factors at mammalian chromosome ends. *Science*, 318(5851): 798-801. https://doi.org/10.1126/science.1147182

Badis, G., Chan, E. T., van Bakel, H., Pena-Castillo, L., Tillo, D., Tsui, K., Carlson, C. D., Gossett, A. J., Hasinoff, M. J., Warren, C. L., Gebbia, M., Talukder, S., Yang, A., Mnaimneh, S., Terterov, D., Coburn, D., Li Yeo, A., Yeo, Z. X., Clarke, N. D., Lieb, J. D., Ansari, A. Z., Nislow, C., Hughes, T. R. (2008). A Library of Yeast Transcription Factor Motifs Reveals a Widespread Function for Rsc3 in Targeting Nucleosome Exclusion at Promoters. *Molecular*

Cell, 32(6): 878-887. https://doi.org/10.1016/j.molcel.2008.11.020

Balk, B., Maicher, A., Dees, M., Klermund, J., Luke-Glaser, S., Bender, K., Luke, B. (2013). Telomeric RNA-DNA hybrids affect telomere-length dynamics and senescence. *Nature Structural and Molecular Biology*, 20: 1199-1205. https://doi.org/10.1038/nsmb.2662

Ben-Aroya, S., Pan, X., Boeke, J. D., Hieter, P. (2010). Making temperature-sensitive mutants. *Methods in Enzymology*, 470: 181-204. https://doi.org/10.1016/S0076-6879(10)70008-2

Berthiau, A. S., Yankulov, K., Bah, A., Revardel, E., Luciano, P., Wellinger, R. J., Géli, V., Gilson, E. (2006). Subtelomeric proteins negatively regulate telomere elongation in budding yeast. *EMBO Journal*, 25(4): 846–856.https://doi.org/10.1038/sj.emboj.7600975

Bilaud, T., Koering, C. E., Binet-Brasselet, E., Ancelin, K., Pollice, A., Gasser, S. M., Gilson, E. (1996). The telobox, a Myb-related telomeric DNA binding motif found in proteins from yeast, plants and human. *Nucleic Acids Research*, 24(7): 1294-1303. https://doi.org/10.1093/nar/24.7.1294

Boeke, J. D., Trueheart, J., Natsoulis, G., Fink, G. R. (1987). [10] 5-Fluoroorotic acid as a selective agent in yeast molecular genetics. *Methods in Enzymology*, 154: 164-175. https://doi.org/10.1016/0076-6879(87)54076-9

Bonetti, D., Anbalagan, S., Lucchini, G., Clerici, M., Longhese, M. P. (2013). Tbf1 and Vid22 promote resection and non-homologous end joining of DNA double-strand break ends. *EMBO Journal*, 32(2): 275–289. https://doi.org/10.1038/emboj.2012.327

Bonetti, D., Clerici, M., Manfrini, N., Lucchini, G., Longhese, M. P. (2010). The MRX complex plays multiple functions in resection of Yku- and Rif2-protected DNA ends. *PLoS ONE*, 5(11): e1412 https://doi.org/10.1371/journal.pone.0014142

Bosio, M. C., Fermi, B., Spagnoli, G., Levati, E., Rubbi, L., Ferrari, R., Pellegrini, M., Dieci, G. (2017). Abf1 and other general regulatory factors control ribosome biogenesis gene expression in budding yeast. *Nucleic Acids Research*, 45(8): 4493–4506. https://doi.org/10.1093/nar/gkx058

Boulton, S. J., Jackson, S. P. (1998). Components of the Ku-dependent non-homologous end-joining pathway are involved in telomeric length maintenance and telomeric silencing. *EMBO Journal*, 17 : 1819-1828. https://doi.org/10.1093/emboj/17.6.1819

Bourgeois, C. A., Laquerriere, F., Hemon, D., Hubert, J., Bouteille, M. (1985). New data on the in situ position of the inactive X chromosome in the interphase nucleus of human fibroblasts. *Human Genetics*, 69: 122-129. https://doi.org/10.1007/BF00293281

Bourns, B.D., Alexander, M.K., Smith, A.M., Zakian, V.A. (1989). Sir proteins, Rif proteins, and Cdc13 bind Saccharomyces telomeres in vivo. *Molecular and Cellular Biology.* 18(9): 5600-5608. https.//doi.org.10.1128/mcb.18.9.5600

Brachmann, C. B., Davies, A., Cost, G. J., Caputo, E., Li, J., Hieter, P., Boeke, J. D. (1998). Designer deletion strains derived from Saccharomyces cerevisiae S288C: A useful set of strains and plasmids for PCR-mediated gene disruption and other applications. *Yeast*, 14(2): 115-132. https://doi.org/10.1002/(SICI)1097-0061(19980130)14:2<115::AID-YEA204>3.0.CO;2-2

Brandl, C. J., Struhl, K. (1990). A nucleosome-positioning sequence is required for GCN4 to activate transcription in the absence of a TATA element. *Molecular and Cellular Biology*, 10(8): 4256-4265. https://doi.org/10.1128/mcb.10.8.4256

Brigati, C., Kurtz, S., Balderes, D., Vidali, G., Shore, D. (1993). An essential yeast gene encoding a TTAGGG repeat-binding protein. *Molecular and Cellular Biology*, 13(2): 1306-1314. https://doi.org/10.1128/mcb.13.2.1306

Buck, S. W., Shore, D. (1995). Action of a RAP1 carboxy-terminal silencing domain reveals an underlying competition between HMR and telomeres in yeast. *Genes and Development*, 9: 370-284. https://doi.org/10.1101/gad.9.3.370

Bupp, J. M., Martin, A. E., Stensrud, E. S., Jaspersen, S. L. (2007). Telomere anchoring at the nuclear periphery requires the budding yeast Sad1-UNC-84 domain protein Mps3. *Journal of Cell Biology*, 179(5): 845-854. https://doi.org/10.1083/jcb.200706040

Cesare, A. J., Reddel, R. R. (2010). Alternative lengthening of telomeres: Models, mechanisms and implications. In *Nature Reviews Genetics*, 11: 319-330. https://doi.org/10.1038/nrg2763

Challal, D., Barucco, M., Kubik, S., Feuerbach, F., Candelli, T., Geoffroy, H., Benaksas, C., Shore, D., Libri, D. (2018). General Regulatory Factors Control the Fidelity of Transcription by Restricting Non-coding and Ectopic Initiation. *Molecular Cell*, 72(6): 955- 969.e7. https://doi.org/10.1016/j.molcel.2018.11.037

Chan, C. S. M., Tye, B. K. (1983). Organization of DNA sequences and replication origins at yeast telomeres. *Cell*, 33: 563-573. https://doi.org/10.1016/0092-8674(83)90437-3

Chan, C. S. M., Tye, B. K., Herskowitz, I. (1983). A family of Saccharomyces cerevisiae repetitive autonomously replicating sequences that have very similar genomic environments. *Journal of Molecular Biology*, 16(3): 505-523. https://doi.org/10.1016/S0022-2836(83)80299-X

Chandra, A., Hughes, T. R., Nugent, C. I., Lundblad, V. (2001). Cdc13 both positively and

negatively regulates telomere replication. *Genes and Development*, 15(4): 404–414. https://doi.org/10.1101/gad.861001

Chappell, A. S., Lundblad, V. (2004). Structural Elements Required for Association of the Saccharomyces cerevisiae Telomerase RNA with the Est2 Reverse Transcriptase. *Molecular and Cellular Biology*, 24(17): 7720-7736. https://doi.org/10.1128/mcb.24.17.7720-7736.2004

Chasman, D. I., Lue, N. F., Buchman, A. R., LaPointe, J. W., Lorch, Y., Kornberg, R. D. (1990). A yeast protein that influences the chromatin structure of UAS G and functions as a powerful auxiliary gene activator. *Genes and Development*, 4(4): 503–514. https://doi.org/10.1101/gad.4.4.503

Chen, Y. (2019). The structural biology of the shelterin complex. *Biological Chemistry*, 400(4): 457–466. https://doi.org/10.1515/hsz-2018-0368

Colin, J., Candelli, T., Porrua, O., Boulay, J., Zhu, C., Lacroute, F., Steinmetz, L. M., Libri, D. (2014). Roadblock termination by reb1p restricts cryptic and readthrough transcription. *Molecular Cell*, 56(5): 667–680. https://doi.org/10.1016/j.molcel.2014.10.026

Conrad, M. N., Wright, J. H., Wolf, A. J., Zakian, V. A. (1990). RAP1 protein interacts with yeast telomeres in vivo: Overproduction alters telomere structure and decreases chromosome stability. *Cell*, 63(4): 739-750. https://doi.org/10.1016/0092-8674(90)90140-A

Cui, Z., Shiraki, T., Hirata, D., Miyakawa, T. (1998). Yeast gene YRR1, which is required for resistance to 4-nitroquinoline N-oxide, mediates transcriptional activation of the multidrug resistance transporter gene SNQ2. *Molecular Microbiology*, 29(5): 1307-1315. https://doi.org/10.1046/j.1365-2958.1998.01027.x

Cusanelli, E., Chartrand, P. (2014). Telomeric noncoding RNA: Telomeric repeat-containing RNA in telomere biology. *Wiley Interdisciplinary Reviews: RNA*, 5(3): 407–419. https://doi.org/10.1002/wrna.1220

Cusanelli, E., Romero, C. A. P., Chartrand, P. (2013). Telomeric Noncoding RNA TERRA Is Induced by Telomere Shortening to Nucleate Telomerase Molecules at Short Telomeres. *Molecular Cell*, 51(6): 780–791. https://doi.org/10.1016/j.molcel.2013.08.029

Dandjinou, A. T., Lévesque, N., Larose, S., Lucier, J. F., Elela, S. A., Wellinger, R. J. (2004). A phylogenetically based secondary structure for the yeast telomerase RNA. *Current Biology*, 14(13): 1148-1158. https://doi.org/10.1016/j.cub.2004.05.054

De Lange, T. (2005). Shelterin: The protein complex that shapes and safeguards human telomeres. In *Genes and Development*, 19:2100-2110.

https://doi.org/10.1101/gad.1346005

Diede, S. J., Gottschling, D. E. (1999). Telomerase-mediated telomere addition in vivo requires DNA primase and DNA polymerases α and δ. *Cell*, 99(7): 723-733. https://doi.org/10.1016/S0092-8674(00)81670-0

Diffley, J. F. X., Stillman, B. (1989). Similarity between the transcriptional silencer binding proteins ABF1 and RAP1. *Science*, 246(4933): 1034-1038 https://doi.org/10.1126/science.2511628

Downs, J. A., Jackson, S. P. (2004). A means to a DNA end: The many roles of Ku. *Nature Reviews Molecular Cell Biology*, 5: 367-378. https://doi.org/10.1038/nrm1367

Ellahi, A., Thurtle, D. M., Rine, J. (2015). The chromatin and transcriptional landscape of native saccharomyces cerevisiae telomeres and subtelomeric domains. *Genetics*. 200(2): 505-521; https://doi.org/10.1534/genetics.115.175711

Emery, P., Strubin, M., Hofmann, K., Bucher, P., Mach, B., Reith, W. (1996). A consensus motif in the RFX DNA binding domain and binding domain mutants with altered specificity. *Molecular and Cellular Biology*, 16(8): 4486-4494. https://doi.org/10.1128/mcb.16.8.4486

Episkopou, H., Draskovic, I., Van Beneden, A., Tilman, G., Mattiussi, M., Gobin, M., Arnoult, N., Londoño-Vallejo, A., Decottignies, A. (2014). Alternative Lengthening of Telomeres is characterized by reduced compaction of telomeric chromatin. *Nucleic Acids Research*, 42(7): 4391-4405. https://doi.org/10.1093/nar/gku114

Evans, S. K., Lundblad, V. (1999). Est1 and Cdc13 as comediators of telomerase access. *Science*, 286(5437) : 117–120. https://doi.org/10.1126/science.286.5437.117

Fedor, M. J., Lue, N. F., Kornberg, R. D. (1988). Statistical positioning of nucleosomes by specific protein-binding to an upstream activating sequence in yeast. *Journal of Molecular Biology*, 204(1): 109-127. https://doi.org/10.1016/0022-2836(88)90603-1

Fell, V. L., Schild-Poulter, C. (2015). The Ku heterodimer: Function in DNA repair and beyond. In *Mutation Research - Reviews in Mutation Research*, 763:15-29 https://doi.org/10.1016/j.mrrev.2014.06.002

Feuerhahn, S., Iglesias, N., Panza, A., Porro, A., Lingner, J. (2010). TERRA biogenesis, turnover and implications for function. In *FEBS Letters*, 584: 3812-3818. https://doi.org/10.1016/j.febslet.2010.07.032

Fisher, T. S., Taggart, A. K. P., Zakian, V. A. (2004). Cell cycle-dependent regulation of yeast telomerase by Ku. *Nature Structural and Molecular Biology*, 11: 1198-1205.

https://doi.org/10.1038/nsmb854

Fourel, G., Boscheron, C., Revardel, É., Lebrun, É., Hu, Y. F., Simmen, K. C., Müller, K., Li, R., Mermod, N., Gilson, É. (2001). An activation-independent role of transcription factors in insulator function. *EMBO Reports*, 2(2): 124–132. https://doi.org/10.1093/embo-reports/kve024

Fourel, G., Miyake, T., Defossez, P. A., Li, R., Gilson, É. (2002). General Regulatory Factors (GRFs) as genome partitioners. *Journal of Biological Chemistry*, 277(44): 41736– 41743. https://doi.org/10.1074/jbc.M202578200

Fourel, G., Revardel, E., Koering, C. E., Gilson, É. (1999). Cohabitation of insulators and silencing elements in yeast subtelomeric regions. *EMBO Journal*, 18(9): 2522–2537. https://doi.org/10.1093/emboj/18.9.2522

Gallardo, F., Laterreur, N., Cusanelli, E., Ouenzar, F., Querido, E., Wellinger, R. J., Chartrand, P. (2011). Live cell imaging of telomerase RNA dynamics reveals cell cycle-dependent clustering of telomerase at elongating telomeres. *Molecular Cell*, 44(5): 819–827. https://doi.org/10.1016/j.molcel.2011.09.020

Gallardo, F., Olivier, C., Dandjinou, A. T., Wellinger, R. J., Chartrand, P. (2008). TLC1 RNA nucleo-cytoplasmic trafficking links telomerase biogenesis to its recruitment to telomeres. *EMBO Journal*, 27: 748-757. https://doi.org/10.1038/emboj.2008.21

Gan, W., Guan, Z., Liu, J., Gui, T., Shen, K., Manley, J. L., Li, X. (2011). R-loop-mediated genomic instability is caused by impairment of replication fork progression. *Genes and Development*, 25: 2041-2056. https://doi.org/10.1101/gad.17010011

Gartenberg, M. R. (2012). Generation of DNA circles in yeast by inducible site-specific recombination. In: Morse R. (eds) Chromatin Remodeling. *Methods in Molecular Biology*, 833:103-113 Humana Press. https://doi.org/10.1007/978-1-61779-477-3_7

Garvik, B., Carson, M., Hartwell, L. (1995). Single-stranded DNA arising at telomeres in cdc13 mutants may constitute a specific signal for the RAD9 checkpoint. *Molecular and Cellular Biology*, 15(11): 6128-6138. https://doi.org/10.1128/mcb.15.11.6128

Gillingham, A. K., Whyte, J. R. C., Panic, B., Munro, S. (2006). Mon2, a relative of large Arf exchange factors, recruits Dop1 to the Golgi apparatus. 281: 2273-2280. *Journal of Biological Chemistry*.

Gilson, E., Londoño-Vallejo, A. (2007). Telomere length profiles in humans: All ends are not equal. In *Cell Cycle*, 6: 2486-2494. https://doi.org/10.4161/cc.6.20.4798

Gilson, E., Roberge, M., Giraldo, R., Rhodes, D., Gasser, S. M. (1993). Distortion of the DNA

double helix by RAP1 at silencers and multiple telomeric binding sites. *Journal of Molecular Biology*, 231(2): 293-310. https://doi.org/10.1006/jmbi.1993.1283

Gotta, M., Laroche, T., Formenton, A., Maillet, L., Scherthan, H., Gasser, S. M. (1996). The clustering of telomeres and colocalization with Rap1, Sir3, and Sir4 proteins in wild- type Saccharomyces cerevisiae. *Journal of Cell Biology*, 134(6): 1349-1363. https://doi.org/10.1083/jcb.134.6.1349

Gottschling, D. E., Aparicio, O. M., Billington, B. L., Zakian, V. A. (1990). Position effect at S. cerevisiae telomeres: Reversible repression of Pol II transcription. *Cell*, 63(4): 751-762. https://doi.org/10.1016/0092-8674(90)90141-Z

Goudsouzian, L. K., Tuzon, C. T., Zakian, V. A. (2006). S. cerevisiae Tel1p and Mre11p are required for normal levels of Est1p and Est2p telomere association. *Molecular Cell*, 24(4): 603-610. https://doi.org/10.1016/j.molcel.2006.10.005

Graf, M., Bonetti, D., Lockhart, A., Serhal, K., Kellner, V., Maicher, A., Jolivet, P., Teixeira, M. T., Luke, B. (2017). Telomere Length Determines TERRA and R-Loop Regulation through the Cell Cycle. *Cell*, 170(1): 72-85.E14. https://doi.org/10.1016/j.cell.2017.06.006

Graham, I. R., Haw, R. A., Spink, K. G., Halden, K. A., Chambers, A. (1999). In Vivo Analysis of Functional Regions within Yeast Rap1p. *Molecular and Cellular Biology*, 19(11): 7481-7490. https://doi.org/10.1128/mcb.19.11.7481

Granneman, S., Kudla, G., Petfalski, E., Tollervey, D. (2009). Identification of protein binding sites on U3 snoRNA and pre-rRNA by UV cross-linking and high-throughput analysis of cDNAs. *Proceedings of the National Academy of Sciences of the United States of America*, 106(24): 9613–9618. https://doi.org/10.1073/pnas.0901997106

Gravel, S., Larrivée, M., Labrecque, P., Wellinger, R. J. (1998). Yeast Ku as a regulator of chromosomal DNA end structure. *Science*. 280(5364) : 741-744. https://doi.org/10.1126/science.280.5364.741

Greenwell, P. W., Kronmal, S. L., Porter, S. E., Gassenhuber, J., Obermaier, B., Petes, T. D. (1995). TEL1, a Gene Involved in Controlling Telomere Length in S. cerevisiae, Is Homologous to the Human Ataxia Telangiectasia Gene. *Cell*, *82*, 823–829.

Greider, C. W., Blackburn, E. H. (1985). Identification of a specific telomere terminal transferase activity in tetrahymena extracts. *Cell*, 43: 405-413. https://doi.org/10.1016/0092-8674(85)90170-9

Greider, C. W., Blackburn, E. H. (1987). The telomere terminal transferase of tetrahymena is a ribonucleoprotein enzyme with two kinds of primer specificity. *Cell*, 51(6): 887-898. https://doi.org/10.1016/0092-8674(87)90576-9

Griesenbeck, J., Boeger, H., Strattan, J. S., Kornberg, R. D. (2003). Affinity Purification of Specific Chromatin Segments from Chromosomal Loci in Yeast. *Molecular and Cellular Biology*, 23(24): 9275-9282. https://doi.org/10.1128/mcb.23.24.9275-9282.2003

Grossi, S., Puglisi, A., Dmitriev, P. V., Lopes, M., Shore, D. (2004). Pol12, the B subunit of DNA polymerase α, functions in both telomere capping and length regulation. *Genes and Development*, 18(9): 992–1006. https://doi.org/10.1101/gad.300004

Hackett, J. A., Feldser, D. M., Greider, C. W. (2001). Telomere dysfunction increases mutation rate and genomic instability. *Cell*, 106(3): 275-286. https://doi.org/10.1016/S0092-8674(01)00457-3

Hardy, C. F. J., Sussel, L., Shore, D. (1992). A RAP1-interacting protein involved in transcriptional silencing and telomere length regulation. *Genes and Development*, 6: 801-814. https://doi.org/10.1101/gad.6.5.801

Hartley, P. D., Madhani, H. D. (2009). Mechanisms that Specify Promoter Nucleosome Location and Identity. *Cell*, 137(3): 445-458. https://doi.org/10.1016/j.cell.2009.02.043

Hayflick, L., Moorhead, P. S. (1961). The serial cultivation of human diploid cell strains. *Experimental Cell Research*, 25(#): 585-621. https://doi.org/10.1016/0014-4827(61)90192-6

Hecht, A., Laroche, T., Strahl-Bolsinger, S., Gasser, S. M., Grunstein, M. (1995). Histone H3 and H4 N-termini interact with SIR3 and SIR4 proteins: A molecular model for the formation of heterochromatin in yeast. *Cell*, 80: 583-592. https://doi.org/10.1016/0092-8674(95)90512-X

Hediger, F., Berthiau, A. S., Van Houwe, G., Gilson, E., Gasser, S. M. (2006). Subtelomeric factors antagonize telomere anchoring and Tel1-independent telomere length regulation. *EMBO Journal*, 25: 857-867. https://doi.org/10.1038/sj.emboj.7600976

Horowitz, H., Thorburn, P., Haber, J. E. (1984). Rearrangements of highly polymorphic regions near telomeres of Saccharomyces cerevisiae. *Molecular and Cellular Biology*, 4(11): 2509–2517. https://doi.org/10.1128/mcb.4.11.2509

Iglesias, N., Redon, S., Pfeiffer, V., Dees, M., Lingner, J., Luke, B. (2011). Subtelomeric repetitive elements determine TERRA regulation by Rap1/Rif and Rap1/Sir complexes in yeast. *EMBO Reports*, 12(6): 587–593. https://doi.org/10.1038/embor.2011.73

Ju, Q. D., Morrow, B. E., Warner, J. R. (1990). REB1, a yeast DNA-binding protein with many targets, is essential for growth and bears some resemblance to the oncogene myb. *Molecular and Cellular Biology*, 10(10): 5226-5234.

https://doi.org/10.1128/mcb.10.10.5226
Kass-Eisler, A., Greider, C. W. (2000). Recombination in telomere-length maintenance. In *Trends in Biochemical Sciences*, 25(4): 200-204. https://doi.org/10.1016/S0968-0004(00)01557-7

Khadaroo, B., Teixeira, M. T., Luciano, P., Eckert-Boulet, N., Germann, S. M., Simon, M. N., Gallina, I., Abdallah, P., Gilson, E., Géli, V., Lisby, M. (2009). The DNA damage response at eroded telomeres and tethering to the nuclear pore complex. *Nature Cell Biology*, 11: 980-987. https://doi.org/10.1038/ncb1910

Ko, E. R., Ko, D., Chen, C., Lipsick, J. S. (2008). A conserved acidic patch in the Myb domain is required for activation of an endogenous target gene and for chromatin binding. *Molecular Cancer*, 7: 1–20. https://doi.org/10.1186/1476-4598-7-77

Koering, C. E., Fourel, G., Binet-Brasselet, E., Laroche, T., Klein, F., Gilson, E. (2000). Identification of high affinity Tbf1p-binding sites within the budding yeast genome. *Nucleic Acids Research*, 28(13): 2519–2526. https://doi.org/10.1093/nar/28.13.2519

Kurtz, S., Shore, D. (1991). RAP1 protein activates and silences transcription of mating-type genes in yeast. *Genes and Development*, 5: 616-628. https://doi.org/10.1101/gad.5.4.616

Larcher, M. V., Pasquier, E., MacDonald, R. S., Wellinger, R. J. (2016). Ku Binding on Telomeres Occurs at Sites Distal from the Physical Chromosome Ends. *PLoS Genetics*, 12(12): e1006479. https://doi.org/10.1371/journal.pgen.1006479

Laroche, T., Martin, S. G., Gotta, M., Gorham, H. C., Pryde, F. E., Louis, E. J., Gasser, S. M. (1998). Mutation of yeast Ku genes disrupts the subnuclear organization of telomeres. *Current Biology*, 8(11): 653-657. https://doi.org/10.1016/s0960-9822(98)70252-0

Larrivée, M., LeBel, C., Wellinger, R. J. (2004). The generation of proper constitutive G-tails on yeast telomeres is dependent on the MRX complex. *Genes and Development*, 18(12): 1391–1396. https://doi.org/10.1101/gad.1199404

Larrivée, M., Wellinger, R. J. (2006). Telomerase- and capping-independent yeast survivors with alternate telomere states. *Nature Cell Biology*, 8: 741-747. https://doi.org/10.1038/ncb1429

Laterreur, N., Lemieux, B., Neumann, H., Berger-Dancause, J. C., Lafontaine, D., Wellinger, R. J. (2018). The yeast telomerase module for telomere recruitment requires a specific RNA architecture. *RNA*, 24:1067-1079. https://doi.org/10.1261/rna.066696.118

Lavoie, H., Hogues, H., Mallick, J., Sellam, A., Nantel, A., Whiteway, M. (2010). Evolutionary tinkering with conserved components of a transcriptional regulatory

network. *PLoS Biology*, 8(3): e1000329. https://doi.org/10.1371/journal.pbio.1000329

Lemieux, B., Laterreur, N., Perederina, A., Noël, J. F., Dubois, M. L., Krasilnikov, A. S., Wellinger, R. J. (2016). Active Yeast Telomerase Shares Subunits with Ribonucleoproteins RNase P and RNase MRP. *Cell*, 165(5): 1171–1181. https://doi.org/10.1016/j.cell.2016.04.018

Lendvay, T. S., Morris, D. K., Sah, J., Balasubramanian, B., Lundblad, V. (1996). Senescence mutants of Saccharomyces cerevisiae with a defect in telomere replication identify three additional EST genes. *Genetics*, 144(4): 1399-1412.

Levy, D. L., Blackburn, E. H. (2004). Counting of Rif1p and Rif2p on. *Society*, 24(24): 10857–10867. https://doi.org/10.1128/MCB.24.24.10857

Li, B., Oestreich, S., De Lange, T. (2000). Identification of human Rap1: Implications for telomere evolution. *Cell*, 101(5): 471-483. https://doi.org/10.1016/S0092-8674(00)80858-2

Lingner, J., Cooper, J. P., Cech, T. R. (1995). Telomerase and DNA end replication: No longer a lagging strand problem? In *Science*, 269(5230): 1533-1534. https://doi.org/10.1126/science.7545310

Lisby, M., Barlow, J. H., Burgess, R. C., Rothstein, R. (2004). Choreography of the DNA damage response: Spatiotemporal relationships among checkpoint and repair proteins. *Cell*, 118(6): 699-713. https://doi.org/10.1016/j.cell.2004.08.015

Liu, Z., Tye, B. K. (1991). A yeast protein that binds to vertebrate telomeres and conserved yeast telomeric junctions. *Genes and Development*, 5: 49-59. https://doi.org/10.1101/gad.5.1.49

Livak, K. J., Schmittgen, T. D. (2001). Analysis of relative gene expression data using real-time quantitative PCR and the 2-ΔΔCT method. *Methods*, 25(4): 402-408. https://doi.org/10.1006/meth.2001.1262

Livengood, A. J., Zaug, A. J., Cech, T. R. (2002). Essential Regions of Saccharomyces cerevisiae Telomerase RNA: Separate Elements for Est1p and Est2p Interaction. *Molecular and Cellular Biology*, 22(7): 22366-2374. https://doi.org/10.1128/mcb.22.7.2366-2374.2002

Longtine, M. S., Mckenzie III, A., Demarini, D. J., Shah, N. G., Wach, A., Brachat, A., Philippsen, P., Pringle, J. R. (1998). Additional modules for versatile and economical PCR-based gene deletion and modification in Saccharomyces cerevisiae. *Yeast*, 14(10): 953-961. https://doi.org/10.1002/(sici)1097-0061(199807)14:10<953::aid-yea293>3.3.co;2-l

Louis, E. J., Haber, J. E. (1992). The structure and evolution of subtelomeric Y' repeats in Saccharomyces cerevisiae. *Genetics*, 131(3): 559-574.

Louis, E. J., Naumova, E. S., Lee, A., Naumov, G., Haber, J. E. (1994). The chromosome end in yeast: Its mosaic nature and influence on recombinational dynamics. *Genetics*, 136(3): 789–802.

Louis, Edward J. (1995). The chromosome ends of Saccharomyces cerevisiae. *Yeast*, 11: 1553-1573. https://doi.org/10.1002/yea.320111604

Luke, B., Panza, A., Redon, S., Iglesias, N., Li, Z., Lingner, J. (2008). The Rat1p 5' to 3' Exonuclease Degrades Telomeric Repeat-Containing RNA and Promotes Telomere Elongation in Saccharomyces cerevisiae. *Molecular Cell*, 32(4): 465-477. https://doi.org/10.1016/j.molcel.2008.10.019

Lundblad, V., Blackburn, E. H. (1993). An alternative pathway for yeast telomere maintenance rescues est1- senescence. *Cell*, 73(2): 347-360. https://doi.org/10.1016/0092-8674(93)90234-H

Lundblad, V., Szostak, J. W. (1989). A mutant with a defect in telomere elongation leads to senescence in yeast. *Cell*, 57(4): 633-643. https://doi.org/10.1016/0092-8674(89)90132-3

Lydeard, J. R., Jain, S., Yamaguchi, M., Haber, J. E. (2007). Break-induced replication and telomerase-independent telomere maintenance require Pol32. *Nature*, 448: 820-823. https://doi.org/10.1038/nature06047

Maicher, A., Kastner, L., Dees, M., Luke, B. (2012). Deregulated telomere transcription causes replication-dependent telomere shortening and promotes cellular senescence. *Nucleic Acids Research*, 40(14): 6649-6659. https://doi.org/10.1093/nar/gks358

Mak, H. C., Pillus, L., Ideker, T. (2009). Dynamic reprogramming of transcription factors to and from the subtelomere. *Genome Research*, 19(6): 1014–1025. https://doi.org/10.1101/gr.084178.108

Marcand, S., Gilson, E., Shore, D. (1997). A protein-counting mechanism for telomere length regulation in yeast. *Science*, 275(5302): 986-990. https://doi.org/10.1126/science.275.5302.986

Marcand, S., Pardo, B., Gratias, A., Cahun, S., Callebaut, I. (2008). Multiple pathways inhibit NHEJ at telomeres. *Genes and Development*, 22: 1153-1158. https://doi.org/10.1101/gad.455108

Martina, M., Clerici, M., Baldo, V., Bonetti, D., Lucchini, G., Longhese, M. P. (2012). A Balance between Tel1 and Rif2 Activities Regulates Nucleolytic Processing and Elongation

at Telomeres. *Molecular and Cellular Biology*, 32(9): 1604-1617. https://doi.org/10.1128/mcb.06547-11

McClintock, B. (1941). The Stability of Broken Ends of Chromosomes in *Zea mays*. *Genetics*, 26(2): 234–282.

McClintock, B. (1939). the Behavior in Successive Nuclear Divisions of a chromosome broken at meiosis. *Proceedings of the National Academy of Sciences of the United States of America*, *25*: 405– 416.

McElligott, R., Wellinger, R. J. (1997). The terminal DNA structure of mammalian chromosomes. *EMBO Journal*, 16: 3705-3714. https://doi.org/10.1093/emboj/16.12.3705

McGee, J. S., Phillips, J. A., Chan, A., Sabourin, M., Paeschke, K., Zakian, V. A. (2010). Reduced Rif2 and lack of Mec1 target short telomeres for elongation rather than double-strand break repair. *Nature Structural and Molecular Biology*, 17: 1438-1445. https://doi.org/10.1038/nsmb.1947

Mersaoui, S. Y., Wellinger, R. J. (2018). Fine tuning the level of the Cdc13 telomere-capping protein for maximal chromosome stability performance. *Current Genetics*, 65: 109-118. https://doi.org/10.1007/s00294-018-0871-3

Misino, S., Bonetti, D., Luke-Glaser, S., Luke, B. (2018). Increased TERRA levels and RNase H sensitivity are conserved hallmarks of post-senescent survivors in budding yeast. *Differentiation*, *100*: 37–45. https://doi.org/10.1016/j.diff.2018.02.002

Mondoux, M. A., Scaife, J. G., Zakian, V. A. (2007). Differential nuclear localization does not determine the silencing status of Saccharomyces cerevisiae telomeres. *Genetics*, 177(4): 2019-2029. https://doi.org/10.1534/genetics.107.079848

Mondoux, M. A., Zakian, V. A. (2007). Subtelomeric elements influence but do not determine silencing levels at Saccharomyces cerevisiae telomeres. *Genetics*, 177(4): 2541-2546. https://doi.org/10.1534/genetics.107.079806

Moretti, P., Shore, D. (2001). Multiple Interactions in Sir Protein Recruitment by Rap1p at Silencers and Telomeres in Yeast. *Molecular and Cellular Biology*, 21(23): 8082-8094. https://doi.org/10.1128/mcb.21.23.8082-8094.2001

Moretti, Paolo, Freeman, K., Coodly, L., Shore, D. (1994). Evidence that a complex of SIR proteins interacts with the silencer and telomere-binding protein RAP1. *Genes and Development*, 8: 2257-2269. https://doi.org/10.1101/gad.8.19.2257

Morin, G. B. (1989). The human telomere terminal transferase enzyme is a ribonucleoprotein that synthesizes TTAGGG repeats. *Cell*, 59(3): 521-529.

https://doi.org/10.1016/0092-8674(89)90035-4
Morrow, B. E., Johnson, S. P., Warner, J. R. (1989). Proteins that bind to the yeast rDNA enhancer. *Journal of Biological Chemistry*, 264(15): 9061–9068.

Mortimer, R. K., Johnston, J. R. (1986). Genealogy of principal strains of the yeast genetic stock center. *Genetics*, 113(1): 35-43.

Muller, J. H. (1938). The remaking of chromosomes. *The Collecting Net*. 8: 182-198.

Olovnikov, A. M. (1973). A theory of marginotomy. The incomplete copying of template margin in enzymic synthesis of polynucleotides and biological significance of the phenomenon. *Journal of Theoretical Biology*, 41(1): 181-190. https://doi.org/10.1016/0022-5193(73)90198-7

Oppikofer, M., Kueng, S., Gasser, S. M. (2013). SIR-nucleosome interactions: Structure-function relationships in yeast silent chromatin. *Gene*, 527(1): 10-25. https://doi.org/10.1016/j.gene.2013.05.088

Peterson, S. E., Stellwagen, A. E., Diede, S. J., Singer, M. S., Haimberger, Z. W., Johnson, C. O., Tzoneva, M., Gottschling, D. E. (2001). The function of a stem-loop in telomerase RNA is linked to the DNA repair protein Ku. *Nature Genetics*, 27(1): 64–67. https://doi.org/10.1038/83778

Pfeiffer, V., Lingner, J. (2012). TERRA promotes telomere shortening through exonuclease 1-mediated resection of chromosome ends. *PLoS Genetics*, 8(6): e1002747. https://doi.org/10.1371/journal.pgen.1002747

Pfingsten, J. S., Goodrich, K. J., Taabazuing, C., Ouenzar, F., Chartrand, P., Cech, T. R. (2012). Mutually exclusive binding of telomerase RNA and DNA by Ku alters telomerase recruitment model. *Cell*, 148(5): 922-932. https://doi.org/10.1016/j.cell.2012.01.033

Polotnianka, R. M., Li, J., Lustig, A. J. (1998). The yeast Ku heterodimer is essential for protection of the telomere against nucleolytic and recombinational activities. *Current Biology*, 8(14): 831-835. https://doi.org/10.1016/s0960-9822(98)70325-2

Poon, B. P. K., Mekhail, K. (2012). Effects of perinuclear chromosome tethers in the telomeric URA3/5FOA system reflect changes to gene silencing and not nucleotide metabolism. *Frontiers in Genetics*, 3: 1-9. https://doi.org/10.3389/fgene.2012.00144

Porter, S. E., Greenwell, P. W., Ritchie, K. B., Petes, T. D. (1996). The DNA-binding protein Hdf1p (a putative Ku homologue) is required for maintaining normal telomere length in Saccharomyces cerevisiae. *Nucleic Acids Research*, 24(4): 582–585. https://doi.org/10.1093/nar/24.4.582

Power, P., Jeffery, D., Rehman, M. A., Chatterji, A., Yankulov, K. (2011). Sub-telomeric core X and Y' elements in S.cerevisiae suppress extreme variations in gene silencing. *PLoS ONE*, 6(3): e17523. https://doi.org/10.1371/journal.pone.0017523

Preti, M., Ribeyre, C., Pascali, C., Bosio, M. C., Cortelazzi, B., Rougemont, J., Guarnera, E., Naef, F., Shore, D., Dieci, G. (2010). The Telomere-Binding Protein Tbf1 Demarcates snoRNA Gene Promoters in Saccharomyces cerevisiae. *Molecular Cell*, 38(4): 614-620. https://doi.org/10.1016/j.molcel.2010.04.016

Pryde, F. E., Louis, E. J. (1999). Limitations of silencing at native yeast telomeres. *EMBO Journal*, 18: 2538-2550. https://doi.org/10.1093/emboj/18.9.2538

Renauld, H., Aparicio, O. M., Zierath, P. D., Billington, B. L., Chhablani, S. K., Gottschling, D. E. (1993). Silent domains are assembled continuously from the telomere and are defined by promoter distance and strength, and by SIR3 dosage. *Genes and Development*, 7: 1133-1145. https://doi.org/10.1101/gad.7.7a.1133

Ribaud, V., Ribeyre, C., Damay, P., Shore, D. (2012). DNA-end capping by the budding yeast transcription factor and subtelomeric binding protein Tbf1. *EMBO Journal*, 31(1): 138–149. https://doi.org/10.1038/emboj.2011.349

Robyr, D., Suka, Y., Xenarios, I., Kurdistani, S. K., Wang, A., Suka, N., Grunstein, M. (2002). Microarray deacetylation maps determine genome-wide functions for yeast histone deacetylases. *Cell*, 109(4): 437-446. https://doi.org/10.1016/S0092-8674(02)00746-8

Rossmann, M. P., Luo, W., Tsaponina, O., Chabes, A., Stillman, B. (2011). A common telomeric gene silencing is affected by nucleotide metabolism. *Molecular Cell*, 42(1): 127–136. https://doi.org/doi:10.1016/j.molcel.2011.03.007

Roy, R., Meier, B., McAinsh, A. D., Feldmann, H. M., Jackson, S. P. (2004). Separation-of-function Mutants of Yeast Ku80 Reveal a Yku80p-Sir4p Interaction Involved in Telomeric Silencing. *Journal of Biological Chemistry*, 279:86-94. https://doi.org/10.1074/jbc.M306841200

Roy, K., Gabulinas, J., Gillespie, A., Ngo, D., Chanfreu, G. F. (2016). Common genomic elements promote transcriptional and DNA replication roadblock. *Genome Research.* 26(10): 1363-1375. https://doi.org/10.1101/gr/204776.116

Sabourin, M., Tuzon, C. T., Zakian, V. A. (2007). Telomerase and Tel1p Preferentially Associate with Short Telomeres in S. cerevisiae. *Molecular Cell*, 27(4): 550-561. https://doi.org/10.1016/j.molcel.2007.07.016

Schoeftner, S., Blasco, M. A. (2008). Developmentally regulated transcription of mammalian telomeres by DNA-dependent RNA polymerase II. *Nature Cell Biology*, 10:

228-236. https://doi.org/10.1038/ncb1685

Seto, A. G., Livengood, A. J., Tzfati, Y., Blackburn, E. H., Cech, T. R. (2002). A bulged stem tethers Est1p to telomerase RNA in budding yeast. *Genes and Development*, 16: 2800-2812. https://doi.org/10.1101/gad.1029302

Seto, A. G., Zaug, A. J., Sobel, S. G., Wolin, S. L., Cech, T. R. (1999). Saccharomyces cerevisiae telomerase is an Sm small nuclear ribonucleoprotein particle. *Nature*, 401(6749): 177–180. https://doi.org/10.1038/43694

Sikorski, R.S., Hieter, P. (1989) A system of shuttle vectors and yeast host strains designed for efficient manipulation of DNA in Saccharomyces cerevisiae. *Genetics.* 122(1):19-27.

Singer, M. S., Gottschling, D. E. (1994). TLC1: Template RNA component of Saccharomyces cerevisiae telomerase. *Science*, 266(5184) : 404-409. https://doi.org/10.1126/science.7545955

Soudet, J., Jolivet, P., Teixeira, M. T. (2014). Elucidation of the DNA end-replication problem in saccharomyces cerevisiae. *Molecular Cell*, 53(6): 954-964. https://doi.org/10.1016/j.molcel.2014.02.030

Southern, E. M. (1975). Detection of specific sequences among DNA fragments separated by gel electrophoresis. *Journal of Molecular Biology*, 98(5): 503-508. https://doi.org/10.1016/S0022-2836(75)80083-0

Stellwagen, A. E., Haimberger, Z. W., Veatch, J. R., Gottschling, D. E. (2003). Ku interacts with telomerase RNA to promote telomere addition at native and broken chromosome ends. *Genes and Development*, 17(19): 2384–2395. https://doi.org/10.1101/gad.1125903

Strahl-Bolsinger, S., Hecht, A., Luo, K., Grunstein, M. (1997). SIR2 and SIR4 interactions differ in core and extended telomeric heterochromatin in yeast. *Genes and Development*, 11: 83-93. https://doi.org/10.1101/gad.11.1.83

Taddei, A., Hediger, F., Neumaan, F. R., Bauer, C., Gasser, S. M. (2004). Separation of silencing from perinuclear anchoring functions in yeast Ku80, Sir4 and Esc1 proteins. *EMBO Journal*, 23:1301-1312. https://doi.org/10.1038/sj.emboj.7600144

Takahashi, Y. H., Schulze, J. M., Jackson, J., Hentrich, T., Seidel, C., Jaspersen, S. L., Kobor, M. S., Shilatifard, A. (2011). Dot1 and Histone H3K79 Methylation in Natural Telomeric and HM Silencing. *Molecular Cell*, 42(1): 118-126. https://doi.org/10.1016/j.molcel.2011.03.006

Teixeira, M. T., Arneric, M., Sperisen, P., Lingner, J. (2004). Telomere length homeostasis is achieved via a switch between telomerase- extendible and -nonextendible states. *Cell*,

117(3): 323-335. https://doi.org/10.1016/S0092-8674(04)00334-4

Teng, S.-C., Zakian, V. A. (1999). Telomere-Telomere Recombination Is an Efficient Bypass Pathway for Telomere Maintenance in *Saccharomyces cerevisiae*. *Molecular and Cellular Biology*. 19(12): 8083-8093. https://doi.org/10.1128/mcb.19.12.8083

Teng, S. C., Chang, J., McCowan, B., Zakian, V. A. (2000). Telomerase-independent lengthening of yeast telomeres occurs by an abrupt Rad50p-dependent, Rif-inhibited recombinational process. *Molecular Cell*, 6(4): 947-952. https://doi.org/10.1016/S1097-2765(05)00094-8

Towbin, H., Staehelin, T., Gordon, J. (1979). Electrophoretic transfer of proteins from polyacrylamide gels to nitrocellulose sheets: Procedure and some applications. *Proceedings of the National Academy of Sciences of the United States of America*, 76(9): 4350-4354. https://doi.org/10.1073/pnas.76.9.4350

Tsukamoto, Y., Kato, J. I., Ikeda, H. (1997). Silencing factors participate in DNA repair and recombination in Saccharomyces cerevisiae. *Nature*, 388: 900-903. https://doi.org/10.1038/42288

Tucey, T. M., Lundblad, V. (2014). Regulated assembly and disassembly of the yeast telomerase quaternary complex. *Genes and Development*, 28(19): 2077–2089. https://doi.org/10.1101/gad.246256.114

Umen, J.G., Guthrie, C. (1996). Mutagenesis of the yeast gene PRP8 reveals domains governing the specificity and fidelity of 3’ splice site selection. *Genetics*. 143(2): 723-739.

Vassetzky, N. (1999). Taz1p and Teb1p, two telobox proteins in Schizosaccharomyces pombe, recognize different telomere-related DNA sequences. *Nucleic Acids Research*, 27(24): 4687-4694. https://doi.org/10.1093/nar/27.24.4687

Vega-Palas, M. A., Venditti, S., Di Mauro, E. (1998). Heterochromatin organization of a natural yeast telomere: Changes of nucleosome distribution driven by the absence of Sir3p. *Journal of Biological Chemistry*, 273(16): 9388–9392. https://doi.org/10.1074/jbc.273.16.9388

Vodenicharov, M. D., Laterreur, N., Wellinger, R. J. (2010). Telomere capping in non-dividing yeast cells requires Yku and Rap1. *EMBO Journal*, 29: 3007-3019. https://doi.org/10.1038/emboj.2010.155

Walmsley, R. W., Chan, C. S. M., Tye, B. K., Petes, T. D. (1984). Unusual DNA sequences associated with the ends of yeast chromosomes. *Nature*, 310 : 157-160. https://doi.org/10.1038/310157a0

Wang, C., Zhao, L., Lu, S. (2015). Role of TERRA in the regulation of telomere length. *International Journal of Biological Sciences*, 11(3): 316-323. https://doi.org/10.7150/ijbs.10528

Wang, H., Nicholson, P. R., Stillman, D. J. (1990). Identification of a Saccharomyces cerevisiae DNA-binding protein involved in transcriptional regulation. *Molecular and Cellular Biology*, 10(4): 1743-1753. https://doi.org/10.1128/mcb.10.4.1743

Wellinger, R. J., Wolf, A. J., Zakian, V. A. (1993). Saccharomyces telomeres acquire single-strand TG1-3 tails late in S phase. *Cell*, 72(1): 51-60. https://doi.org/10.1016/0092-8674(93)90049-V

Wellinger, R. J., Zakian, V. A. (2012). Everything you ever wanted to know about Saccharomyces cerevisiae telomeres: Beginning to end. *Genetics*, 191(4): 1073–1105. https://doi.org/10.1534/genetics.111.137851

Wotton, D., Shore, D. (1997). A novel Rap1p-interacting factor, Rif2p, cooperates with Rif1p to regulate telomere length in Saccharomyces cerevisiae. *Genes and Development*, 11: 748-760. https://doi.org/10.1101/gad.11.6.748

Wu, Y., Zakian, V. A. (2011). The telomeric Cdc13 protein interacts directly with the telomerase subunit Est1 to bring it to telomeric DNA ends in vitro. *Proceedings of the National Academy of Sciences of the United States of America*, 108(51): 20362-20369. https://doi.org/10.1073/pnas.1100281108

Wyrick, J. J., Holstege, F. C. P., Jennings, E. G., Causton, H. C., Shore, D., Grustein, M., Lander, E. S., Young, R. A. (1999). Chromosomal landscape of nucleosome-dependent gene expression and silencing in yeast. *Nature*, 402 : 418-421. https://doi.org/10.1038/46567

Xie, W., Gai, X., Zhu, Y., Zappulla, D. C., Sternglanz, R., Voytas, D. F. (2001). Targeting of the Yeast Ty5 Retrotransposon to Silent Chromatin Is Mediated by Interactions between Integrase and Sir4p. *Molecular and Cellular Biology*, 21(19): 6606-6614. https://doi.org/10.1128/mcb.21.19.6606-6614.2001

Yassoura, M., Kaplana, T., Fraser, H. B., Levin, J. Z., Pfiffner, J., Adiconis, X., Schroth, G., Luo, S., Khrebtukova, I., Gnirke, A., Nusbaum, C., Thompson, D. A., Friedman, N., Regev, A. (2009). Ab initio construction of a eukaryotic transcriptome by massively parallel mRNA sequencing. *Proceedings of the National Academy of Sciences of the United States of America*, 106(9): 3264-3269. https://doi.org/10.1073/pnas.0812841106

Yu, T. Y., Kao, Y. W., Lin, J. J. (2014). Telomeric transcripts stimulate telomere recombination to suppress senescence in cells lacking telomerase. *Proceedings of the National Academy of Sciences of the United States of America*, 111(9): 3377-3382.

https://doi.org/10.1073/pnas.1307415111

Zhang, Q., Wang, J., Deng, F., Yan, Z., Xia, Y., Wang, Z., Ye, J., Deng, Y., Zhang, Z., Qiao, M., Li, R., Denduluri, S. K., Wei, Q., Zhao, L., Lu, S., Wang, X., Tang, S., Liu, H., Luu, H. H., Haydon, R. C., He, T-C., Jiang, Li. (2015). TqPCR: A touchdown qPCR assay with significantly improved detection sensitivity and amplification efficiency of SYBR Green qPCR. *PLoS ONE*. 10(7): e0132666. https://doi.org/10.1371/journal.pone.0132666

Zhong, Z., Shiue, L., Kaplan, S., de Lange, T. (1992). A mammalian factor that binds telomeric TTAGGG repeats in vitro. *Molecular and Cellular Biology*, 12(11): 4834-4843. https://doi.org/10.1128/mcb.12.11.4834

Zhu, X., Gustafsson, C. M. (2009). Distinct differences in chromatin structure at subtelomeric X and Y' elements in budding yeast. *PLoS ONE*, 4(7): e6363. https://doi.org/10.1371/journal.pone.0006363

Zill, O. A., Scannell, D., Teytelman, L., Rine, J. (2010). Co-evolution of transcriptional silencing proteins and the DNA elements specifying their assembly. *PLoS Biology*, 8(11): e1000550. https://doi.org/10.1371/journal.pbio.1000550

Zou, S., Wright, D. A., Voytas, D. F. (1995). The Saccharomyces Ty5 retrotransposon family is associated with origins of DNA replication at the telomeres and the silent mating locus HMR. *Proceedings of the National Academy of Sciences of the United States of America*, 92(3): 920-924. https://doi.org/10.1073/pnas.92.3.920